

## INFORMATION TO USERS

The most advanced technology has been used to photograph and reproduce this manuscript from the microfilm master. UMI films the text directly from the original or copy submitted. Thus, some thesis and dissertation copies are in typewriter face, while others may be from any type of computer printer.

The quality of this reproduction is dependent upon the quality of the copy submitted. Broken or indistinct print, colored or poor quality illustrations and photographs, print bleedthrough, substandard margins, and improper alignment can adversely affect reproduction.

In the unlikely event that the author did not send UMI a complete manuscript and there are missing pages, these will be noted. Also, if unauthorized copyright material had to be removed, a note will indicate the deletion.

Oversize materials (e.g., maps, drawings, charts) are reproduced by sectioning the original, beginning at the upper left-hand corner and continuing from left to right in equal sections with small overlaps. Each original is also photographed in one exposure and is included in reduced form at the back of the book. These are also available as one exposure on a standard 35mm slide or as a 17" x 23" black and white photographic print for an additional charge.

Photographs included in the original manuscript have been reproduced xerographically in this copy. Higher quality 6" x 9" black and white photographic prints are available for any photographs or illustrations appearing in this copy for an additional charge. Contact UMI directly to order.

# U·M·I

University Microfilms International  
A Bell & Howell Information Company  
300 North Zeeb Road, Ann Arbor, MI 48106-1346 USA  
313/761-4700 800/521-0600

**Order Number 9000675**

**A neuroanatomical study of the connectivity of the pretectal  
lentiform nucleus of the mesencephalon in chicken**

**Bodnarenko, Stefan Roman, Ph.D.**

**City University of New York, 1989**

**Copyright ©1989 by Bodnarenko, Stefan Roman. All rights reserved.**

**U·M·I**  
300 N. Zeeb Rd.  
Ann Arbor, MI 48106

**PLEASE NOTE:**

**BEST COPY AVAILABLE, FILMED AS RECEIVED.**

**U·M·I**

A

A NEUROANATOMICAL STUDY OF THE CONNECTIVITY OF THE PRETECTAL  
LENTIFORM NUCLEUS OF THE MESENCEPHALON IN CHICKEN

by

STEFAN R. BODNARIENKO

A dissertation submitted to the Graduate Faculty in Psychology in partial  
fulfillment of the requirements for the degree of Doctor of Philosophy,  
The City University of New York.

1989

© 1989

STEFAN R. BODNARENKO

All Rights Reserved

This manuscript has been read and accepted by the Graduate Faculty in Psychology in satisfaction of the dissertation requirement for the degree of Doctor of Philosophy.

3/29/89  
Date

*Oliver C. McKenna*  
Chair of Examining Committee

Date  
*March 31, 1989*

Executive Officer  
*Herbert D. Saltzstein*

Dr. H. P. Ziegler

Dr. J. Gordon

Dr. M. Gottlieb

Dr. K. Fite

Supervisory Committee

## ABSTRACT

## A NEUROANATOMICAL STUDY OF THE CONNECTIVITY OF THE PRETECTAL LENTIFORM NUCLEUS OF THE MESENCEPHALON (LM) IN CHICKEN

by

Stefan R. Bodnarenko

Advisers: Dr. Olivia McKenna and Dr. H. P. Ziegler

The lentiform nucleus of the mesencephalon (LM) is a retinorecipient pretectal nucleus in the avian brain thought to receive retinal slip signals and in turn relay these signals to oculomotor pathways through which horizontal optokinetic nystagmus (OKN) is generated. Because of their common derivation from the tectal plate and similar positioning within the pretectum, it has been suggested that the LM in birds is homologous to the nucleus of the optic tract (NOT) in mammals.

The objective of this dissertation was to identify the boundaries of the LM nucleus within the chicken pretectum, and then, to describe the organization of the afferent and efferent connectivity of the LM in an effort to better understand the organization of this region and the neuroanatomical substrate which may mediate the generation of horizontal optokinetic pursuit in birds.

The position of the LM in the chicken pretectum was identified on the basis of the position of cells in Klüver-Barrera stained sections, the position of retinal terminals after intraocular injections of horseradish peroxidase (HRP) and the regional accumulation of 2-deoxy-D-glucose (2-DG) label in response to horizontal large-field motion. The sources of afferent projections to the LM and the distribution of the projection neurons and the spatial organization of these projections were described with the HRP retrograde tract tracing technique. The efferent projection targets of the LM were identified with the tritiated amino acid

and HRP anterograde tract tracing techniques. The size and position of projection neurons in the LM were identified after HRP injections into the efferent target nuclei.

The LM in chickens was found in the pretectum medial to the optic tectum (OT) and lateral to the pretectal superficial synencephalic nucleus (SS). The LM consists of two subdivisions, the magnocellular portion (LMmc) and the parvocellular portion (LMpc), both of which receive retinal afferents.

The sources of afferent input to the LM were identified to be the contralateral retina, the ipsilateral accessory hyperstriatum (HA) of the visual Wulst, the ipsilateral nucleus of the basal optic root (nBOR), and ipsilateral OT. Retinal ganglion cells that project to the LM were distributed in all four retinal quadrants in a wide horizontal belt lying along both sides of the retinal equator stretching from the temporal to the nasal retina. The HRP-labeled ganglion cells, which appeared either round or oval, ranged from 25-840  $\mu\text{m}^2$  in cross-sectional area with most in the smaller size range. Results of HRP injections into portions of the LM and metabolic mapping patterns in the LM produced by stimulation of half the retina with horizontal visual motion and injections of 2-DG were in agreement in that there was an orderly mapping of the retina onto the LM. The inferior temporal quadrant projected to the rostradorsal LM; the inferior nasal quadrant projected to the caudadorsal LM. The superior temporal quadrant projected to the middle and ventral LM, extending from the rostral to the caudal pole, whereas the superior nasal quadrant projected to a small zone in the caudal LM.

A spatially organized projection of nonretinal afferents originating from the ipsilateral HA was identified after HRP injections into the LM. Retrogradely labeled round or stellate-shaped neurons, with somata measuring 678.9  $\mu\text{m}^2$  on average, were confined to the lateralmost portion of the HA layer, throughout its

caudal to rostral extent, except for the rostralmost portion of the HA. Injections into portions of the LM revealed a spatial organization of this projection. The ventral LM received projections from rostrally and dorsally positioned neurons within the HA whereas the dorsal LM received projections from caudally and ventrally placed neurons. The projection from the HA to the LM is of particular interest since it has been suggested that its postnatal development may account for postnatal changes in horizontal OKN. The terminal innervation pattern of the HA projection within the LM was found to be similar in both hatchlings and older chickens after anterograde tract tracing experiments. In addition to the non-retinal afferent projection from the HA, the LM was found to receive a projection from medium (10-19 $\mu$ m) and large (20-29 $\mu$ m), round or stellate shaped neurons distributed throughout all three subdivisions of the ipsilateral nBOR, and small (6-9 $\mu$ m) and medium (10-19 $\mu$ m) sized neurons, round or elongated in shape in layers 2, 4, 8, 10, 13, and 14 of the ipsilateral OT.

The results of the anterograde tract tracing experiments suggested that the LM projects to various thalamic, pretectal, mesencephalic, and brainstem nuclei. Ascending efferent projections of the LM were found to terminate in ipsilateral dorsal and ventral thalamic areas including the ventrolateral geniculate nucleus (GLv), the magnocellular portion of the dorsolateral nucleus of the anterior thalamus (DLAmc), the lateral portion of the dorsolateral nucleus of the anterior thalamus (DLL), and the intercalated nucleus of the thalamus (ICT). The pretectal efferent targets of the LM were all ipsilateral and included the pretectal area (AP), the pretectal nucleus (Pt), and the principal precommissural nucleus (PPC). The mesencephalic targets included the ipsilateral layers 4, 7, 9, 11, 12, 13 of the OT, the ipsilateral nucleus Darkschewitsch (nD), the nBOR bilaterally, the contralateral lateral reticular formation (FRL), the ipsilateral ventral nucleus of the deep mesencephalon (MPv) and the ipsilateral papilliform nucleus (nPap).

The efferent targets of the LM in the brainstem were the ipsilateral lateral pontine (LP), medial pontine (MP), and inferior olive (IO). A direct projection from the LM to the cerebellum (Cb) was found to terminate bilaterally in folia VI, VIII a and b, and IX a and c.

The results of the HRP retrograde tracing experiments from several of the descending efferent targets of the LM suggested a differential projection from different sized neurons. Small (10-19  $\mu\text{m}$ ), medium (20-29  $\mu\text{m}$ ), and large (30-39  $\mu\text{m}$ ) neurons within both the LMmc and LMpc project to the nBOR and pontine nuclei whereas medium and large cells in the LMmc were found to project to the IO and Cb. The LM projection to nD was found to originate primarily from medium neurons in the LMmc.

The results of the present study have demonstrated the elaborate organization of the retinal representation within the LM both directly and indirectly via the visual Wulst and other afferent pathways that may bring retinal slip information into the LM. Furthermore, the description of the organization of the efferent projections of the LM provides connectivity information regarding the pathways that may be involved in the generation of horizontal optokinetic pursuit in chickens. Finally, the results of this study provides further evidence in support of the notion that the LM in birds is homologous to the NOT in mammals.

## Acknowledgements

This doctoral dissertation is authored by a single individual, although, it is in reality, the product of a group effort that involved many of my friends and colleagues at Hunter and City College. Their advice throughout all the phases of my doctoral research was greatly appreciated. A special thanks to Ximena Rojas for her contribution in the metabolic mapping experiments, to Michael Gottlieb for his advice on technical matters and his general musings, and to the rest of my dissertation committee for their contribution in the development of this doctoral thesis. Most of all, thanks to Olivia McKenna, my friend and thesis adviser, for her patience, advice and guidance throughout the course of my doctoral studies. She provided me with a great laboratory environment for learning and an opportunity to grow both emotionally and professionally. In addition, several other individuals should be recognized. I am forever indebted to my friend and colleague, Dr. Donald Hutchings, who many years ago, opened the doors to neuroscience research for me both literally and figuratively, and in effect, helped pave the way to this milestone in my development as a research scientist. This one's for you, Don! I am especially grateful to my closest friend Lisa "B." Leicach, who supported me throughout this endeavor, at that darkest hour, just before the dawn.

This doctoral thesis is dedicated to the memory of my grandfather Alexander Sadczenko, who, along with my grandmother and parents, taught me the importance of learning.

## TABLE OF CONTENTS

Abstract	iv
Acknowledgements	viii
Table of Contents	ix
Abbreviations	x
List of Tables	xii
List of Figures	xiii
Chapter 1: Introduction	1
Chapter 2: Background	5
Chapter 3: Methods	34
Chapter 4: The Topography of the LM in the Chicken Pretectum	41
Chapter 5: The Organization of the Retinal Projection to the LM	48
Chapter 6: The Organization of the Non-retinal Afferent Projections to the LM	67
Chapter 7: The Organization of the Efferent Projections of the LM	83
Chapter 8: General Discussion	93
Appendix A: Tables	107
Appendix B: Figures	114
References	201

## ABBREVIATIONS

AOS	Accessory optic system
AP	Area pretectalis
BCP	Brachium cerebellopetale
BDH	Benzidine Dihydrochloride
BHRP	$\beta$ -subunit Cholera toxin horseradish peroxidase
Cb	Cerebellum
2-DG	2-deoxy-D-glucose
DLAmc	Dorsolateral nucleus of the anterior thalamus, magnocellular portion
DLL	Dorsolateral nucleus of the anterior thalamus, lateral portion
DTN	Dorsal terminal nucleus
FRL	Lateral reticular formation of the mesencephalon
GLv	Lateral geniculate nucleus, ventral portion
GT	Tectal grey
HA	Accessory hyperstriatum
HD	Dorsal hyperstriatum
HIS	Hyperstriatum intercalatus superior
HV	Ventral hyperstriatum
HRP	Horseradish peroxidase
HRP-WGA	Wheat germ agglutinated horseradish peroxidase
ICT	Intercalated nucleus of the thalamus
IO	Inferior olivary nucleus
LFM	Supreme frontal lamina
LFS	Superior frontal lamina
LM	Lentiform nucleus of the mesencephalon
LMmc	Lentiform nucleus of the mesencephalon, magnocellular portion
LMpc	Lentiform nucleus of the mesencephalon, parvicellular portion

LP	Lateral pontine nucleus
MP	Medial pontine nucleus
MPv	Ventral portion of the deep nucleus of the mesencephalon
MTN	Medial terminal nucleus
NE	Nucleus externus
NOT	Nucleus of the optic tract
nBOR	Nucleus of the basal optic root
nBORl	Nucleus of the basal optic root, lateral portion
nBORd	Nucleus of the basal optic root, dorsal portion
nBORp	Nucleus of the basal optic root, proper
nD	Nucleus Darkschewitsch
nPap	Nucleus Papilliformis
nRTP	Reticular nucleus of the tegmentum of the pons
OKN	Optokinetic nystagmus
OPT	Principal optic nucleus of the thalamus
OT	Optic tectum
PPC	Principal precommissural nucleus
Pt	Pretectal nucleus
SCE	Stratum cellulare externum
SS	Superficial synencephalic nucleus
TeO	Optic tectum
TMB	Tetramethyl benzidine dihydrochloride

## LIST OF TABLES

Table 1. Alternative nomenclatures used by various authors to describe the LM and SS	108
Table 2. Summary of the distribution of labeled retinal ganglion cells in retinal quadrants after HRP injections into LM	110
Table 3. Summary of the frequency of HRP-labeled neurons in the LM after injections into efferent target nuclei	112

## LIST OF FIGURES

1. Schematic line drawings of a series of coronal sections from the rostral through the caudal pole of the LM	115
2. Photomicrographs of coronal Klüver-Barrera stained sections of the LM	118
3. High magnification photomicrograph of a coronal section through the rostral pretectum	120
4. Photomicrographs of coronal sections showing HRP-labeled terminals within the LM after intraocular injection of the contralateral eye with HRP-WGA	122
5. Photomicrograph of HRP-labeled retinal ganglion cells after injection into LM	124
6. Frequency histograms of HRP-labeled retinal ganglion cells in the superior temporal, inferior nasal and inferior temporal quadrants	126
7. Photomicrographs of HRP injection site in the dorsorostral LM and the resultant distribution of labeled retinal ganglion cells	128
8. Photomicrographs of HRP injection site in the dorsocaudal LM and the resultant distribution of labeled retinal ganglion cells	130
9. Photomicrographs of HRP injection site in the ventral LM and the resultant distribution of labeled retinal ganglion cells	132
10. Photomicrographs of HRP injection site in the LM and the resultant distribution of labeled retinal ganglion cells	134

11. Autoradiograms and matched stained sections illustrating the pattern of label in the LM after stimulation of the superior retina with horizontal visual motion and injection of 2-DG	136
12. Autoradiograms and matched stained sections illustrating the pattern of label in the LM after stimulation of the inferior retina with horizontal visual motion and injection of 2-DG	138
13. Autoradiograms and matched stained sections illustrating the pattern of label in the LM after stimulation of the temporal retina with horizontal visual motion and injection of 2-DG	140
14. Autoradiograms and matched stained sections illustrating the pattern of label in the LM after stimulation of the injection of 2-DG	142
15. Line drawing of a parasagittal view of the LM showing mapping of each retinal quadrant onto the nucleus and the retinotopic mapping onto the optic tectum	144
16. Photomicrographs of a coronal sections through the middle of the telencephalon	146
17. Photomicrographs of the HRP injection site in the LM and a schematic illustration of the injection site with the resultant distribution of labeled cells in HA	148
18. Frequency histogram of HRP-labeled neurons in HA after injection into LM and photomicrographs of HRP-labeled neurons	150
19. Line drawing of the HRP injection site in the dorsal	

LM and a rostrocaudal series of line drawings of the resultant distribution of labeled neurons in HA	152
20.Line drawing of the HRP injection site in the dorsal LM and a rostrocaudal series of line drawings of the resultant distribution of labeled neurons in HA	154
21.Line drawing of the HRP injection site in the ventral LM and a rostrocaudal series of line drawings of the resultant distribution of labeled neurons in HA	155
22.Line drawing of the HRP injection site in the ventral LM and a rostrocaudal series of line drawings of the resultant distribution of labeled neurons in HA	156
23.Composite drawing of the distribution of labeled cells within the HA after HRP injections into portions of LM	158
24.A rostrocaudal series of line drawings and darkfield photomicrographs showing the distribution of labeled terminals in the LM after injections into the HA of older chickens	160
25.A rostrocaudal series of line drawings and darkfield photomicrographs showing the distribution of labeled terminals in the LM after injections into the HA of hatchlings	163
26.A line drawing of the nBOR and photomicrographs of HRP-labeled neurons after injection into LM	165
27.A line drawing of the OT and photomicrographs of HRP-labeled neurons after injection into LM	167
28.Schematic representations of the mapping of the	

retinal quadrants in the HA and LM	169
29. Photomicrographs of HRP injection site in the LM and a line drawing of the resulting anterograde labeling of three bundles of axons	171
30. Line drawings of a rostrocaudal series of coronal sections and a parasagittal section of the Cb showing the distribution of labeled axons and terminals after injection into the LM	173
31. A brightfield photomicrograph of a coronal section through the rostral OT and a darkfield photomicrograph showing the resultant anterograde labeling in the OT after injection into LM	175
32. A brightfield photomicrograph of a coronal section through the nD and a darkfield photomicrograph showing the resultant anterograde labeling in nD after injection into LM	177
33. A brightfield photomicrograph of a coronal section through the nBOR and a darkfield photomicrograph showing the resultant anterograde labeling in nBOR after injection into LM	179
34. A brightfield photomicrograph of a coronal section through the MP and a darkfield photomicrograph showing the resultant anterograde labeling in MP after injection into LM	181
35. A brightfield photomicrograph of a coronal section through the IO and a darkfield photomicrograph showing the resultant anterograde labeling in IO after injection	

into LM	183
36.A brightfield photomicrograph of a coronal section through the LP and a dark field photomicrograph showing the resultant anterograde labeling in LP after injection into LM	185
37.A brightfield photomicrograph of a parasagittal section through the Cb and a dark field photomicrograph showing the resultant terminal labeling in folia IXc of Cb	187
38.Photomicrographs of HRP-labeled neurons in LM after injection into nBOR	189
39.Photomicrographs of HRP-labeled neurons in LM after injection into LP and MP	191
40.Photomicrographs of HRP-labeled neurons in LM after injection into nD	193
41.Photomicrographs of HRP-labeled neurons in LM after injection into IO	195
42.Photomicrographs of HRP-labeled neurons in LM after injection into Cb	197
43.Summary diagram of the afferent and efferent connectivity of the LM in chicken	199

## Chapter 1: INTRODUCTION

Whenever an animal moves within its environment, its eyes must move in a compensatory fashion to avoid blurring by keeping the visual world stationary on the retina. This stabilization is accomplished by two interrelated neural reflexes that are similar in most vertebrates. For the vestibulo-ocular reflex, movement of the head detected by the stimulation of the semicircular canals results in the movement of the eyes in the opposite direction, but at almost the same velocity as the head, thus compensating for the apparent movement of the world. For the optokinetic reflex, the visual system detects retinal slip, the movement of a large portion of the visual field on the retina, providing a signal for the generation of optokinetic pursuit in the same direction and at approximately the same velocity as the moving object thus stabilizing the retinal image. These two reflexes are usually invoked together in the natural environment, their interaction resulting in the generation of the appropriate compensatory eye movements.

The aim of this dissertation was to investigate, in the avian brain, the anatomical connectivity of a nucleus in the optokinetic system that receives retinal slip signals and is responsible for mediating optokinetic eye movements. Evidence strongly suggests that the visual input for horizontal optokinetic nystagmus, the movement of the eye in a temporal to nasal, or nasal to temporal direction in response to slow large field horizontal visual stimulation, is transmitted along a pathway from the retina to a pretectal nucleus. In mammals, this nucleus is the nucleus of the optic tract (NOT). The NOT is a diffuse superficial cell aggregation in the pretectum with most of its cells embedded in the fibers of the brachium of the superior colliculus. Neurophysiological recordings in the cat and rabbit NOT show that these cells have very large receptive fields, respond best to large moving random dot patterns, are velocity tuned to a range of .01-30 deg/sec and are directionally selective preferring

movement in the temporal to nasal direction. This stimulus direction is best in eliciting OKN in the horizontal plane (Collewijn, 1975; Hoffmann and Schoppmann, 1981). Furthermore, it has been reported in rabbits that stimulation of the NOT triggers horizontal OKN and lesioning this nucleus eliminates this type of nystagmus (Collewijn, 1975).

It has been suggested that the lentiform nucleus of the mesencephalon (LM) of birds is homologous to the NOT of mammals on the basis of its embryological derivation and position in the pretectum, its neurophysiological properties, and behavioral changes in OKN resulting from lesions (Kuhlenbeck and Miller, 1942; Winterson and Brauth, 1985; Gianni et al., 1983). In birds, the LM is located in the pretectum, medial to the rostral optic tectum (OT), lateral to the superficial synencephalic nucleus (SS) and rostral to the nucleus of the basal optic root (nBOR). It consists of two subdivisions, the LM magnocellular portion (LMmc) and the parvocellular portion (LMpc). All portions receive direct retinal projections although the density of terminals in the LMmc is much greater (Cowan, 1961; Gottlieb and McKenna, 1986). Evidence that the LM mediates horizontal retinal slip signals comes both from a 2-deoxy-D-glucose (2DG) metabolic mapping study and from a neurophysiological study demonstrating that the LM responds best to slow large-field horizontal motion (McKenna and Wallman, 1985a; Winterson and Brauth, 1985). In their study of the response properties of single units within the pigeon LM, Winterson and Brauth (1985) found that the response properties of the LM units are indeed similar to those in the NOT of rabbits and cats in that units respond best to large visual field stimuli and are directionally selective, that is, their firing rate increased above spontaneous levels when the stimulus moved in preferred directions and decreased below the spontaneous levels when the stimulus moved in the non-preferred directions. Furthermore, Gianni, et al. (1983) showed that lesions of the LM area produce

severe deficits in the optokinetic pursuit produced by motion in a temporal to nasal direction and a lesser deficit in optokinetic pursuit produced by motion in the opposite, nasal to temporal, direction.

The pathways underlying the processing of horizontal retinal slip signals and the generation of horizontal optokinetic pursuit have been elucidated only to some degree, and mostly in mammals. However, in mammals, anatomical studies of the connectivity of the NOT are confounded by the ill-defined borders of the NOT and neighboring pretectal nuclei, its location in the brachium of the superior colliculus and the technical problem of false positive labeling associated with the uptake of tracers by broken axons in passage. In contrast, the accessibility of the LM nucleus in chicks to injection with tract tracing agents and its position away from major fiber tracts allows for the thorough elucidation of the connectivity of this nucleus.

The LM in birds is known to receive afferent input from both the contralateral retina (Ehrlich and Mark, 1983; Cowan, 1961; Gamlin and Cohen, 1988a) and the visual telencephalon (Karten, et al. 1973; Miceli et al., 1979). However, all of these studies used various anterograde tracing techniques, rather than retrograde techniques, to describe the projection into the LM rather than identifying the projection neurons, their location and their morphology. With respect to the efferent targets of the LM, a study in pigeons (Gamlin and Cohen, 1988b) suggest that the LM may project to the vestibulocerebellum, the lateral pontine nucleus (LP), the inferior olivary nucleus (IO), the ventral nucleus of the deep mesencephalon (MPv), and the nucleus papillioformis (nPap). Furthermore, retrograde tracing experiments suggest that different neurons within the LM may project to these different target areas (Gamlin and Cohen, 1988b). No such connectivity evidence is presently available for chickens.

The goals of this investigation were first, to define the location of the

retinorecipient LM and its subdivisions in relation to neighboring nuclei and second, to identify the sources of afferent projections to the LM, the morphology and distribution of the projection neurons and the spatial organization of the projection neurons and their terminals. The afferent telencephalic projection to the LM is of particular interest since it has been suggested that its postnatal development may account for postnatal changes reported in horizontal OKN. In mammals, it has also been suggested that this projection develops postnatally, and its development may account for changes in horizontal optokinetic pursuit. Thus, the third goal is to determine whether this projection develops postnatally. Finally, the fourth goal is to describe the efferent targets of LM projections and then identify and characterize the different sized neurons and their position within the subdivisions of the LM that give rise to these projections. A description of the efferent connectivity of the LM related to oculomotor functions is important in that it will provide neuroanatomical data upon which available physiological and behavioral data can be interpreted.

The overall result of this study was the definition of the specific brain regions which contribute to the chickens' horizontal optokinetic responsiveness and the elucidation of pathways into and out of the LM by which retinal slip signals may effect a motor response of the eye. Furthermore, evidence of the topography and connectivity of the LM, together with the available embryological and neurophysiological evidence, lend support for the notion that the greater the concordance among avian and mammalian characteristics, the stronger the justification for the inference that the LM in avians and the NOT in mammals are indeed homologous and fit a general vertebrate pattern.

## Chapter 2: BACKGROUND

### Behavior

Optokinetic nystagmus (OKN) is one of the simplest forms of visuomotor behavior. It is elicited by the movement of a large portion of the visual field on the retina providing a stimulus for the generation of compensatory eye movements in the same direction and at approximately the same velocity as the stimulus movement. As a result, the visual world is stabilized on the retina with respect, both, to movements of the animal and the visual environment.

Optokinetic nystagmus, which is typically studied by measuring the eye movements of animals placed inside a rotating drum, consists of two phases, a slow following movement and a fast movement of the eyes in the opposite direction. The gain of OKN, a measure of retinal image stabilization, is calculated as the quotient of the eye velocity and stimulus velocity and usually remains less than 1.0, the value that would represent perfect retinal image stability.

Although the OKN appears to be essential for all vertebrates, there are differences in its features among various species, perhaps as a function of the position of the eyes within the cranium. These differences become most evident when large-field motion is presented in the temporal to nasal and nasal to temporal direction to only one eye. In adult humans, monkeys and cats, whose eyes are positioned frontally, the optomotor response to monocular optokinetic stimulation is almost completely symmetrical, that is, the eye follows stimulus movement at approximately the same velocity in both the temporal to nasal and nasal to temporal directions (Atkinson, 1979; Naegele and Held 1982). In contrast, in rabbits and rats, whose eyes are placed laterally, the adult OKN is asymmetrical, that is, the eye follows when the stimulus moves in the temporal to nasal direction but does not follow as well in response to nasal to temporal large field motion (Cazin, 1981; Collewijn, 1969). Most frontal-eyed species possess

both contralateral and ipsilateral central visual pathways, a wide binocular field, and a well developed visual cortical influence on midbrain visual structures. The lateral-eyed species, on the other hand, possess almost a complete decussation of the optic nerve, little cortical influence on midbrain visual structures, and essentially two independent visual fields with little binocular overlap. The appearance of an increased cortical afference to midbrain visual structures is correlated with the migration of the eyes from a lateral to a frontal position in the head and with the development of binocular vision (Braun and Gault, 1969). Alternatively, it has been suggested that a bidirectional optomotor response is not dependent on the presence of the uncrossed retinal fibers, but rather on the existence of a fovea or area centralis. It has been demonstrated that most foveate animals show a symmetric optomotor response to monocular optokinetic stimulation whereas afoveate animals show an asymmetric response (Tauber and Atkins, 1968). Arguments against this notion are that two reptiles examined possess a fovea but nevertheless possess an asymmetrical nystagmus, and that these authors classify the pigeon as afoveate even though it does have a fovea (Galifret, 1968), and asymmetrical OKN. Therefore, it seems more plausible that the asymmetry of nystagmus is associated with the lateral position of the eyes and symmetrical nystagmus to the frontal position of the eyes.

The position of the eyes within the cranium greatly affects the perception of movement of the visual field during locomotion. In a lateral-eyed animal, forward motion will generate movement of the visual field in a predominantly backward and nasal to temporal direction whereas in the frontal eyed animal, forward motion will generate movement of the visual field in a predominantly vertical direction. The reduced ability of the eye to generate optokinetic pursuit in the nasal to temporal direction has evolved presumably to reduce the tendency for OKN to be initiated by forward locomotion, because it would be counterproductive

to have the eyes tracking the passing scenery rather than being directed to the front. Furthermore, the asymmetries present in horizontal OKN are most prominent when large portions of the visual field move at faster velocities, velocities likely to be generated during forward locomotion (Wallman and Velez, 1985; Grasse and Cynader, 1986). Thus, the directional asymmetries in horizontal OKN which are characteristic of the lateral eyed species such as the rabbit or chicken seem to specifically reflect the differences in evolutionary pressure.

#### Horizontal Optokinetic Nystagmus in Mammals

In general, the characteristics of horizontal OKN are similar among the mammalian species studied. In rabbits (lateral-eyed mammal), when one eye is stimulated with an optokinetic stimulus, OKN is observed in only the temporal to nasal direction. For slow stimulus velocities of up to about 2 deg/sec the gain for the rabbit is about 0.8. Gain decreases for stimulus velocities higher than 10 deg/sec and becomes negligible at stimulus velocities above 60 deg/sec (Collewijn, 1969).

In contrast, for cats (frontal-eyed mammal), when one eye is stimulated by a large field stimulus, OKN is observed in both temporal to nasal and nasal to temporal directions. For cats, the eye velocity is almost equal to the stimulus velocities from 0.1-40 deg/sec, but decreases precipitously for higher velocities (Cynader and Harris 1980; Hoffmann, 1981).

The nucleus of the optic tract (NOT) has been considered to play a major role in the generation of horizontal optokinetic nystagmus in mammals. The main support for this idea comes from lesion and electrical stimulation experiments. In lateral-eyed mammals such as the rabbit and rat, stimulation of the NOT elicits slow horizontal eye movements only in the contralateral eye in a temporal to nasal direction while lesions of this area abolish temporal to nasal optokinetic

pursuit (Collewijn, 1975a; Cazin, 1980).

In frontal-eyed mammals such as monkeys, unilateral lesions of the NOT result in the failure to respond with the contralateral eye to large field visual motion in the temporal to nasal direction but do not affect OKN in response to nasal to temporal stimulation. In cats, unilateral lesions of the NOT also abolish OKN in response to temporal to nasal stimulation but the nasal to temporal following is not affected (Precht and Strata, 1980; Precht, 1981).

The nasal to temporal following of the eyes appears to be mediated by the visual cortex. In cats, after bilateral lesions of the visual cortex, the OKN elicited monocularly is asymmetrical with a severe reduction or eradication of following in the nasal to temporal direction. Furthermore, there is a reduction in the OKN in the temporal to nasal direction at higher stimulus velocities (Strong et al. 1984; Wood et al., 1973; Hoffmann, 1981). Effects after unilateral cortical ablation are less severe. Thus, the nature of changes in OKN caused by cortical lesions supports the notion that the visual cortex has two important roles in the OKN system of the cat. First, it mediates OKN in response to nasal to temporal motion of the visual environment during monocular viewing. Second, it expands the range of the OKN system to allow responses to higher stimulus velocities in the temporal to nasal direction. These results are similar to those reported for monkeys (Pasik et al., 1959; Pasik and Pasik, 1964).

In lateral-eyed mammals such as the rabbit, ablation of the visual cortex has been reported to have little effect on the horizontal OKN (Ter Braak, 1936; Hobbelein and Collewijn, 1971). However, the identification of a nystagmogenic region (low frequency stimulation will elicit optokinetic pursuit in the nasal to temporal direction) in the region at the border of A 17, 21, and 22 of the cerebral cortex, suggests some role for the visual cortex in OKN. Single shock stimulation of this area evoked single or multiple responses in half of the NOT units analyzed

and suggests some type of direct cortical modulation of the NOT in rabbits (Pettorossi and Troiani, 1983).

#### Development of Horizontal OKN in Mammals

The asymmetric horizontal OKN found in frontal-eyed adult mammals after bilateral cortical ablation is similar to the characteristics of OKN elicited in mammalian neonates. Developmental studies of OKN in neonatal monkeys and humans indicate that under monocular conditions, elicitation of OKN is strongly biased for temporal to nasal motion (Atkinson 1979; Naegele and Held 1982). With increasing age OKN becomes increasingly symmetrical until the adult form is achieved. As a consequence of the similarity in horizontal OKN between bilaterally ablated cortical mammals and neonatal frontal-eyed mammals and the reports of postnatal development of the visual cortex, it has been suggested that the postnatal development of the corticopretectal pathway may be responsible for the postnatal changes seen in the development of horizontal OKN.

#### Horizontal Optokinetic Nystagmus in Birds

Early descriptions of horizontal OKN in pigeons comes from Mowrer (1936) who described an asymmetry in following of a stimulus presented monocularly; optokinetic pursuit was observed in the temporal to nasal direction but little optokinetic pursuit was observed in the nasal to temporal direction.

Gioanni et al. (1981) studied both the monocular and binocular elicitation of OKN in pigeons. They found, that during the presentation of the stimulus to one eye, OKN was asymmetrical with better following (higher gain) in the temporal to nasal direction. In a binocular stimulation situation, the OKN remained asymmetrical with better following for the temporal to the nasal direction for the stimulated eye.

Parallel evidence comes from a 2-DG metabolic mapping study demonstrating

that the pretectal LM in chicken accumulates label when a slow horizontal temporal to nasal moving stimulus is presented to the contralateral eye, but less label is found in the LM after nasal to temporal stimulation (McKenna and Wallman, 1981).

A lesion study in pigeons implicates the LM in the neural circuitry that generates horizontal OKN (Gioanni et al., 1983). Lesions of the LM eliminate OKN in the contralateral eye in the temporal to nasal direction and reduced the OKN in the nasal to temporal direction suggesting that the LM is essential for OKN in the temporal to nasal direction but also participates in OKN in the nasal to temporal direction. Unilateral lesions also produce an increase in OKN when the ipsilateral eye is stimulated in a temporal to nasal direction and a smaller increase in the nasal to temporal direction. These increases suggest some kind of inhibitory or disfacilitatory interaction between the LM on opposite sides of the brain.

#### Development of Horizontal OKN in Birds

Wallman and Velez (1985) investigated the development of the directional asymmetry in horizontal OKN in hatchlings and older chickens. They found substantial asymmetries between opposite directions of stimulus motion when the stimulus is presented to one eye. In hatchlings, the ability of the eye to follow in the temporal to nasal direction is better than in the nasal to temporal direction whereas in older birds this asymmetry increases due to the reduction in the ability of the eye to follow in the nasal to temporal direction. The authors suggest that the changes in OKN over the first weeks of life are related to corresponding changes in the anatomy of the horizontal OKN system, and in particular the development of the telencephalic input to the LM. Coupled with early descriptions of the OKN in decerebrate birds which suggest that the OKN response becomes somewhat more symmetrical than in normal birds (Visser and Rademaker, 1934), and the anatomical finding of a projection from the visual

telencephalon to the pretectum, it is plausible that the development of the telencephalic features of the OKN circuit may mediate these developmental changes. However, in contrast to the symmetrical OKN of frontal-eyed species, an asymmetrical adult form of horizontal OKN is exhibited by a great many lateral-eyed species. Wallman and Velez (1985) speculate that the influence from the visual forebrain to the pretectum may be similar to that found in frontal-eyed mammals, but inhibitory in nature resulting in an increase in the degree of asymmetry of OKN. Furthermore, this input may be responsible for the enhanced high velocity OKN responses of the older birds.

### Neurophysiology

Neurophysiological investigations of the pretectal region in mammals have implicated the NOT as a relay nucleus receiving retinal slip signals and then transmitting these signals to the neural circuitry mediating horizontal OKN. The characteristics of single unit recordings in the NOT of cats, rats and rabbits suggest that units within the NOT have a rather high spontaneous discharge rate and respond in a non-habituating manner to the movement of large random dot pattern or striped pattern stimuli in a directionally selective manner over a large range of velocities.

#### Response Properties of the NOT in Mammals

Neurophysiological recordings of units within the rabbit NOT suggest that the units typically maintain a discharge rate of 25-50 impulses per second and have large receptive fields (up to 40 by 150 degrees) in the visual streak of the contralateral eye. They are excited by motion in the temporal to nasal direction and inhibited by motion in the opposite (180 deg) direction. Most units are excited by temporal to nasal motion over a wide range of stimulus velocities (0.01-20 deg/sec), and are maximally stimulated at velocities below 1 deg/sec. A stimulus

area of 2 by 2 degrees is minimally effective in exciting NOT units with an increase in responsivity as the area of the stimulus increases. The conduction velocities measured in direction selective fibers in the NOT suggest that w-fibers make up the bulk of retinal inputs to the rabbit NOT (Collewijn, 1975). Similar evidence has been reported for the rat NOT. Rat NOT units are excited most frequently by slow moving (1 deg/sec) large field stimuli presented to the contralateral eye moving in a temporal to nasal direction (Cazin, 1980).

Neurophysiological studies of the cat NOT report similar characteristics for the units within this area. Units in the cat NOT, found lying within the scattered retinal terminal fields and not within dense retinal terminal clusters, were identified by their strong direction specific responses to slow horizontally drifting large field stimuli (Ballas and Hoffmann, 1985; Hoffmann and Schoppmann, 1981). With a spontaneous discharge rate of 30 impulses/sec, units in the NOT are maximally stimulated by large random dot patterns moving in a temporal to nasal direction and inhibited by nasal to temporal movement over a broad velocity range (0.1- 100 deg/sec), although stimulus velocities between 1-10 deg/sec are most effective. All cells are driven by the contralateral eye and unlike in the rabbit and rat, 50% are also driven by the ipsilateral eye. Receptive fields of these units were isolated within the visual streak of the retina, similar to rabbits. Taken together, units in the mammalian NOT have a high spontaneous discharge rate, respond in a non-habituating manner to the movement of a large random dot pattern or striped pattern stimuli, and are directionally selective. However, in the lateral-eyed mammals such as rats and rabbits, all units in the NOT are driven only by the contralateral eye. In contrast, in the frontal-eyed cat, 50% of the units in the NOT are also driven by the ipsilateral eye. The conduction velocities measured suggest that like those in rabbits, the direction selective cells in the cat NOT receive a direct input from retinal w-cells. In addition to the direction

selective units in the NOT, direction unselective neurons, sensitive to high stimulus velocities (jerk neurons), were also identified (Ballas and Hoffmann, 1985).

#### Response Properties of Retinal Ganglion Cells that Project to the NOT

The retinal input to the NOT has been studied in some detail in both rabbits and cats. Approximately one-quarter of the rabbit's retinal ganglion cells have been described as direction selective; that is the neurons respond maximally to movement in a preferred direction but do not respond to movement of the same stimulus in the opposite (null) direction. These direction selective cells can be divided into on-off and on-type subgroups (Barlow et al., 1964) that differ in the velocities to which they preferentially respond. Oyster and Barlow (1967) suggest that the output of the on-off units could be used as error signals in the optokinetic system. However, Oyster et al., (1972) measured the velocity preferences of both on-off and on-type units and found that the on-off cells scarcely responded to stimuli in the velocity range of less than 1 deg/sec which is most effective for eliciting nystagmus in rabbits. The on-type direction selective cell however, with receptive fields of about 3 deg in diameter, had a markedly different velocity response curve. These units were extremely sensitive to stimulus velocities of less than 1 deg/sec and did not respond in the optimum velocity range for the on-off units. Furthermore, there was little inhibition evidenced in null directions at the retinal level. This data suggests that retinal on-type direction selective cells represent the input stage of the optokinetic loop in the rabbit.

The fact that the NOT receptive fields are very large and the retinal direction selective units receptive fields are small, suggests that there is a heavy convergence of retinal inputs onto units in the NOT. The units within the NOT are excited by temporal to nasal motion and inhibited by nasal to temporal

motion. Moreover, many NOT units respond to a large range of stimulus velocities (0.01-20 deg/sec) in rabbits, and it has been suggested that both on and on-off retinal types converge on NOT units in the rabbit (Oyster et al., 1972).

Hoffmann and Stone (1985) studied the physiological properties of ganglion cells in the retina of the cat. All of the direction selective cells they recorded from were w-cell types with slow conducting axons. The majority of cells are on-center cells, as in the rabbit. However, there is some question as to whether the direction selectivity of NOT cells in the cat is fully determined in the retina. First, the direction selective ganglion cells recorded from are only a fraction of the total population of w-cells antidromically activated from the NOT. Second, not all of the preferred directions are strictly horizontal. Even so, these results do not entirely preclude the notion that direction selective on-center w-cells form a major retinal input to the NOT. Ganglion cells which prefer stimulus movement in the temporal to nasal direction might form the excitatory input and ganglion cells preferring nasal to temporal or non-horizontal movements could form the inhibitory input.

#### Response Properties of the Corticopretectal Projection

The elimination of horizontal OKN in the nasal to temporal direction after bilateral cortical ablation in cats suggests a role for the visual cortex in the optokinetic reflex. Schoppmann (1981) investigated the response properties of cortical cells activated antidromically from the NOT and found they were located in layer V of A 17 and 18. These units responded well to stimulation with large area random dot patterns moving across the visual field at velocities between 1 and 10 deg/sec. As compared with the NOT units, the cortical units were more sharply tuned for stimulus velocities, preferring faster movement. These findings suggest a strong convergent projection to the NOT from cortical units in A 17 and 18.

Subsequently, Schoppmann (1985) investigated the functional development of the corticopretectal pathway to the NOT. The electrical stimulation of units in A 17 and 18 evoked postsynaptic orthodromic activity in up to 18% of the cells in the NOT at four weeks of age increasing to 60% in adult cats. In the adults, successful stimulation depended on the retinotopic matching of stimulation and recording sites. In adult cats, a high incidence of direction and velocity tuning was seen in NOT cells driven by the cortex as opposed to cells not driven by the cortex. Cortex-driven NOT cells in cats and kittens received convergent retinal input mainly from w-fibers and have a higher incidence of directional bias and a preference for a restricted stimulus velocity range.

#### Response Properties of the LM in Birds

Lesion studies have suggested that the specific oculomotor function of the LM may be to relay neural signals of horizontal visual field motion to oculomotor circuits in which optokinetic pursuit movements are generated (Gioanni et al., 1983). In order to elucidate the role for the LM in mediating horizontal retinal slip signals, the response properties of single units within the pigeon LM have been examined (Winterson and Brauth, 1985). Single units in the pigeon LM have high rates of spontaneous activity and respond exclusively to visual stimulation of the contralateral eye. These units are direction and velocity selective responding preferentially to large stimuli with many visual contrasts. The preferred directions of LM units are largely oriented along the horizontal meridian although a large proportion of units preferred non-horizontal directions as well. Preferred velocities for LM units ranged from 0.2 deg/sec to 80 deg/sec. More than half of the pigeon LM units preferred high velocities (>10 deg/sec). Those LM units preferring low velocities almost exclusively preferred temporal to nasal movement and were found almost exclusively in the LMmc. The large receptive fields appeared retinotopically organized with units in the dorsal LM having

receptive fields in the temporal portion of the visual field and units in the ventral LM having receptive fields in the nasal visual field.

Using the 2-DG metabolic mapping technique, McKenna and Wallman (1985) studied the postnatal changes in the responsivity of the LM to horizontal retinal slip in chickens. Monocular stimulation with horizontal large field motion results in the labeling of the contralateral LM. In hatchlings visual motion in both temporal to nasal and nasal to temporal directions results in labeling of both the LMmc and the LMpc. In older birds temporal to nasal motion results in labeling of only the LMmc whereas nasal to temporal motion produces labeling in both the LMmc and LMpc. These results suggest that the LM continues to develop its response properties postnatally perhaps as a result of the postnatal development of a telencephalic projection.

### Neuroanatomy

Neuroanatomical studies of the connectivity of the NOT in mammals, are constrained by two factors. First, because the NOT is a diffuse aggregation of cells, it is difficult to define its precise boundaries and second, because these neurons are embedded in the fibers of the brachium of the superior colliculus, connectivity studies may be confounded by false-positive labeling problems as a result of the uptake of tracers by broken fibers in passage. Consequently, there are few studies which describe the neuroanatomical features and connectivity of this area in mammals and these need to be interpreted carefully.

### Topography of the NOT

Despite the difficulty in defining the precise boundaries of the NOT within the pretectum, certain topographical features of the NOT appear to be similar in the mammalian species studied. The NOT, in non-primate mammals such as rabbits (Kuhlenbeck and Miller, 1942), rats, mice, tree shrews, cats (Scalia, 1972;

Kaneseiki and Sprague, 1974; Berman, 1977) and primates such as squirrel monkeys and rhesus monkeys (Hutchins and Weber, 1985), occupies a similar position in the pretectum. The NOT lies at the dorsolateral border of the pretectal complex and extends along its full length. The rostral pole of the NOT is anterior to the superior colliculus but the bulk of the nucleus also extends along its lateral surface for some distance. The NOT is composed of darkly staining cells collected in small groups or interspersed individually between the fascicles of the superior collicular brachium. Its cells are large compared with those of other pretectal nuclei. In addition to the magnocellular aspect of the NOT there is a parvicellular portion which lies medial to the large-celled subdivision, extending not quite as rostrally as the latter, but further caudally. It consists of rather densely packed small and medium size cells (Kuhlenbeck and Miller, 1942).

Further cytological information about the NOT is limited to a single Golgi study of the NOT in rats (Gregory, 1985) which suggests that there are three types of neurons within the NOT. The first, the horizontal cell, is usually found within the superficial part of the brachium of the superior colliculus and has a fusiform cell body with one or two primary dendrites arising from each end of the soma. These dendrites radiate in a transverse direction parallel to the surface of the brachium. The primary dendrites usually branch close to the cell body before extending for some 300-400  $\mu\text{m}$ . Additional branching may occur more distally. The second type of neuron within the NOT is the large multipolar NOT cell which has a large to medium size soma. These cells probably account for the large cell bodies seen in Nissl stained sections of the NOT and are usually found in the more ventral part of the NOT within its central region. In the transverse plane these large multipolar NOT cells have a more dispersed dendritic arborization pattern with more dendritic appendages and spines than the horizontal cells. Their dendrites extend out in a transverse plane predominantly

parallel to the long axis of the NOT. The third kind of cell in the NOT is the medium and small multipolar cell. These cells have considerable variation in their dendritic architecture and were not classified along this criterion.

#### Connectivity of the NOT

There are several anatomical studies describing the afferent connectivity of the NOT in mammals. However, most of these studies are of the anterograde tract tracing variety, which describe the pattern of terminations of the afferent inputs within the NOT, but do not characterize the source of that input. These studies have identified three major inputs into the LM, the retina, the visual cortex and the medial terminal nucleus (MTN) of the accessory optic system (AOS). Similarly, there are few studies describing the efferent connectivity of the NOT in mammals. These studies describe the efferent projection targets in several mammalian species but lack a description of the projection neurons within the NOT that project to these targets.

#### Synaptic Organization

There is little information available regarding the synaptic organization of the NOT in mammals. However, in cats, two preliminary studies have suggested that there are several types of terminals in the NOT, including retinal and cortical terminals. In one study, the NOT was examined after intravitreal injections of HRP and tritiated amino acids. Most of the terminal labeling was found in large axon terminals containing round synaptic vesicles and a pale mitochondrian matrix which terminated on presynaptic dendrites. Similar large axon terminals with round synaptic vesicles and pale mitochondria were previously reported in the dorsal lateral geniculate nucleus and the superficial gray of the superior colliculus and considered to be axon terminals of optic fibers (Nakamura, 1981).

In a preliminary study of the cat NOT, the ultrastructure of retinal or visual

cortical terminals in the NOT, studied either by anterograde degeneration or by anterograde HRP histochemistry, was classified. In all cases retinal terminals in the NOT were classified as RLP profiles (round and large synaptic vesicles, pale mitochondria) in contact with single medium to large dendrites. Visual cortical terminals are of two types, RSD (round, small, densely packed vesicles) and RLD (round, large and densely packed vesicles) profiles. Labeled RSD and RLD profiles typically are found in contact with dendrites of small to medium diameter while RLD profiles are found presynaptic along various regions of dendrites. Both retinal and visual cortical inputs appear to terminate in clusters. In combined Wallerian degeneration and anterograde HRP preparations, it appears that axons from both retinal and cortical neurons do indeed synapse on single NOT cells (Hutchins and Weber, 1986).

A study of the ultrastructure of the NOT in rats describes four types of presynaptic terminals on neurons in the NOT. The R-terminals have round vesicles, electronlucent mitochondria and asymmetric contact zones; the F-terminals have flattened vesicles, opaque mitochondria and symmetric contact zones. The RLD-terminals have spherical vesicles and electron-dense mitochondria and asymmetric contact zones whereas the P-terminals have pleiomorphic vesicles and electron-lucent or opaque mitochondria and asymmetric synaptic thickenings. These different types of terminals are found in the neuropil or in clusters of synapses (Cardozo and Van Der Vant, 1987).

## Afferent Projections to the NOT

### Retinal Projection

Early degeneration studies in which the eye was enucleated (cat: Laties and Sprague, 1966) or the retina lesioned (rat, mouse, rabbit, tree shrew: Scalia, 1972) suggest an exclusively contralateral retinal projection to the NOT. The results of these degeneration studies have been verified by studies using anterograde

autoradiographic tract tracing techniques. In cats, after intraocular injections of labeled amino acids, labeled fibers enter the contralateral NOT via the brachium of the superior colliculus. In the contralateral NOT, label is confined to two or three finger like strips, elongated in the dorsolateral and ventromedial dimensions. These strips are 150-200  $\mu\text{m}$  wide and are separated by unlabeled regions 400-600  $\mu\text{m}$  wide. These strips form two oblique slabs oriented from posterolateral to anteromedial. The labeling tends to be confined to the vicinity of the large, densely stained cells of the NOT. Furthermore, in contrast to the degeneration studies, label is also found in the ipsilateral NOT in the form of oblique strips though they are less dense than those on the contralateral side (Berman, 1977). The retinal projection to both the ipsilateral and contralateral NOT has been verified by a degeneration study (Kanesecki and Sprague, 1974) and by an autoradiography study (Koontz et al., 1985) in cats.

The retinal projection to the NOT has also been reported in primates. Hutchins and Weber (1985) report that after injections of labeled amino acids a dense aggregation of silver grains is observed over the dorsal regions of the contralateral NOT with the label becoming less dense over the ventral and lateral regions. The amount of ipsilaterally transported label, although present, is significantly less when compared with the contralateral side. The label in the ipsilateral NOT is confined to the more dorsal aspect of the nucleus in primates.

The presence of the ipsilateral pathway is apparently related to the degree of telencephalization of vision and to the position of the eyes in the skull. On the one hand, in lissencephalic mammals with laterally placed eyes, where there is little binocular overlap, (mice, rats, rabbits, and hamsters) the retinal input to the NOT is almost exclusively contralateral (Scalia and Arango, 1972; 1979). On the other hand, in animals where large amounts of the neocortex are devoted to vision, the eyes are frontally placed and there is a large degree of binocularity

(cats and primates), an ipsilateral retinal pathway to the NOT is present in varying degrees (Latic and Sprague, 1966; Garcy and Powell, 1968; Kaneseki and Sprague, 1974; Berman, 1977; Hutchins and Weber, 1985).

Scalia and Arango (1972; 1979) suggest that the retinal projection to the pretectal nuclei in rats is retinotopically organized. Each of the three retinorecipient pretectal nuclei receives a different map. The inferior peripheral retina is represented in the rostral pole of the NOT (anteromedially); the superior peripheral retina is mapped in the caudal end of the NOT (posterolaterally). The nasal retina is represented in ventral NOT and the temporal retina is represented in dorsal NOT. A similar topographical retinal projection has been reported in the cat. In a study of the retinal representation within the pretectum, it was found that, in the cat as in the rat, the inferior to superior retinal axis maps along the long axis of the pretectal complex from rostromedial to caudolateral. The manner in which the temporal to nasal retinal axis maps onto the pretectal complex was not described (Koontz, 1985).

Attempts to describe the retinotopic organization in the primate pretectum have yielded limited information. Upper and lower retinal quadrant lesions in the tree shrew result in terminal degeneration within the rostral and caudal pretectum respectively. These findings agree with the rat data (Scalia and Arango, 1979) only so far as the superior and inferior retinal projection is concerned. Lesions placed in the temporal and nasal quadrants produced only minimal separation of terminal fields of label within the complex (Hutchins and Weber, 1985).

Few studies are available regarding the morphology of the retinal ganglion cells that project to the NOT, or their distribution in the retina. In a study by Ballas et al. (1981), HRP was iontophoretically injected into the NOT and the retina wholemounted after NOT units were identified on the basis of their

characteristic responses to visual stimulation and their antidromic activation by electrical stimulation from the inferior olive. The results suggest that, with the exception of a few labeled alpha cells (large cell bodies with a diameter of about 30  $\mu\text{m}$ , very thick axons and 5-6 large dendrites), most retinal ganglion cells projecting to the NOT were identified as gamma cells due to their small cell bodies and thin long dendrites. These labeled cells are found primarily along a horizontal band approximating the visual streak on the retina. The input to the NOT from the contralateral retina is 10 times more numerous than the ipsilateral one with the highest concentration of labeled cells found near the area centralis in both retinas.

#### Non-retinal Afferent Projections to the NOT

In addition to the retinal projection, the NOT in mammals receives a projection from the visual cortex. In rats, after focal lesions of the visual cortex, degenerating terminal fibers have been reported in the pretectal area including the lateral and medial divisions of the NOT. Similarly, in the cat, various investigations have documented a projection from the visual cortex to the NOT. After small lesions of the visual cortical areas A 17, 18, 19, in adult cats, degenerating fibers have been found in the brachium of the superior colliculus entering the pretectum with degenerating terminals in the NOT (Kawamura et al., 1974). Another study of the corticofugal projections to the pretectum with discrete injections of tritiated amino acids into A 17, 18, 19 in the cat visual cortex suggests that there is a sparse projection from all three cortical areas to the NOT (Updyke, 1977). This projection is reported to originate from layer V complex cells in primary and secondary visual areas (Hollander et al., 1974).

To explore the possibility of postnatal developmental changes, the corticopretectal projection was studied in cats from 1-13 weeks old (Schoppmann, 1985b). Large injections of HRP into areas 17 and 18 result in terminal labeling

in the ipsilateral NOT but only after the fourth week of life. However, it may be erroneous to conclude that the time of the initial appearance of terminal label reflects the actual birth of corticopretectal contacts. The labeling of this cortical input appears more diffusely distributed throughout the NOT than the retinal input. Most pretectal neurons receive converging retinal and cortical input, and the termination patterns of the retinal and cortical afferents probably reflects differential spatial distribution of synaptic contacts at the dendritic trees and or somata of recipient cells. Although the Schoppmann study replicates the earlier findings of Kawamura et al.,(1974) and of Updyke (1977), there is some controversy as to whether the corticopretectal projection is fully developed at birth. Two studies in cats suggest that the corticopretectal projection is present at birth in kittens (Tsumoto, et al., 1983; Stein and Edwards, 1979). The disparity in the results of these two studies may be a result of the techniques employed.

A direct projection from the visual cortex to the NOT of rabbits has also been reported. After lesions of primary visual cortex, degenerating terminals were seen in the albino rabbit NOT (Giolli and Guthrie, 1971). A subsequent autoradiographic study of the projections of the visual cortex in the albino rabbit by the same authors however, did not demonstrate a projection to the NOT (Giolli et al., 1978). However, another autoradiographic study of subcortical projections of the visual cortex in pigmented rabbits suggests that the NOT does indeed receive a projection from the visual cortex (Hollaender et al., 1979). This disparity in the results is not easily reconciled. Although there are no discrete boundaries among pretectal nuclei, it seems unlikely that a different criterion was applied in the identification of these nuclei by the same authors in different studies of the albino rabbit. It seems more likely, however, in light of the evidence that there indeed does exist a projection from the striate cortex in rabbits to the NOT. The lack of a projection from the albino rabbit visual cortex to the NOT after amino

acid injections may be due to the incomplete sampling by injection of the entire VI area.

The studies mentioned above provide evidence for a projection from the primary visual cortex to the NOT in rats, rabbits and cats. Although the study by Giolli et al., (1978) failed to demonstrate terminals in the NOT, the demonstration of degenerating terminals in the NOT after cortical lesions in albino rabbits and an autoradiographic confirmation of this projection in pigmented rabbits provide strong support for the existence of this projection in most rabbits. Thus, the bulk of the evidence indicates that there indeed is a projection from primary visual cortex to the NOT of the pretectum in mammals.

There is little evidence available regarding other sources of afferent projections to the NOT. In mammals, a nucleus of the AOS have been reported to project to the NOT. In rabbits and rats, this projection is dense, originating from the medial terminal nucleus (MTN) (Yamamoto, 1979.)

#### Efferent Projections of the NOT

The studies of the efferent connections of the NOT in mammals must be interpreted cautiously in light of the nebulous boundaries of pretectal nuclear masses and the fiber tracts passing through the area. Degeneration (Itoh, 1977) and autoradiography (Graybiel, 1974) studies of the NOT efferents in cats usually include not only the NOT but also other neighboring pretectal nuclei. In these studies the pretectal area including the NOT is shown to project to the ipsilateral dorsal lateral geniculate nucleus, ventral lateral geniculate nucleus, pulvinar, zona incerta, thalamic reticular nucleus, Field H of Forel, MTN, superior colliculus, mesencephalic reticular formation, interstitial nucleus of Cajal, nucleus of Darkschewitsch, and the dorsal cap of the inferior olive. The autoradiography study differs from the degeneration study in a number of ways. It suggests an ipsilateral projection to the nucleus of the reticular tegmentum of the pons while

the degeneration study suggests a termination in the pontine nuclei. In addition, the autoradiography study suggests a contralateral projection to the anterior pretectal nucleus and the interstitial nucleus of Cajal as well as fibers in the posterior commissure. In a study in which small injections were more or less confined to single nuclei of the pretectum, Berman (1977) reported that the NOT in cats projects to the ipsilateral pulvinar, dorsal medial geniculate (MGd), labels fibers in the posterior commissure and projects to the contralateral NOT and nucleus of the posterior commissure.

A study of the efferent projections of the rat NOT implicates many targets which are similar to those in the cat (Terasawa et al., 1975). After lesions of the rat NOT, labeling was found in the ventral lateral geniculate nucleus, pulvinar, zona incerta, superior colliculus, pontine nuclei, nucleus of the reticular tegmentum of the pons, the inferior olive, fibers in the posterior commissure, contralateral NOT, and dorsal terminal nucleus (DTN) of the AOS. The results differ from those in cats in that no direct ipsilateral projection to the MTN of the AOS was reported, and in that the investigation of rat NOT did not demonstrate terminal labeling in several nuclei that are reported to be efferent targets of the pretectum in cats. The differences between these studies may be related to the larger lesions or injections in the cat studies that included other neighboring pretectal structures along with the NOT. On the other hand, these differences may be species-specific. A study of the efferent projections of the NOT in the tree shrew suggests that the NOT projects to targets similar to those in rats and cats including, the ventral lateral geniculate, zona incerta, reticular nucleus of the thalamus, nucleus of the posterior commissure (also contralaterally), MTN of the AOS, superior colliculus, mesencephalic reticular formation, nucleus of Darkschewitsch, pontine nuclei, inferior olive and, unique to the tree shrew, contralaterally to Nucleus VI (Weber and Harting, 1980).

A study of the efferent projections of the rabbit NOT suggests similarities and differences in the efferent targets of the NOT in rabbits, cats, rats, and tree shrews. Similar to the cat and rat, the rabbit NOT projects to the lateral dorsal nucleus, the dorsal lateral geniculate nucleus, the ventral lateral geniculate nucleus, pulvinar, reticular nucleus of the thalamus, anterior pretectal nucleus, contralateral NOT, MTN, superior colliculus, mesencephalic reticular formation, pontine nuclei, and the inferior olive. Other targets of rabbit NOT efferent projections include Nucleus Z, MGd/posterior complex, the pretectal olivary nucleus, posterior pretectal nucleus, contralateral DTN (found only in rat), parabigeminal nucleus, medullary reticular formation, Nucleus VI, Nucleus VII (also contralateral), prepositus hypoglossi nucleus, and the lateral reticular nucleus (Holstege and Collewijn, 1982). These latter efferent targets have not been confirmed by retrograde labeling and indeed may be artifactual or may represent species-specific differences between rabbits and other mammals.

#### Anatomy of the LM in Birds

The results of anatomical studies of the pretectal nuclei in birds are confounded by a few or all of the following problems; the lack of definition of nuclear groups within the pretectal area, the lack of drawings identifying the course of projections afferent and efferent to this area and no consistent nomenclature for the ill-defined nuclear groups within the pretectum. Particularly confusing is the use of similar names for different nuclear masses.

#### Topography of the LM

The suggestion has been made that the LM is homologous to the NOT of mammals on the basis of its similar embryological derivation and its position in the pretectum (Kuhlenbeck, 1942). The common embryological derivation of the LM in birds and the NOT in mammals from the mesencephalic tectal plate

provides the most basic structural evidence for the homology of the avian LM to the mammalian NOT. Furthermore, the position of the LM within the pretectum as described by Kuhlenbeck (1939) is similar to that described for the NOT by Kuhlenbeck and Miller (1942). According to this study (Kuhlenbeck, 1939), the magnocellular portion of the LM (LMmc) forms the most rostral and dorsal part of the mesencephalic lentiform group located in the angle between the dorsal and ventral rami of the optic tract. Its cells are larger and stain darker than other cells in the pretectum. It receives fibers from the optic tract and has fiber connections with the tectum and other pretectal nuclei. Internuclear fibers connect it with the laterally positioned parvicellular portion of the LM, the LMpc. The LMpc is an extensive part of the lentiform nucleus consisting of irregularly scattered small and medium size cells. This cell mass has connections with the ventral tecto-thalamic tract and direct short connections with the tectum and other pretectal nuclei.

The topographical and cytological features of the LMmc in chickens have been described by Gottlieb and McKenna (1986). In coronal sections, the LMmc in its most rostral aspect appears as a crescent shaped structure embedded in the optic tract; it is concaved medially and contains darkly stained large neurons. In its rostral aspect, the LMmc is located medial to the most rostral tip of the optic tectum and lateral to the superficial synencephalic nucleus (SS). In more caudal sections, the LMmc lengthens dorsoventrally extending between the optic tract on both dorsal and ventral surfaces of the midbrain, narrowing in its mediolateral aspect. At the ventral aspect of this nucleus, large cells are seen extending into the optic tract; this clump of cells is seen extending caudally to the level of the lateral nucleus of the basal optic root (nBOR1).

The LMmc is reported to contain both large and small neurons. These neurons are separated from one another by myelinated fibers running between and around

the cells. The cytological features of large neurons include a smooth contoured cytoplasmic membrane and an eccentrically located nucleus. The cytoplasm contains large clumps of rough endoplasmic reticulum (RER). The shape of the large neurons varies from round to elongated. The small neurons, similar to the large, have an eccentrically located ovoid nucleus but unlike the large neurons, do not contain clumps of RER (Gottlieb and McKenna, 1986). No such description is presently available for the LMpc.

It is the unique topography of the LM that distinguishes it from its pretectal neighbors. The commonly used atlas of the avian brain by Karten and Hodos (1967) employs to some degree the nomenclature proposed by Kuhlenbeck (1939) in defining the pretectal region of birds. However, much like the other available atlases of the avian brain (which utilize a different nomenclature) (Huber and Crosby, 1929; van Tienhoven and Juhasz, 1960) they lack a precise definition of the various nuclear groups within this region. Although more recent investigations of primary visual centers in the pretectum of birds (Reperant, 1973; Ehrlich and Mark 1984a; Gamlin and Cohen, 1988a) provide relatively precise schematic illustrations, they in turn lack a consistent nomenclature applied to nuclei in this area. Most frequently, the LM is defined as consisting of two subdivisions, by Kuhlenbeck (1939) and Gottlieb and McKenna (1986), but is designated as two different nuclei by other authors. Both Huber and Crosby (1929) and Ehrlich and Mark (1984a) designate the LMmc as the nucleus externus (NE) and the LMpc as the tectal grey (GT). An alternative nomenclature utilized by Reperant (1973) is the superficial synencephalic nucleus (SS) for the LMmc and the nucleus griseum tectalis (GT) for the LMpc. This area should not be confused with the area of medium size cells medial to the LM and lateral to the nucleus rotundus designated as the SS by Ehrlich and Mark, (1984), Huber and Crosby, (1927) and Gottlieb and McKenna (1986) (for a complete review of

alternative nomenclatures for the pretectal nuclei see Ehrlich and Mark, 1984a).

Gamlin and Cohen (1988a) choose to name the LMmc of Kuhlenbeck (1939) and Gottlieb and McKenna (1986), the LM lateralis, the SS of these authors the LM medialis, and the LMpc, the griseum tectalis. This latter terminology for the LMpc is that of Reperant, (1973) and Ehrlich and Mark (1984a). The 2-DG metabolic mapping study of McKenna and Wallman (1981) confirms the definition of two subdivisions within a single LM nucleus and follows the nomenclature used by Kuhlenbeck (1939). The accumulation of 2-DG metabolic marker in response to horizontal large field motion in both subdivisions of the LM lends further support for this definition. Moreover, the labeling of the LMmc and not the LMpc in response to temporal to nasal large-field motion suggests that the LM region is indeed one nucleus with two functional subdivisions.

#### Connectivity of the LM

There are a few anatomical studies that describe sources of afferents to the LM of birds. These studies have identified three major inputs to the avian LM, from the retina, visual telencephalon, and the nBOR of the AOS. However, these studies use anterograde labeling to describe the pattern of terminations rather than characterizing the source of that input. Furthermore, as a consequence of the poor definition of the pretectal nuclei in birds, there is only one study of the efferent projections of the LM in pigeons which itself is confounded by an altogether new nomenclature and different definition of the LM region.

#### Synaptic Organization

Ultrastructural evidence suggests that two types of axosomatic profiles and three types of axodendritic profiles are present in the LM. Both large and small neurons in the LMmc have axosomatic synapses with the larger neurons having a somewhat greater number. Presynaptic profiles were classified into two categories

based on the presence of round (type R) or flat (type F) vesicles. Type R presynaptic profiles contain round vesicles, 55-60 nm in diameter, relatively large mitochondria, and form asymmetrical synapses. The Type F presynaptic profiles contain mostly flat synaptic vesicles 25-30 by 60 nm and account for 80% of all presynaptic profiles forming axosomatic synapses. The Type F profile usually contains relatively few, small mitochondria and form symmetrical synaptic contacts with the cell soma (Gottlieb and McKenna, 1986).

In addition, two types of axodendritic profiles and a third dendrodendritic profile were classified. The Type R axodendritic profile is largest and most numerous (about 67%). It contains large, round synaptic vesicles and often synapses on several dendritic profiles. The Type F axodendritic profile contains flat vesicles and accounts for about 32% of all axodendritic synapses examined. The third type of presynaptic profile encountered only occasionally is reported to be dendrodendritic with a small number of pleiomorphic vesicles. The five different types of axonal terminals, two types of axosomatic profiles, two axodendritic and one dendrodendritic profiles may represent different sources of afferent input into the LM of chickens (Gottlieb and McKenna, 1986).

#### Retinal Projection to the LM

The termination of retinal axons within the LM in birds has been reported by various investigators. Although the nomenclatures differ as mentioned above Cowan et al. (1961), Reperant (1973), Ehrlich and Mark (1984a), Gamlin and Cohen (1988a), and Gottlieb and McKenna (1986) all reported that there is a predominantly contralateral projection from the retina to the LM as well as other pretectal structures. Both Cowan et al. (1961) (pigeons) and Ehrlich and Mark (1984a) (chickens) reported that degeneration and autoradiography studies revealed a strong retinal terminal field within the NE and GT. Similarly, Reperant (1973), reports a similar strong contralateral retinal projection to the SS

(corresponding to the LM region). Gottlieb and McKenna (1986) reports that the LMmc receives a relatively dense retinal input as compared with the LMpc. Both LMmc and LMpc receive their retinal afferents primarily from the contralateral eye although there is an additional sparse ipsilateral projection from the retina to this nucleus. However, all of these above-mentioned studies are of the anterograde variety and provide no information concerning the source of the retinal input, a description of the projection neurons nor their distribution.

Both Ehrlich and Mark (1984b) (chickens) and Gamlin and Cohen (1988a) (pigeons) report a topographical organization of the retinal projection to the LM region. Comparisons of the results from these studies are extremely difficult due to the differences in the identification of the nucleus, in the nomenclatures used and in the interpretation of the results. Both of these studies, one using small laser lesions (Ehrlich and Mark, 1984b) and the other using small injections of tritiated amino acids (Gamlin and Cohen, 1984a) demonstrate that the superior retina projects to the ventral LM and the inferior retina to the dorsal LM. The projections from the temporal and nasal portions of the retina have not been mapped convincingly in either of these studies as they do not sample large portions of the retina including the superior nasal quadrant.

#### Nonretinal Afferent Projections to the LM

Studies describing the telencephalic input to the LM region have utilized various avian species including pigeons, chickens, ravens, African lovebirds, owls, and herring gulls. Adamo (1967) in a degeneration study of the visual telencephalon or Wulst in chicken, lovebirds and ravens, describes an efferent projection from the Wulst to the pretectal area. However, no clear schematic drawings are provided nor is there any definition of nuclear groups within the pretectal area on the drawings provided. Karten et al., (1973), in a degeneration study of the owl and pigeon visual telencephalon also described an efferent

projection to the pretectal nuclei but do not define nor schematically represent the specific nuclei within the pretectum which receive this projection. Miceli et al. (1978; 1985), in an autoradiography study of the pigeon, chicken, herring gull visual telencephalon, described in far greater detail the efferent projections of the Wulst to the pretectum. However, the authors adopted a specific nomenclature without providing detailed schematic drawings for this poorly defined area and as a result definitive comparisons of the telencephalic projection to the LM among these species cannot be made. Furthermore, all of the above studies simply reported the existence of terminals from the visual telencephalon within the LM without defining the morphology of the projection neurons, their distribution within the visual Wulst or the topography of this projection to the LM.

The LM in birds is also reported to receive and afferent input from the nBOR of the AOS. Brecha et al. (1980) in an autoradiography study of the nBOR, report that after injections of the nBOR ipsilateral terminal labeling is found within the LM in pigeons. A unilateral injection of HRP that included the LM retrogradely labels medium and large cells in all three subdivisions of the nBOR (Brecha et al., 1980).

#### Efferent Projections of the LM

The only available study of the efferent projections of the pretectal nuclei in birds is that of Gamlin and Cohen (1988b). However, the interpretation of this study in pigeons is confounded by an altogether different nomenclature proposed for pretectal nuclei and by a different definition of the LM region. Furthermore, only one injection into the LM region is illustrated. However, if the LM of Gamlin and Cohen (1988b) at least in part coincides with the LM<sub>mc</sub> as defined by Kuhlenbeck (1939) and Gottlieb and McKenna (1986), the LM region has predominantly descending projections to the inferior olive, the cerebellum, parts of the lateral pontine nucleus, the nucleus papilliformis, the nucleus of the basal

optic root, pars dorsalis, the nucleus mesencephalicus profundus, pars ventralis, the nucleus principalis precommissuralis, and the stratum cellulare externum. The LM may project to the optic tectum and the medial pontine nucleus. Attempts to verify these apparent efferent projections of the LM using retrograde techniques were conducted only for the cerebellum, ventromedial pons, and the inferior olive. These results suggest that a separate population of cells in the LM region were labeled after these injections. Thus, large cells in the LM project to the cerebellum, small cells project to the inferior olive, and medium cells within the LM project to the medial pontine nucleus. These results, however, must be interpreted carefully in light of the identification of the LM offered by these authors (Gamlin and Cohen, 1988b).

Additional evidence for some of the efferent targets of the LM region comes from HRP studies of the inferior olive, lateral pontine and tectum. The retrograde filling of cells within the LM region after injections into these targets suggests that the LM projects to the ipsilateral optic tectum (Brecha, 1978), the lateral pontine nucleus and the cerebellum (Clarke, 1977), and the inferior olive (Brauth and Karten, 1977).

## Chapter 3: METHODS

### Subjects

White Leghorn chickens (*Gallus gallus domesticus*) of both sexes were used in this study. All of the subjects were hatched, raised and housed in our laboratory under standard conditions. Five to six week old chickens were used in the histological study of the pretectal nuclei and the tract tracing portions of the study, whereas both hatchlings and six week old chickens were used in the developmental portion of the study. For the metabolic mapping study, two to three week old chickens were used in the metabolic mapping study.

Subjects used in the tract tracing experiments were administered 0.5 cc of 0.685% Atropine and anesthetized with 20mg/100g of Ketaset (Bristol Laboratories) and 12mg/100g of chloral hydrate solution (Fort Dodge Laboratories) and placed in a modified pigeon holder on a Kopf stereotaxic frame. The beakbar was adjusted so that a line between it and the earbars formed an angle of 25° with the horizontal axis of the stereotaxic frame, approximating the position of the head in a free-standing chicken (personal observation). The adopted coordinates of the areas studied were determined in preliminary lesion experiments. After the individual injections were completed the injection micropipette or syringe was removed, the hole through the skull was cleaned, packed with Gelfoam, and the skin sutured.

### Histological Study

To study the LM and its neighboring nuclei at the light microscopic level, animals were anesthetized with sodium pentobarbital (60mg/kg IM) and perfused intracardially with a 0.75% saline solution followed by 10% buffered formalin followed by a 10% sucrose in 10% buffered formalin wash. After fixation, the animals were decapitated and the brains excised and postfixated in a 20% sucrose

formalin solution for seven days. Following postfixation, the brains were either embedded in paraffin, sectioned at 10  $\mu\text{m}$  thick in the coronal, sagittal or horizontal planes and stained following a standard Klüver-Barrera staining protocol, or tissue was frozen and sectioned in a coronal plane at 25  $\mu\text{m}$  and stained for Nissl substance using a standard cresyl violet staining protocol.

#### Horseshoe Peroxidase (HRP) Experiments

To study the retinal afferents to the LM, intracocular injections of 1-10  $\mu\text{l}$  of 1% HRP-WGA (Sigma) or 0.1-0.5  $\mu\text{l}$  of 1% BHRP (List Biological) were made in either eye with a Hamilton syringe. For intracranial injections, either pressure injections of 0.1-0.5  $\mu\text{l}$  of 20-30% HRP (Boehringer Mannheim Grad 1) with a Hamilton syringe or iontophoretic injections with a glass micropipette, 10-40  $\mu\text{m}$  in diameter at the tip, filled with 20-40% HRP (Boehringer Mannheim Grad 1) in .05M Tris-HCl buffer, pH 8.0, were made through a hole in the skull 3 mm wide, drilled over the desired region of the brain. For iontophoretic injections, a positive DC current of 1.5  $\mu\text{A}$  was applied on an alternating cycle (7 seconds on, 7 seconds off) for 45 to 75 minutes. In all cases, a continuous negative current of 0.15  $\mu\text{A}$  was passed during the removal of the micropipette to prevent passive leakage of HRP.

Following survival times of 22-66 hours, the subjects were anesthetized, with 65 mg/kg of Nembutal, then perfused intracardially with 0.75% saline solution followed by a mixture of 1% paraformaldehyde and 1.25% glutaraldehyde in 0.1M phosphate buffer, pH 7.4 rinsed with a 10% sucrose in 0.1M phosphate buffer, pH 7.4 solution at 4° C.. Brain tissue was then sectioned at 40  $\mu\text{m}$  in the coronal plane and the sections collected in 0.1M phosphate buffer and processed for HRP histochemistry.

To visualize the injected HRP, two different chromogens were used. Use of the benzidine dihydrochloride (BDH) chromogen resulted in clear visualization of

the center of the injection site. For this procedure, serial sections that included the LM were preincubated in a BDIH, acetate buffer and sodium nitroprusside solution for 25 minutes (Mesulam, 1976). After stabilization, the sections were rinsed in water, mounted, air dried, and counterstained with 1% neutral red for Nissl substance. Injection sites were marked on drawings of coronal sections through the pretectum and subsequently photographed.

Because of its high sensitivity, the tetramethyl benzidine (TMB) chromogen was used to visualize the retrogradely labeled ganglion cell bodies and anterogradely projecting fibers and terminals (Mesulam, 1978). Brain tissue sectioned at 40  $\mu\text{m}$  was preincubated in a TMB and sodium nitroprusside solution for 20 minutes and then incubated in a similar fresh solution with hydrogen peroxide for 20 minutes. Afterwards, the reaction product was stabilized by rinsing in an acetate buffer solution. Tissue was then mounted on gelatinized slides, dried and alternating sections counterstained with 1% neutral red.

To identify HRP-labeled retinal ganglion cells, retinas in eyecups were preincubated in a TMB and sodium nitroprusside solution for 40 minutes and then incubated in a similar fresh solution with hydrogen peroxide for 40 minutes; the reaction product was stabilized by rinsing the tissue in an acetate buffer solution. After stabilization, the eyecups with the retinas were embedded in albumin-gelatin blocks and fixed in formalin vapors for 2-3 days.

The proper orientation of the chick retina was crucial to the assignment of ganglion cells in the retinal quadrants. The orientation of the major landmark in the chick retina, the pecten, was determined in two birds in the following manner. The head of the perfused subject was placed into the stereotaxic apparatus with the beakbar adjusted as previously described and the outer portion of the eye removed thus exposing the retina. At this head orientation, the pecten was found in the temporal inferior retina at a 78° angle from a horizontal line

drawn at its base. Every effort was made to position the retinas in the albumin-gelatin blocks at this angle. The eyecups were then sectioned in a transverse plane from inferior to superior at  $40\ \mu\text{m}$ ; every fourth section was mounted on gelatinized slides air dried and subsequently counterstained with 1% neutral red.

To reconstruct the retinas all sections were projected and drawn at a magnification of 17.5x. HRP labeled cells, which were identified in the light microscope, were marked in their appropriate positions on the drawing of the individual sections. Next, the length of each section, the positions of each conspicuous group of labeled cells and of the pecten relative to the midpoint of each section were measured using a digitalizing tablet coupled with a computer programmed with the appropriate software algorithm. With these measurements the retinas were reconstructed according to the equidistant polar projection of Galifret (1968). This method, which assumes that the retina is a hemispherical shell, involves projecting the retina onto a plane tangent to the polar end of the hemisphere; the height of the center of the projection is chosen such that the projections of two equal arcs on the retina are equal on the tangent plane. Those reconstructed retinas in which the alignment of the pecten deviated from the  $78^\circ$  angle established previously, were rotated along a central axis until they were properly oriented. To determine whether the regional distribution of the total ganglion cell population in the reconstructed retinas resembled that of a whole mount of a chick retina reported by Ehrlich (1981), a retina from an uninjected animal was reconstructed as described above, and the total population of ganglion cells estimated by counting retinal ganglion cells at  $100\ \mu\text{m}$  intervals and marking them on the drawings. A close agreement was found between the distribution of the retinal ganglion cells in the reconstructed and in the wholemount retinas.

A total of 304 ganglion cell somata were drawn at a magnification of 1890x

with a Zeiss microscope equipped with a drawing tube. Only those neurons whose somata appeared completely filled with HRP reaction product were drawn. The areas of the cells were measured with the aid of a computer interfaced with a digitizing pad. A chi-square test was performed in order to determine whether more than one population of retinal ganglion cells could be identified based on cell size. Next, the long and short axes of each cell body were measured from the drawings and the ratios were calculated. To determine whether there was a correlation between these ratios and the size of the cell bodies, a scatter diagram was constructed and the correlation coefficient was calculated.

To analyze the results of the other retrograde and anterograde tracing experiments, brain sections were magnified on an Aus Jena projector at 17.5x and drawn. For the retrograde experiments, HRP-labeled neurons were identified and drawn at a magnification of 1890x on a Zeiss microscope equipped with a drawing tube and marked in their appropriate positions on the individual drawings. Only those neurons whose somata appeared filled with HRP reaction product were drawn. The long and short axes of these neurons were measured with an eyepiece reticule; these neurons were then classified according to the size of their longest axis. Some of these neurons were photographed.

For the anterograde experiments, HRP-labeled fibers and terminals were identified in both stained and unstained sections, with both light and dark-field microscopy, and drawn in their appropriate position on the brain section drawings. The criteria for determining terminal labeling within structures included both the finding of fibers entering these areas and the appearance of terminal labeling. Examples of HRP-labeled terminals in the various efferent target areas of the LM were photographed.

#### Metabolic Mapping Study

For the metabolic mapping study of the retinal projection to the LM, selected

portions of the retina were visually stimulated by first covering the eyes with hemi-occluders that allowed vision in only half of the retina, and then placing the animals in an optokinetic drum that rotated on a vertical axis. Since the eyes move in response to this visual stimulus, resulting in the exposure of larger areas of the retina than the occluded portion, the eyes were immobilized with an adhesive. For this procedure, animals were anesthetized with halothane and a small incision was made in the skin and conjunctiva above the eye, close to the upper border of the orbit, exposing the posterior part of the eyeball. The eye was displaced slightly and a drop of Histoacryl surgical adhesive (Braun Meslungen) placed at the back of the eye to adhere the eye to the orbit. Repeated observations of the eyes during stimulation in an optokinetic drum indicated that the procedure resulted in minimal eye movements. After recovery from the anesthesia, both eyes were covered with translucent hemi-occluders that exposed only the superior inferior, temporal or nasal retina.

All subjects were injected intravenously into the brachial vein with  $^{14}\text{C}$ -2-deoxy-D-glucose (0.16  $\mu\text{C}/\text{gm}$ ; specific activity 300-350 mCi/mM) (Amersham) placed immediately into an acrylic container with a beak bar used to immobilized the head and then into the center of a vertically striped drum. The drum rotated on a vertical axis by means of a variable speed motor at 4-5 deg/sec or at a variable speed (40 deg/sec the first 10 min and then 4-5 deg/sec). Because both eyes were open one eye viewed temporal to nasal motion and the other viewed nasal to temporal motion. After 45 minutes animals were removed injected with an overdose of urethane and decapitated. The brains were subsequently processed according to a protocol described previously (McKenna and Wallman, 1985a).

The same sections used for autoradiography were later stained with thionine, drawn at a magnification of 17.5x, and superimposed on the corresponding autoradiograms to identify the  $^{14}\text{C}$  labeled portions of the LM. These drawings

were then charted on drawings of coronal sections of the pretectum similar to those used in the HRP study.

#### Amino Acid Autoradiography Study

For the anterograde tracing of the telencephalic projection to the LM and the efferent projections of the LM, iontophoretic injections of  $^3\text{H}$  proline and  $^3\text{H}$  leucine cocktails (1:1 ratio, 10-30  $\mu\text{Ci}/\mu\text{l}$ ; New England Nuclear) in .01M acetic acid were made using a single barrelled micropipette, 10-40  $\mu\text{m}$  in diameter at the tip. For injection, a positive DC current of 1.5  $\mu\text{A}$  was applied on an alternating cycle (7 seconds on 7 seconds off) for 45-75 minutes. Following survival periods from 3 to 5 days, chicks were anesthetized, perfused with 10% formalin and brain tissue postfixed for seven days in 30% sucrose-formalin. Brains were then sectioned at 40  $\mu\text{m}$ ; sections were mounted, dehydrated and coated with Kodak emulsion for an exposure time of 4-6 weeks. Following exposure to emulsion, the sections were developed in Kodak D-19 developer and alternating sections counterstained with cresyl violet stain. Sections were then magnified at 17.5x on an Aus Jena projector and drawn. After viewing sections under both light and dark field illumination, terminal labeling was marked on the drawn sections. Examples of terminal labeling were subsequently photographed.

## Chapter 4: THE TOPOGRAPHY OF THE LM IN THE CHICKEN PRETECTUM

### Introduction

In vertebrates, a nucleus in the pretectal region has been implicated in the processing of horizontal retinal slip signals, i.e., slow large field horizontal visual motion across the retina, and in mediating the generation of horizontal optokinetic pursuit. It has been previously suggested that this area in birds, the LM, is homologous to the NOT in mammals (Kuhlenbeck and Miller, 1942). To further validate this notion of homology between the avian LM and the mammalian NOT, a study of the anatomical connectivity of the LM was essential. As noted previously, anatomical investigations of the pretectal region in birds have been hindered both by the difficulty in defining the small and diffuse nuclei within this region and by the various nomenclatures adopted by authors. The commonly used atlases of the avian brain (Huber and Crosby, 1929; Kuhlenbeck, 1937; van Tienhoven and Juhasz, 1960; Karten and Hodos, 1967) provide only a scant representative illustration of the pretectum and lack a precise definition of nuclear groups within this region. Although more recent investigations of primary visual centers in the pretectum of birds (Reperant, 1973; Ehrlich and Mark, 1984; Gamlin and Cohen, 1988a) provide relatively precise schematic illustrations, they, in turn, lack a consistent nomenclature for the nuclei in this area.

Prior to initiating a study of the connectivity of the chicken LM, a precise topographical definition of the LM within the chicken pretectum was needed. In the present study, a combination of staining and tract tracing techniques were used to define the the location of the retinorecipient LM and its subdivisions in the pretectal region.

## Results

The LM in chicken was initially identified on the basis of its position in the pretectum and its cellular composition. The LM was found in the pretectum, medial to the rostral optic tectum and extended between the dorsal and ventral optic tracts, lateral to another retinorecipient pretectal area, the superficial synencephalic nucleus (SS) (see Ehrlich and Mark, 1984 for alternative nomenclature). Although the nucleus measured 1.5 mm in its rostrocaudal extent, most of the LM lies in the rostral 650  $\mu\text{m}$ ; at this point it tapered to a small ventral group of cells (Fig. 1) that could be traced caudally to the level of the nucleus of the basal optic root (nBOR) of the accessory optic system (AOS).

As it was traced caudally in coronal sections through the pretectum, the LM, which is composed of two portions, a magnocellular portion (LMmc) and a parvicellular portion (LMpc), appeared as a thin sheet-like nucleus (Fig. 1), measuring approximately 350  $\mu\text{m}$  in its mediolateral extent. In coronal sections treated with Klüver-Barrera stain, at its rostral pole the LM first appeared as the LMmc with its large neurons measuring between 20-39  $\mu\text{m}$  in diameter embedded in the optic tract. These neurons, as well as smaller ones, were dispersed among the stained myelinated fibers of the optic tract running between and around the cells (Fig. 1a and 2a). Further caudally, the LM lengthened dorsoventrally extending between the dorsal and ventral optic tracts (Fig. 1b-d). Approximately 200  $\mu\text{m}$  from the rostral pole, the smaller cells of the LMpc (9-19  $\mu\text{m}$  in diameter) appeared medial to the optic tectum, and lateral to the large neurons of the LMmc (Fig. 1e and 2b). Beginning at approximately 300  $\mu\text{m}$  from the rostral pole (Fig. 1g), the LMmc narrowed into a thin line of large neurons extending dorsoventrally and lying on the extreme medial border of the LM, subsequently becoming separated into a dorsal and ventral limb by the intrusion of the LMpc (Fig. 1i,j). In more caudal regions, at approximately 500  $\mu\text{m}$  from the rostral pole

(Fig. 1k and 2c), the LMpc began to separate into a dorsal and ventral limb by the narrowing of its mediolateral aspect so that by approximately 600  $\mu\text{m}$  from the rostral pole (Fig. 1l, m) the LMpc was completely separated into a dorsal and ventral component and began merging with the layers of the OT (Fig. 1n, o, p and 2d). Further caudally, the dorsal component of the LMmc disappeared and the ventral limb consisted of only a few large neurons which were embedded in the ventral optic tract. These LMmc neurons could be traced caudally for another 900  $\mu\text{m}$  until they merged with the lateral subdivision of the nBOR (nBORl). When viewed in the parasagittal plane, the LM is ovoid in shape with an indentation at the caudal surface.

The LM was easily distinguished from the SS in the Kluver-Barrera stained sections on the basis of their position within the pretectum and their different cell sizes. The SS, although also a crescent shaped nucleus, was already found to be elaborated rostral to the rostral pole of the LM. Further caudally, where the LM and SS lie adjacent to one another the strikingly large cells of the LMmc, extending from dorsal to ventral at the medial border, formed a rather distinct boundary between the LM and the small cells of the SS (Fig. 3). Furthermore, the fiber matrix within which the cells of the LMmc are situated was not apparent in the SS, clearly defining it from the LM. Further caudally, approximately 200  $\mu\text{m}$  from the rostral pole of the LM, the SS was found medial only to the ventral portion of the LM and was clearly separated from it by a distinct thin fiber tract.

An alternate method of demarcating the extent and boundaries of the LM was provided by the visualization of the retinal afferents within the LM after intraocular injections of HRP-WGA or BHRP. There was no difference in the results after HRP-WGA or BHRP injections. As illustrated in Fig. 4, labeled terminals were found throughout the contralateral LM and were confined to the same areas of the pretectum that had been designated as LMmc and LMpc

respectively in the Klüver-Barrera stained sections (compare 2a-d with 4a-d). In addition, the intraocular injections of HRP allowed for the visualization of the retinal terminals on the neurons of the LMmc in the ventral limb in the caudalmost portions of the LM until they merge with the nBORI. The density of label within the LMmc suggested that its neurons receive a relatively strong retinal input as compared with the LMpc. Like other primary visual structures in the chick, the LM receives its retinal afferents primarily from the contralateral eye, though careful examination of the LM ipsilateral to the injected eye revealed the presence of a sparse retinal input into this nucleus.

#### Discussion

Much of the confusion regarding the definition of the LM is the result of a lack of serial schematic drawings defining the position of the LM relative to the SS nucleus in the pretectum of birds combined with several different nomenclatures adopted by different authors (see Ehrlich and Mark, 1984a). The representative schematic drawings of Huber and Crosby (1929) and Reperant (1973) refer to the LM as the nucleus superficialis synencephalis (SS) whereas Ehrlich and Mark (1984a) have divided this area into the nucleus externus (NE) and the griseus tectalis (GT). This same area is designated as the LM in the atlas of Karten and Hodos (1967) and agrees with the definition of the LM by Kuhlenbeck (1936). This latter nomenclature, adopted for the present study (Table 1), is chosen for several reasons. First, one can distinguish this area from the adjacent crescent shaped SS region without changing familiar terms (we certainly do not need more new names for the LM). Second, the nomenclature for the LM is derived from embryological investigations of the pretectal cell masses which suggest that both the LMmc and the LMpc are derived from the mesencephalic tectal plate (Kuhlenbeck, 1936). Defining two separate areas (NE and GT) within the LM region is based on cytoarchitectural criteria and is of little

use in comparing this avian pretectal region with that of other mammalian species. Third, metabolic mapping studies in chickens have described both the LMmc and the LMpc as being responsive to horizontal large field visual motion implicating both subdivisions in the horizontal optokinetic reflex (McKenna and Wallman, 1981; 1985a). This has been verified in the present study (see next chapter).

The coronal sections stained with Klüver-Barrera stain, clearly labeled the fiber tracts and nuclei of the chick pretectum allowing for a precise description of the topographically complex LM nucleus along its entire rostrocaudal extent. The Klüver-Barrera stained sections showing the strikingly large cells of the LMmc, form a distinct medial boundary between the LM and the SS. Furthermore, these large cells are embedded in a matrix of optic nerve fibers. These features are unique to the LM and not the SS and allows one to clearly distinguish between the LM region and the more medial SS. This distinction is important as several authors have included the SS into their definition of the LM area (LM-PTO complex: Brecha, 1978; LMn/LMl: Gamlin and Cohen, 1988a).

The terminal labeling seen after intraocular injections of HRP indicates that retinal afferents that are almost exclusively contralateral are distributed to all parts of the LMmc and LMpc though the innervation to the magnocellular division is more dense. These results are similar to those reported by Ehrlich and Mark (1984a) for the NE and GT after retinal laser lesions and injections of tritiated amino acids.

This investigation defines clearly the topography of the LM within the pretectum and distinguishes it from the adjacent SS. Thus, in conjunction with the neurophysiological and 2DG metabolic mapping studies which functionally implicate both the LMmc and the LMpc in the horizontal optokinetic reflex, the results presented here clearly support the claim that the LM is a single nucleus.

The designation of the LM as a pretectal nucleus also bears some consideration. It has been suggested that there is a unifying theme among retinorecipient nuclei designated as pretectal in nonmammalian vertebrates. Characteristics such as the embryological derivation from the tectal plate and any other features that reflect a pattern which parallels that of the tectum are representative of this unifying theme (Fite, 1985). According to this notion, the LM should be considered a pretectal nucleus whereas the SS, which is also a retinorecipient area but is presumably derived from the thalamic plate (Kuhlenbeck, 1939), should not be considered as such. Thus, it is questionable whether the pretectum, generally defined as an area on the basis of location adjacent to or nearby the tectum, can be considered a single entity.

#### Comparison with Mammals

The topographical features of the avian LM mentioned above are similar to those of the mammalian NOT. The NOT of nonprimate mammals such as rabbits (Kuhlenbeck and Miller 1942), rats, mice, tree shrew, cats (Scalia, 1972) and primate mammals such as the squirrel and rhesus monkeys (Hutchins and Weber, 1985) is located similarly within the brachium of the superior colliculus. Its rostral pole is anterior to the colliculus but the bulk of the NOT extends along its lateral side for some distance. It is composed of darkly staining cells collected in small groups or interspersed individually between fascicles of the collicular brachium. Its cells are large compared with those of other pretectal nuclei. In addition to the magnocellular aspect of the NOT, there is a parvicellular portion which lies medial to the large-celled subdivision extending not as far rostrally as the latter but further caudally. It consists of rather densely crowded small and medium sized cells (Kuhlenbeck and Miller, 1942).

The similarity between the LM and NOT also extends to their embryological derivation. Kuhlenbeck and Miller (1942) demonstrated that the LM in birds and

the NOT in rabbits and humans not only occupy a similar position in the pretectum but are also derived from a homologous precursor, the mesencephalic tectal plate.

It has been suggested by Campbell and Hodlos (1970) that the concept of homology in the nervous system should be based on various types of data including similarities in embryological derivation, topology, topography, morphology of neurons, behavioral changes resulting from lesions, neurophysiology, and fiber connections. Thus, the available metabolic mapping, neurophysiological and embryological studies taken together with the topographical and cytoarchitectural data presented here provide evidence for the homology of the avian LM and the mammalian NOT. This will be supplemented with connectivity data, presented in subsequent chapters.

## Chapter 5: THE ORGANIZATION OF THE RETINAL PROJECTION TO THE LM

### Introduction

In birds, the LM is known to receive a direct retinal projection that is extensively contralateral (Reperant, 1973; Ehrlich and Mark, 1984a; Gottlieb and McKenna, 1986) and has been shown to accumulate 2-DG when birds view large-field patterns moving in horizontal directions (chickens: McKenna and Wallman, 1985a; pigeons: Chown et al., 1984). The functional relationship to horizontal OKN has been demonstrated by the finding that lesions of the LM result in the elimination of temporal to nasal eye movements evoked by slow moving large-field visual patterns (Gioanni, 1983). A neurophysiological study of the LM has demonstrated that single units in the pigeon LM are direction selective mostly for horizontal directions and have large visual receptive fields ranging from 55° to 84°, which, in most cases, include some portion of the retinal equator (Winterson and Brauth, 1985). The position of the receptive fields of units in the LM suggests a possible retinotopic mapping within the nucleus; in dorsal regions, the receptive fields tend to be located in the temporal visual field, whereas in ventral regions receptive fields tend to be located in the nasal visual field.

Although the functional characteristics of this pretectal nucleus are fairly well understood, less is known about the innervating retinal ganglion cells and the spatial distribution of their terminals within the nucleus. In frogs (Montgomery et al., 1985) and cats (Ballas et al., 1981), the ganglion cells that project to the LM and the NOT, respectively, and their distribution within the retina have been described, but a retinotopic organization of the LM or NOT has not been reported. In birds, while an orderly arrangement of the retinal projection within several visual pretectal nuclei has been suggested (Ehrlich and Mark, 1984b; Gamlin and Cohen, 1988a), the results are difficult to interpret because of differences both in the nomenclature used for the pretectal nuclei and

in the identification of the retinal quadrants which were based on the orientation of the pecten of the avian retina.

In the present study, the HRP retrograde technique was used to describe the sizes and distribution of retinal ganglion cells that project to the chicken LM and to determine the mapping of the retinal ganglion cells onto the LM. The position of the LM adjacent to the optic tectum and other visual pretectal nuclei, however, made it imperative that another technique be used to verify the results found with HRP. By taking advantage of the selective sensitivity of the LM to horizontal retinal slip and the 2-DG metabolic mapping technique, the projection onto the LM was mapped by localizing the accumulated label produced by the visual stimulation of portions of the retina. A similar anatomical and functional retinotopic mapping of the LM was demonstrated by both techniques.

## Results

### HRP Injections into the LM

Nine injections were made into the LM. Because of the shape of the target nucleus and the proximity of neighboring pretectal nuclei, none of these injections was complete in the sense of including all parts of the nucleus, and some injections extended from the LM into neighboring nuclei and the optic tract. The injections reported here were restricted to the rostral 650  $\mu\text{m}$  of the LM. No injections were attempted into the caudal ventral limb of the LMmc due to the difficulty in making a discrete injection into the area containing the few LMmc neurons at this level. Since it is difficult to distinguish a boundary between the LMmc and the LMpc, and because the two subdivisions are unusually thin in their mediolateral aspect, every injection included some portion of both the LMmc and the LMpc but neither one exclusively.

To allow for ready comparisons between different injection sites, a

reconstructed parasagittal view of the LM was derived from coronal sections through the LM and the position of the injected HRP indicated by crosshatching. Table 2 shows the nine injection sites in the parasagittal sections and the resulting quadrantal distribution of labeled ganglion cells.

#### Retrogradely Labeled Retinal Ganglion Cells

After HRP injections restricted to the LM, labeled cells were identified in sectioned retinas in the ganglion cell layer, only in the contralateral retina (Fig. 5). The labeled cell bodies were round or oval and measured 25-840  $\mu\text{m}^2$ , with a mean area of 230  $\mu\text{m}^2$  ( $n=304$ ). As seen in the histogram (Fig. 6), the distribution of cell sizes is positively skewed indicating the greater frequency of smaller cells (78.6% < 300  $\mu\text{m}^2$ ). The chi-square test suggests that more than one population of cells based on cell body size, was labeled ( $\chi^2=118.38$ ,  $df=15$ ;  $p>.05$ ). Although the cell sizes may have been underestimated because of the difficulty of measuring cells labeled with HRP, the smallest size measured falls within the size range of stained retinal ganglion cells reported previously for the chick retina (Ehrlich, 1981). Other features such as cell shape or dendritic arborization patterns were not useful in distinguishing the number of possible populations present because no correlation was found between the shape (ratio of the long axis to the short axis) and the area of the cells ( $r=0.023$ ) and because, at best, only the proximal portions of dendrites were filled with HRP. In addition, no relationship was found between cell shape and quadrantal location within the retina. The cell sizes, however, tended to be differentially distributed among the retinal quadrants; many small cells were found in the superior temporal quadrant (mean= 161  $\mu\text{m}^2$ ) inferior nasal quadrant (mean= 231  $\mu\text{m}^2$ ) whereas the cells in the inferior temporal quadrant were, on the average, larger (mean= 404  $\mu\text{m}^2$ ) (Fig. 6) Cells found in the superior nasal quadrant were too lightly labeled to be measured accurately.

The total number of labeled retinal ganglion cells after LM injections varied with each injection because of differences in the size of the injection, the position of the injection within the LM and the variability inherent in the HRP technique. As seen in Table 2, when all the injections are considered, labeled retinal ganglion cells were found in all retinal quadrants. Taken together, the majority of cells were seen in the superior temporal quadrant whereas relatively few cells were found in the superior nasal quadrant. In addition, the number of labeled cells in the center of the retinas was noticeably sparse (Fig. 7-10) considering that this is the area of highest ganglion cell density in the chick retina (Ehrlich, 1981).

Labeled displaced retinal ganglion cells, which are found at the inner margin of the inner plexiform layer, were encountered only when the injection site extended beyond the LM into the surrounding optic tract. The cell bodies, which ranged in size from  $5 \times 5 \mu\text{m}$  to  $12 \times 17 \mu\text{m}$ , are smaller than the population of displaced retinal ganglion cells that projects to the nBOR of the accessory optic system of pigeons (Fite et al., 1981; Karten, et al., 1977; Reiner et al., 1979).

#### Retinal Projection to the LM

In general, injections into the dorsal half of the LM resulted in the labeling of retinal ganglion cells in the inferior retina whereas injections into the ventral half of the LM labeled cells in the superior retina. Of the nine injections into the LM reported here, four injection sites and their resulting HRP labeled ganglion cells, in retinas reconstructed as described previously, are illustrated in Figures 7-10.

#### Injections Into Dorsal LM

Two injections (HRP-27, HRP-48), which were positioned primarily in the dorsal LM, resulted in the labeling of ganglion cells in the inferior retina with the majority of cells lying in the proximity of the equator. Although both injection

sites extended the full rostrocaudal length (650  $\mu\text{m}$ ) of the LM, the center of each injection site, as defined by the position of the heaviest label, differed with the center of HRP-27 lying more caudally than that of HRP-48. As seen in Fig. 7a-d and Table 2, the center of the injection site of HRP-27 was placed more than 400  $\mu\text{m}$  from the rostral pole with very little injected HRP in the rostral 200  $\mu\text{m}$  (Fig. 7a,b). After this injection, a majority of labeled ganglion cells (80.6%) as shown in Table 2, were found in the inferior nasal quadrant with most lying near the equator. As seen in HRP-48 (Fig. 8a-d, Table 2), when the center of the injection site was positioned in the rostral 200  $\mu\text{m}$  of the LM (Fig. 8b), almost all the labeled cells (88.8%) were found in the inferior temporal quadrant, again near the equator (Fig. 8c).

A third larger injection, HRP-57, illustrated in Table 2, covered the entire dorsal LM region with a heavy HRP label from rostral to caudal, and resulted in the labeling of cells in both the inferior temporal (26.7%) and inferior nasal quadrants (73.3%), as one would predict from the results of HRP-27 and HRP-48.

#### Injections Into the Middle and Ventral LM

Five injections (HRP-115, HRP-70, HRP-153, HRP-14, HRP-15) were placed into a portion of the ventral half of the LM, and in most cases excluded the dorsal LM. These injections consistently resulted in the labeling of ganglion cells in the superior retina. As seen in Fig. 9a-d and in Table 2, the injection site for HRP-115 was positioned in the ventral half of the LM throughout its rostrocaudal extent although it was heavier in the rostral 500  $\mu\text{m}$ ; in the last 100  $\mu\text{m}$  it tapered off to include only the medial edge of the ventral caudal limb (Fig. 9d). After this injection, all the labeled cells were found in the superior temporal retina with most of the cells lying near the equator. The injection site for HRP-70, illustrated in Table 2, was positioned, like HRP-115, in the middle of the LM along its dorsoventral extent, but not in the ventral LM. Following this injection, almost

all the labeled ganglion cells (98%), like those of HRP-115, were found in the superior temporal retina with a majority of the cells lying near the equator. The results of these two injections suggest that the retinal ganglion cells in the superior temporal retina project to a large area within the LM including the middle and ventral portions and extending from the rostral pole to the caudal pole.

The third injection site, HRP-153, was remarkably similar to HRP-70 in its location in the middle of the LM along its dorsoventral axis, but it also extended rostrally to include the rostralmost portion of the nucleus (Table 2). Like HRP-115 and HRP-70, most of the labeled ganglion cells (73.2%) after this injection were found in the superior temporal retina. In addition, a few labeled cells were found in the superior nasal quadrant.

Two additional injections, HRP-14 and HRP-15, considerably larger than the preceding three injections, spread into the optic tract and areas outside the LM, but otherwise appeared to be a combination of injection sites HRP-115, HRP-70, and HRP-153 (see Table 2). As would be predicted from the position of these three injection sites, most ganglion cells were found within the superior temporal quadrant (HRP-15: 81.4%; HRP-14: 86.5%). The few cells labeled in the inferior retina might be due to the spread of injected HRP into the dorsal LM region; this is suggested by the findings from HRP-27 and HRP-48. In addition, a few labeled cells were found in the superior nasal quadrant. The labeling of displaced retinal ganglion cells at the inner margin of the inner plexiform layer following these two injections was probably due to the encroachment of the injected HRP into the optic tract and surrounding areas.

#### Nearly Complete Injection

The injection site of HRP-36 was the most complete injection of the nucleus, confined exclusively to the LM without encroaching into any adjacent

retinorecipient nuclei, or into the optic tract. As illustrated in Fig. 10a-d and Table 2, the injected HRP heavily labeled the entire LM along its dorsoventral extent in the rostral 300  $\mu\text{m}$  of the LM; as the label was traced caudally it became lighter and in the caudalmost regions it was confined to only the dorsal limb of the LM. After this injection labeled ganglion cells were found distributed in a wide horizontal belt lying along both sides of the equator and stretching from the temporal to the nasal retina. Labeled ganglion cells were found in all four quadrants. The relatively low number of HRP positive cells in the superior temporal quadrant, surprising in light of the findings reported above for injections such as HRP-115 and HRP-70, might be due to the light deposit or complete lack of HRP in the ventrocaudal LM. A surprisingly high proportion of labeled cells was found in the superior nasal quadrant after this injection. However, these cells lie very close to the equator suggesting that their quadrantal assignment may have been affected by the reconstruction of the retinal cross-sections.

Taken together, the results of the HRP injections into the LM suggest that there is a general mapping of the retina onto the LM nucleus such that the inferior retina projects to the dorsal LM and the superior retina projects to the middle and ventral LM (see Fig. 15). Furthermore, within the inferior retina, temporally located ganglion cells project to the rostradorsal LM while the nasally positioned ganglion cells project to the caudodorsal LM with a probable area of overlap in the central LM. Ganglion cells in the superior temporal retina, an area of greater ganglion cell density in the chick retina, project to the middle and ventral LM from the rostral to the caudal pole. In most of the injections very few cells were found in the superior nasal quadrant suggesting a very sparse projection to the LM, a finding supported by the 2DG results described below. Since relatively few cells were labeled in the superior nasal quadrant, it is difficult to decipher the mapping of this quadrant onto the LM. The distribution

of labeled retinal ganglion cells after injections into portions of the LM matches the distribution of labeled ganglion cells after the nearly complete injection into the LM.

#### Metabolic Mapping Patterns in the LM Produced by Optokinetic Stimulation of Half of the Retina.

The metabolic mapping patterns in the LM were examined in four experimental groups. In both eyes of each chick tested, one half of the retina was masked with a translucent hemi-occluder while the other half --either superior, inferior, temporal or nasal -- was exposed to large-field horizontal visual motion. Since both eyes of the animals were open during testing in the optokinetic drum, one eye viewed temporal-to-nasal motion and the other viewed nasal-to-temporal motion. The LM contralateral to the eye viewing either direction of horizontal motion was expected to accumulate 2-DG since in chicks the optic nerves are extensively crossed. In many birds, the LM contralateral to the eye stimulated with temporal-to-nasal motion was more heavily labeled than the nucleus contralateral to the eye stimulated with nasal-to-temporal motion; in others the labeling appeared equal. The pattern of labeling within each LM was not affected by the direction of horizontal movement, except in those birds with the nasal half of the retina exposed. In these birds, label was consistently absent from the LM contralateral to the eye viewing nasal to temporal motion.

*Superior retina.* In the three birds of this group, stimulation of the superior retina with horizontal visual motion resulted in accumulation of 2-DG labeling primarily in the ventral LM. Only in the rostralmost LM was the dorsal half of the nucleus labeled (Fig. 11a); as the LM was followed caudally, the label was located exclusively in the ventral half of the nucleus (Fig. 11b-d), and in the caudalmost part (480 to 600  $\mu\text{m}$  from the rostral pole) only the ventral limb of the nucleus was labeled (Fig. 11f). In addition, in two of the three birds the

nBORI, which in a previous study was shown to be responsive to horizontal motion (McKenna & Wallman 1981), was labeled (Fig. 11g).

*Inferior retina.* In contrast to the above, in three birds, stimulation of the inferior retina with horizontal visual motion resulted in the accumulation of label primarily in the dorsal LM. This label was particularly heavy in the dorsal half of the LM in its rostralmost portion (Fig. 12a); as the nucleus was traced caudally, between 120 and 240  $\mu\text{m}$  from the rostral pole, the label became lighter and extended ventrally (Fig. 12b-c). In the caudal half of the nucleus, the label was restricted to the dorsal limb (Fig. 12d,e) and was absent in the caudalmost extreme (between 500 and 600  $\mu\text{m}$ , Fig. 12f) in two of the three birds.

Along the dorsoventral axis of the LM the pattern of label found after stimulation of the inferior retina was complementary to the one obtained after stimulation of the superior retina: superior retinal stimulation caused labeling of the ventral LM and inferior retinal stimulation caused labeling of the dorsal LM; only in the rostral third of the nucleus did the label produced by these two conditions overlap somewhat (compare Figs. 11a,b and 12a,b). This zone of overlap could be due to the central retina being stimulated with either occluder worn; alternatively, it might imply that both the superior and the inferior retina project to the rostral LM.

*Temporal retina.* In all four animals tested, stimulation of the temporal retina with horizontal visual motion resulted in very heavy label that extended along the full dorso-ventral axis in the rostral half of the LM (up to 360  $\mu\text{m}$  from the rostral pole, Fig. 13a-c). As the nucleus was traced caudally, the label became lighter and, in two brains, was concentrated in the ventral limb of the nucleus (Fig. 13d-f). In the other two brains, the label was not detected in the caudal third of the nucleus. The light labeling or lack of it in this portion of the nucleus suggests that the level of metabolic activity produced by stimulation of the

temporal retina is near the limit of sensitivity of the method.

*Nasal retina.* In the four birds of this group, stimulation of the nasal retina with horizontal visual motion resulted in very light labeling of the LM. Label, which was absent from the rostral half of the LM (Fig. 14a-c), first appeared at approximately 360  $\mu\text{m}$  from the rostral pole, where it extended along the entire dorsoventral extent of the nucleus (Fig. 14d). At more caudal levels the label was found mainly in the dorsal portion of the LM (Figs. 14e,f).

Thus, stimulation of temporal and nasal retina showed complementary patterns of labeling of the LM: stimulation of the temporal retina labeled the entire rostral LM and the ventral part of the central and caudal portions of the nucleus, whereas stimulation of the nasal retina resulted in label mainly in the dorsal half of the LM, excluding the rostral part (compare Figs. 13 and 14). The zone of overlap, in the central LM (compare Figs. 13d and 14d), may have been produced by stimulation of the same region of the retina under both experimental conditions, or it might imply a zone of the LM that receives projections from both the temporal and the nasal retina.

From these results we can infer the labeling pattern in terms of retinal quadrants. The metabolic mapping pattern in the LM during superior retinal stimulation (Fig. 11) overlaps to a large extent with that obtained after temporal retinal stimulation (Fig. 13); both cover the ventral LM from the rostral to the caudal pole. One can then assume that this region of the LM would be labeled after stimulation of the superior temporal retina, the quadrant of overlap for these two experimental conditions. In contrast, the label after superior retinal stimulation (Fig. 11) overlaps very little with that after nasal stimulation (Fig. 14), except for a small region just rostral to the separation of the nucleus into a dorsal and a ventral limb. Although this zone of overlap is quite reduced and is not present in all the birds of these two experimental groups, and the fact that

HRP injections that include this zone of the LM resulted in labeling of ganglion cells in the superior nasal retina, suggests that the superior nasal quadrant may be represented in this region of the caudal LM.

Since the dorsalmost portion of the nucleus was labeled after stimulation of the inferior, either nasal or temporal, retina (Fig. 12) we can infer that the label resulting from stimulation of the inferior temporal quadrant would cover the rostradorsal nucleus (similar positions of 2-DG label in Figs. 12a-c and 13a-c) and stimulation of the inferior nasal quadrant would cover the dorsocaudal nucleus (similar position of 2-DG label in Figs. 12d-e and 14d-e).

*Overall pattern of projections to the LM.* Taken together, the results of the HRP injections into the LM and the 2-DG study suggest that there is a general mapping of the retina onto the LM such that the inferior retina projects to the dorsal LM and the superior retina projects to the middle and ventral LM (Fig. 15). Furthermore, the inferior temporal retina projects to the rostradorsal LM whereas the inferior nasal retina projects to the caudadorsal LM. The superior temporal quadrant projects to the middle and ventral LM extending from the rostral to the caudal pole, whereas the superior nasal quadrant projects to a small zone in the caudal LM just rostral to the separation of the nucleus into its dorsal and ventral components. Both the HRP and the 2-DG results suggest that the superior nasal quadrant is weakly represented in the LM.

### Discussion

The present study has three principle findings. First, more than one population of ganglion cells, based on size, projects from the retina to the LM; second, these retinal ganglion cells are distributed in a horizontal band near the equator; and third, these ganglion cells project onto the LM in a retinotopic manner.

### Rationale for Using Both HRP and 2-DG Techniques

The use of the HRP technique has enabled the identification of the ganglion cell types that project to the LM and description of their distribution within the retina. Unfortunately, the injection technique has drawbacks, including the possibility of breaking optic fibers in or near the nucleus and the possibility of diffusion of injected HRP into neighboring retinorecipient nuclei resulting in some falsely labeled ganglion cells. In contrast, use of the 2-DG method has neither of these risks, although it cannot be used for identification of the retinal ganglion cells. Since previous studies have shown that large-field horizontal visual motion results in the accumulation of 2-DG in the LM and not in the neighboring retinorecipient nuclei (McKenna and Wallman, 1985a), its use allowed for the description of the retinotopic organization of the entire LM including its caudoventral tail, which is too small for a confined injection of HRP. Although one technique traces the anatomical projection and the other detects metabolic activity, the results from both procedures are in agreement.

#### Cell Types Projecting to the LM

The finding in this study of more than one population of retinal ganglion cells, many of which are small in size, projecting to the LM of chicken, is consistent with findings in other species. In frogs, at least two classes of ganglion cells, many of which are small in size, project to the LM (Montgomery et al., 1985). In cats, of the total population of cells projecting to the NOT, 95% were the smaller  $\gamma$ -cells and 5% were the larger  $\alpha$ - cells (Ballas et al., 1981). The finding of a predominant  $\gamma$ -cell input into the NOT agrees with electrophysiological studies that identified the retinal input to the NOT in cats as w-type, the physiological counterpart to the  $\gamma$ -cell, and that identified some of these ganglion cells as directionally selective (Hoffmann and Schoppmann, 1975; Hoffmann and Stone, 1985).

### Distribution of Retinal Ganglion Cells Projecting to the LM

The retinal ganglion cells labeled after HRP injections into the LM were distributed in all quadrants and lay in a horizontal band near the equator stretching from the temporal to the nasal retina. This distribution is in agreement with the finding in the pigeon that most of the directionally selective units in the LM had receptive fields that included some portion of the retinal equator (Winterson and Brauth, 1985). The direction sensitive ganglion cells, many of which respond best to temporal-to-nasal movement of the visual world, a direction of motion preferred by the units of the LM (Winterson and Brauth, 1985), also tended to lie near the equator (see Fig. 5 Pearlman and Hughes, 1976). The distribution of retinal ganglion cells within the quadrants was not uniform. The greatest concentration of labeled cells was found in the superior temporal quadrant, and relatively few cells were found in the superior nasal quadrant. In addition, few ganglion cells were labeled in the centralmost portion of the retina. It has been reported previously that in the chick retina, the area of highest ganglion cell density, the area centralis, is in the central retina. However, the contours of the isodensity map of chick retinal ganglion cells suggests that the superior temporal quadrant is an additional area of high ganglion cell density (Ehrlich, 1981; pers. observ.). Thus, the results of the present study indicate that although many of the ganglion cells projecting to the LM do not lie within the area centralis, many are found in an area of high ganglion cell density. It is not surprising that few cells were found in the area centralis since in other avians, this area projects to the lateral nucleus of the anterior thalamus (pigeons: Gamlin and Cohen, 1988a), or to both the optic tectum and thalamus (owls: Bravo and Pettigrew, 1981).

The location, near the retinal equator, of the pretectal-projecting ganglion cells appears to be a common property among vertebrates. In cats (Ballas, et al., 1981)

and frogs (Montgomery et al., 1985), retinal ganglion cells projecting to the NOT and LM, respectively, are localized near the retinal equator with the highest concentration of cells in and around the area centralis. The finding in rabbits (Dubois and Collewijn, 1979) and humans (Howard and Ohmi, 1984) that horizontal OKN is driven more effectively when a moving stimulus is presented to the central region of the retina may be a reflection of the position of retinal ganglion cells which mediate horizontal OKN in these species.

The functional importance of the distribution of these ganglion cells within the retina is not readily apparent. The finding of large receptive fields within the LM suggests that a relatively large number of retinal ganglion cells converge onto units in the LM. For this reason, as long as a large portion of the visual field is sampled, the location of the retinal ganglion cells along the equator does not appear to have a functional significance.

#### Retinotopic Organization of the LM

Results of the present study suggest that the retinal projection to this nucleus in chicken is organized in a retinotopic manner (Fig. 15). The results of both the HRP and 2-DG studies suggest that the ganglion cells in the inferior retina map onto the dorsal LM; the inferior nasal retina projects to the caudodorsal LM whereas the inferior temporal retina projects to the rostradorsal LM. In addition, the ganglion cells in the superior retina project to the middle and ventral LM from the rostral to the caudal poles, excluding only the dorsal portion; most of these cells lie within the superior temporal quadrant. As suggested by the metabolic mapping results, ganglion cells from the superior temporal quadrant probably also project to the caudoventral tail of the LM. Relatively few retinal ganglion cells in the superior nasal quadrant project to the LM as evidenced by the paucity of labeled cells found in this quadrant even after large HRP injections into the LM and by the small zone of overlap of metabolic activity after

stimulation of the superior and nasal hemi-retinas. This zone is found in the caudal LM, just rostral to the separation of the nucleus into its dorsal and ventral components.

The retinotopic mapping of the LM in birds has been reported in several studies using a variety of methodological approaches. Comparisons of the results from each of these studies with the present study are extremely difficult, due to the differences in the identification of the nucleus, in the nomenclature used for it and in the interpretation of the results. However, when in one case the illustrations are examined (Gamlin and Cohen, 1988a) and in the other case the retinal wholemounts are rotated to align the pecten to the same angle as the pecten in retinas used in this study (Ehrlich and Mark, 1984b), our results are in close agreement. Both these anatomical studies, one using small laser lesions of the chick retina (Ehrlich and Mark, 1984b) and the other using small injections of tritiated amino acids into the pigeon retina (Gamlin and Cohen, 1988) demonstrated that the superior retina projects to the ventral LM and inferior retina to the dorsal LM. This superior-inferior inversion of the retina on the LM has also been shown in an electrophysiological study that mapped receptive field positions (see Fig 6 in Winterson and Brauth, 1985). The projection of the inferior temporal and the inferior nasal quadrants to the rostradorsal and caudadorsal LM found in the present investigation has not been demonstrated convincingly by any of these studies. The notion that these quadrants are mapped separately is supported by both the retrograde HRP and the metabolic mapping techniques. The finding in the present study of a topographic mapping of the superior nasal quadrant in the LM was not confirmed by the other anatomical studies since neither lesions nor amino acid injections were made into this quadrant. A retinotopic organization of the NOT in mammals has also been demonstrated anatomically though the functional significance of this organization has not been

discussed (cat: Updyke, 1977; rat: Scalia and Arango, 1979).

The orderly mapping of the retinal projection onto the LM may be a consequence of two factors, a common embryological anlage and the arrangement of retinal axons as they enter each nucleus from the optic tract.

#### Similarity of the Retinotopic Organization of the LM and Optic Tectum

As shown in Fig. 15, the mapping of retinal quadrants in the LM is similar to that reported in the optic tectum in both chicken (Crossland and Uchwat, 1979) and pigeon (McGill, et al. 1966). For both areas, the inferior retina projects to the dorsal portion whereas the superior retina projects to the ventral portion. Furthermore, the inferior temporal retina and inferior nasal retina project, respectively, to the rostradorsal and rostrocaudal LM and optic tectum. The similarity of this organization is also found in the projection of the superior nasal retina to the middle caudal portion and the superior temporal retina to the remaining ventral portion. The similarity of the retinal mapping in both areas suggests that the same developmental mechanisms for axonal targeting might be responsible.

I suggest that a common embryological anlage together with the arrangement of retinal axons in the optic tracts that supply both the LM and optic tectum are important factors in establishing a retinotopic organization of the LM. In birds, both the optic tectum and the LM develop embryologically from the tectal plate (Kuhlenbeck, 1939). This common derivation may result in the presence of similar molecular markers that direct the retinal axons to their targets. The derivation of other pretectal nuclei from the diencephalic plate may explain the finding that these nuclei, although they lie adjacent to the LM, have a different retinotopic organization (Ehrlich and Mark, 1984b; Gamlin and Cohen, 1988b).

The arrangement of retinal axons in the optic nerve and tract is another factor that may account for the similar organization of the LM and optic tectum. It has

been reported recently in the chick (Rager, et al., 1986), that as the retinal fibers travel from the eye toward the optic tectum they maintain a high degree of order. The retinal quadrants preserve their neighboring relationships, suggesting that the representation of the retinal image is maintained within the nerve. Optic fibers arriving at the rostral surface of the tectal/pretectal area separate so that fibers from the inferior retina form the dorsal optic tract and the fibers from the superior retina form the ventral optic tract (Ehrlich, 1981). Fibers running along the inner border of the optic tracts, which originate from the temporal retina, terminate rostrally, whereas fibers running along the outer border, which originate from the nasal retina, terminate caudally. Although these findings were reported for the optic tectum, I suggest that a similar distribution of optic fibers into the LM occurs, since the same optic tracts deliver the retinal axons to the LM (Repérant, 1973). As a consequence, the retinotopic organization of both these areas would be conferred by the organization of the optic tracts. When the retinal axons have entered the individual nuclei, one would expect different developmental mechanisms to come into play for further refinement of the map. In the optic tectum, one could well imagine in early stages of development an excess of axon terminals that are subsequently pruned back producing the small receptive fields of units found in the adult. In contrast, the presence of very large receptive fields in the LM suggests a clustering of terminals originating from retinal ganglion cells that are distributed over a relatively large area of the retina.

#### A Comparison of the Retinal Projection to the Pretectum and the AOS

The nBOR of the AOS of birds has been shown to receive retinal slip signals which are probably used to generate vertical and torsional optokinetic stabilizing eye movements. This similarity to the LM in function suggests that the morphological organization of the retinal projection to each nucleus might be similar. This, however, does not appear to be the case. Although both the LM and

nBOR have a similar function in the stabilization of the visual world, the morphological organization of the retinal projection to each system appears to be quite different. The LM receives a retinal projection from more than one population of ganglion cells, based on somal size, whereas the nBOR receives all its retinal afferents from displaced ganglion cells of similar size. The ganglion cells in the pretectal system are found distributed near the equator in all four quadrants with a majority in the superior temporal retina. In chickens, the displaced ganglion cells of the AOS, which are found in the inner plexiform layer, are scattered throughout the retina, evenly distributed among the retinal quadrants (Reiner et al 1979). Although both the LM and the nBOR have a retinotopic organization, they differ in that there is only a partial mapping of the retina onto the nBOR. Electrophysiological evidence in chicken suggests that the frontal and lateral visual fields (temporal and nasal retina) are mapped onto the dorsal and ventral nBOR respectively, with very few units near the optic axis (Burns, 1985); this latter finding is very similar to that found in the present study. There is no evidence for a retinotopic order in the mapping of the superior and inferior retina onto the nBOR as there is onto the LM in this species. Thus, in birds, the retinal projection to the LM in the pretectum appears to be organized differently from the retinal projection to the nBOR of the AOS. The reasons for these differences are, at the moment, inexplicable.

The findings in the present study of more than one population of retinal ganglion cells many of which are small in size, located near the retinal equator which project to the LM in a topographically organized manner are similar to those reported for the retinal projection to the mammalian NOT. The similarity of these particular features of the primary projection to the optokinetic pretectal area in avians and mammals lends more credence to the notion of homology and suggests a general pattern homologous among vertebrates. To continue this

comparison of the connectivity of the avian and mammalian horizontal optokinetic reflex the following portion of this investigation will define the nonretinal afferent projections to the I.M

## Chapter 6: THE ORGANIZATION OF THE NON-RETINAL AFFERENT PROJECTIONS TO THE LM

### Introduction

The previous chapter describes the retinal ganglion cells that are a source of afferents to the LM and the orderly mapping of the retina onto the LM. This portion of the study addresses the question of the other sources of afferents to the LM and the organization of these projections. These non-retinal afferent projections may provide additional pathways along which retinal slip signals may reach the LM or pathways that may modulate the activity of LM units. Previous studies that used a variety of anterograde tract tracing techniques have suggested a number of non-retinal sources of afferents to the LM including the visual telencephalon, the nBOR of the AOS, and the OT.

Three investigations of the efferent connectivity of the visual telencephalon describe a projection to the pretectum in a variety of birds (Adamo, 1967; Karten et al., 1973; Miceli et al., 1978). However, all of these studies suffer from a basic deficiency in that they do not provide a precise definition of nuclear groups within the pretectum. As a result, the drawings provided do not allow for a precise analysis of the terminal labeling within the individual pretectal nuclei and thus do not allow for a definitive determination of a telencephalic projection to the LM. Furthermore, the above mentioned studies report simply the evidence of terminals in the pretectum originating from the telencephalon without defining the cells of origin within this multilayered region. Thus, one aim of the present study was to define, with the HRP retrograde tracing technique, the morphology of the projection neurons, their distribution within the telencephalon and the spatial organization of this projection to the LM.

Several behavioral studies of the horizontal optokinetic response provide additional evidence for the existence of a telencephalic projection to the LM in

birds. These studies suggest that such a projection may be important in mediating the asymmetrical response patterns of horizontal optokinetic pursuit in birds and that the development of this pathway may mediate the developmental changes reported in horizontal OKN postnatally. Early reports in birds suggest that after bilateral telencephalic ablation, the asymmetrical horizontal OKN response found in normal birds becomes somewhat more symmetrical, similar to that found in hatchlings (Fox, 1926; Visser and Rademaker, 1934). Furthermore, it has been reported that an asymmetry in the horizontal OKN response patterns of hatchling chicks becomes more pronounced with increasing age (Wallman and Velez, 1985). This change may be reflected in the change in differential labeling of the LM in hatchling and older birds demonstrated in 2-DG metabolic mapping experiments (McKenna and Wallman, 1985a). This finding suggests that there indeed may be an anatomical change taking place in the innervation pattern of the LM, perhaps as a consequence of the development of a projection from the visual telencephalon to the LM (McKenna and Wallman, 1985a). Thus, another aim of this study was to determine, with anterograde tracing techniques, whether a change in the innervation pattern of the HA projection to the LM occurred postnatally.

The nBOR of the AOS in birds has been shown to provide an afferent projection to the LM. After injections of tritiated amino acids into the nBOR in pigeons, terminal labeling was reported in the LMmc but not the LMpc or the nucleus parageniculatis tecti optici (PTO) (Brecha et al., 1980); the latter may be equivalent to the SS in chickens. Furthermore, HRP injections, centered within the LM but also including the optic tract and optic tectum, retrogradely labeled medium and large sized cells within all three subdivisions of the nBOR (Brecha et al., 1980). In the present study the HRP retrograde tracing technique was used to determine whether the LM of chickens receives an afferent projection from the nBOR, the location of the projection neurons, and their morphology.

It has also been suggested that the optic tectum projects to the pretectal nuclei in pigeons. After injections of tritiated amino acids into the tectum, a projection was reported to the LMmc, the LMpc and the GT (Hunt and Kunzle, 1976). Similarly, after HRP injections into the tectum, anterogradely transported label was observed in terminals within the entire extent of the LM-PTO complex (Brecha, 1978). A comparison of schematic drawings provided in these studies suggest that the GT of Hunt and Kunzle is equivalent to the PTO of Brecha in pigeons and may be equivalent to the SS in chickens. However, the cells of origin of the tectal projection have not been previously described. Thus, another aim of the present study was to determine with the HRP retrograde tracing technique, whether a similar projection exists in chickens and to define the location of the projection neurons within the multilayered OT.

Because the SS may be the equivalent of the PTO as defined by Brecha (1978) and the GT as defined by Hunt and Kunzle (1976), and has been included in the definition of the pigeon LM by Gamlin and Cohen (1988a), several HRP injections were made into the SS in the present study to determine whether the SS also receives a projection from the nBOR and the OT.

The results of the retrograde tracing experiments described here reveal for the first time in birds, the location and distribution of the neurons within the telencephalon that project to the LM, their morphological appearance, and the spatial organization of the projection neurons in the HA and their terminals within the LM. In addition, the distribution of terminal labeling within the LM from the telencephalon, demonstrated with anterograde tract tracing techniques, was compared in both hatchlings and older chickens in an effort to determine whether the terminal innervation pattern from the telencephalon changes postnatally. Finally, the results of the present investigation demonstrate additional non-retinal sources of afferent input to the LM from the nBOR of the

AOS, and the OT in chickens.

## Results

### Topography of the Hyperstriatum

The hyperstriatum occupies the dorsalmost position within the rostral telencephalon of birds, bulging out onto the dorsal surface of the cerebrum. In six week old chickens, this region extends from the midline to the vallecule, a shallow groove at the lateral border, and stretches posteriorly from the olfactory bulb about 5mm along the body axis. In Klüver-Barrera stained coronal sections, four layers can be recognized (Fig. 16). In order from ventral to dorsal, they are the the dorsal hyperstriatum (HD), the hyperstriatum intercalatus superior (HIS), the nucleus intercalatus hyperstriatum accessorium (IHA), and the hyperstriatum accessorium (HA) (Fig. 16b). The four dorsal layers are often referred to as the visual Wulst. Although the configuration of the layers changes from rostral to caudal portions of the Wulst, the layers maintain a similar relationship relative to each other. In the rostral half of the Wulst, the layers lie nearly perpendicular to the dorsal surface of the telencephalon while in the caudal half, the layers become narrower and oriented nearly parallel to the dorsal surface. The layers of the Wulst can be differentiated by their cytoarchitectonic characteristics. The HA, which contains dispersed medium to large-sized cells, is clearly distinguished from the IHA granule cell layer which contains cells oriented approximately into columns that lie perpendicular to the borders of the layer. Ventral to the IHA is the HIS which contains a more dispersed group of cells. Ventral to the HIS is the supreme frontal lamina (LFM), a thin fiber layer that separates the HIS from the HD layer which contains cells that are elongated in a mediolateral direction. Another fibrous layer, the superior frontal lamina (LFS) separates a deeper hyperstriatal layer, the ventral hyperstriatum (HV) from the rest of the Wulst.

### Telencephalic Projection to the LM

Injections of HRP were made into the LM of ten animals; two animals from the study of retinal afferents were included in this sample. Because of the shape of the target nucleus, none of these injections included all parts of the LM. All of the injections reported in this portion of the study were made into some portion of the rostral 650  $\mu\text{m}$  of the LM. No injections were attempted into the caudal ventral limb of the LMmc because of its small size (see chapter 2). Because the LMmc and LMpc are unusually thin in their mediolateral aspect, every injection included some portion of both the LMmc and LMpc. Of the ten injections, five representative examples are described below; one was a nearly complete injection of the LM, two were located primarily in the dorsal LM, one was in the middle LM and one was in the ventral LM.

In general, after HRP injections into the LM, retrogradely labeled projection neurons were found exclusively in the ipsilateral Wulst, within the lateral portions of the HA layer. The area containing these projection neurons extends approximately 4.0 mm rostrally from the caudal pole of the HA, but not in the rostralmost portions of the HA, which is considered somatosensory by virtue of its neuroanatomical connectivity (Karten et al., 1973). Furthermore, after injections into different portions of the LM, labeled cells were observed in different portions of the HA, suggesting an orderly mapping of the projection neurons and their terminals.

### Population of Telencephalic Neurons Projecting to LM

Retrogradely labeled neurons were found exclusively in the ipsilateral HA after a nearly complete injection of HRP (HRP-36) that was confined exclusively to the LM. As seen in Fig. 17a-d, the injection site was restricted to the LM without encroaching into any adjacent retinorecipient nuclei or into the optic tract and included all but the caudal ventral limb of the LM. As seen in Fig. 17e-j, this

projection area extended rostrally approximately 4.0 mm from the caudal pole of the HA and was confined to the lateral portions of this layer, on the border of the next adjoining layers, the HIS more medially and the IHA more laterally. Furthermore, within this lateral portion of the HA, labeled cells were found distributed from the dorsal to the ventral limits and throughout the rostrocaudal extent of the HA; this area is hereafter referred to as the HA projection area.

#### Morphology of Retrogradely Labeled Neurons Projecting to LM

The cell bodies of HRP labeled projection neurons measured 260.7-1378.9  $\mu\text{m}^2$  with a mean area of 678.9  $\mu\text{m}^2$  (S.D.= 173.8; n=185). As seen in the histogram in Fig. 18a, the distribution of neuronal areas suggests that a single population of neurons, based on size, projects to the LM. The cell bodies of these projection neurons tended to be round or stellate-shaped (Fig. 18b,c).

#### Spatial Organization of Telencephalic Projection to LM

*Injections into dorsal LM.* Two injections were made into the dorsal LM. Both of the injection sites (HRP-4 and HRP-27) were positioned primarily in the dorsal half of the LM (Fig. 19a and 20a). After these injections, retrogradely labeled neurons were found in the lateral portions of the ipsilateral IHA, up to 4.0 mm from the caudal pole and within the HA projection area. However, the neurons labeled after these dorsal injections were distributed primarily in the ventral HA with a greater concentration of neurons in the caudal portion of the projection area (Fig. 19b-g and 20b-g). Although both injections into dorsal LM resulted in the labeling of neurons within ventral portions of the HA, there were some subtle differences between the two dorsally placed injections discussed here that may account for differences in the position of the labeled neurons. The injection site of HRP-27 did not include a substantial portion of the rostral and caudal regions of the dorsal LM (Fig. 20a) and perhaps, as a result, did not label as many neurons in

ventral HA as did HRP-4 (compare Fig. 19c-g to Fig. 20 c-g). Furthermore, unlike HRP-4, the injection site of HRP-27 spread more ventrally in the LM (compare Fig. 19a and 20a) and perhaps as a result labeled a few neurons in the dorsal portions of the HA (compare 19c-g and 20c-g).

*Injections into ventral LM.* An injection into the ventral LM (HRP-59) included the entire ventral half of the LM in its rostral 300  $\mu$ m but became limited to the middle third of the LM further caudally (Fig. 21a). Labeled neurons were found throughout the entire rostrocaudal extent of the projection area up to 4.0 mm from the caudal pole. However, within the projection area, the labeled neurons were distributed primarily in the dorsal HA with a greater concentration of neurons in rostral HA (Fig. 21b-g). The smaller number of cells labeled in the caudodorsal HA (compare Fig. 21c with g) may be a consequence of the incomplete filling of the caudoventral LM with HRP (Fig. 21a).

*Injections into middle LM.* An injection (HRP-6) was restricted to the middle third of the LM along its dorsoventral axis from its rostral to caudal poles (Fig. 22a). Following this injection, labeled neurons were found extending up to 3.5 mm from the caudal pole, but not in the rostral 0.5 mm of the projection area in the HA. Within the projection area these neurons were distributed centrally and not in the dorsalmost or ventralmost limits of the projection area (Fig. 22 b-g).

Thus, as seen in a summary diagram of the position of cells within the HA resulting from these four injections (Fig. 23), a spatial organization of the telencephalic projection to the LM in chicks is found such that the ventral LM receives a projection from neurons distributed in dorsal and more rostral HA whereas the dorsal LM receives a projection from neurons in the caudal and more ventral HA. Neurons lying in middle portions of the projection area along its dorsoventral axis project to and terminate in the LM midway along its

dorsoventral axis. The position of the distribution of labeled neurons within the HA after injections into specific portions of the LM illustrated in Fig. 23 matches the position of the distribution of labeled neurons within the HA after the nearly complete injection into the LM (compare Fig. 17 and Fig. 23).

#### Anterograde Tracing of the Hyperstriatal-LM Projection in Older Chicken

Large pressure injections of tritiated proline and leucine or HRP into the HA projection area of seven chickens resulted in the labeling of the septomesencephalic tract, the major efferent outflow bundle of the Wulst, and in the labeling of terminals in the OT and a number of pretectal nuclei including the LM. As seen in Fig. 24, the labeling of terminals was distributed over the entire LMmc and the LMpc throughout their rostrocaudal extent. There was no apparent difference in the density of terminal labeling between the LMmc and the LMpc, nor was there any suggestion of a differential distribution of label within either subdivision of the LM.

#### Anterograde Tracing of the Hyperstriatal-LM Projection in Hatchlings

Large pressure injections of tritiated proline and leucine or HRP into the HA projection area of six hatchlings resulted in a pattern of labeling similar to that seen in older birds. As illustrated in Fig. 25, the terminal labeling is seen throughout the entire rostrocaudal extent of the LMmc and the LMpc. There was no difference in the density of terminal labeling between the LMmc and the LMpc nor was there any suggestion of differential labeling within either subdivision of the LM or between the magnocellular and parvicellular portions of the LM.

#### The Accessory Optic System Projection to the LM

After HRP injections that were restricted to the LM of five additional chickens, retrogradely labeled neurons were found throughout the entire rostrocaudal extent and within all three subdivisions of the nBOR, the nBORp, the

nBORd, and the nBORl (Fig. 26a). There was no apparent spatial organization to this projection. Retrogradely labeled neurons (Fig. 26b) were generally medium (10-19  $\mu\text{m}$  along the longest axis) (Fig. 26c) or large sized (20-29  $\mu\text{m}$  along the longest axis) (Fig. 26 d,e) cells, round or stellate in shape and were found within all three subdivisions.

#### The Tectal Projection to the LM

After HRP injections that were restricted to the LM of five chickens, the same injections used to describe the AOS projection, retrogradely labeled neurons were found in the optic tectum (Fig. 27 a, b). The labeled neurons were found throughout layers 2, 4, 8, 10, 13 and 14 and predominantly in the rostral half of the optic tectum. This was perhaps a consequence of the small discrete injections into LM because larger injections labeled more neurons in the caudal OT. There was no apparent spatial organization of this projection. Retrogradely labeled cells were small (6-9  $\mu\text{m}$  along the longest axis) and medium (10-19  $\mu\text{m}$  along the longest axis) in size and round or elongated in shape (Fig. 27 c,d,e). These results suggest that the LM receives a projection from the OT.

#### HRP Injections into the SS

Injections of HRP were restricted to the SS, adjacent to the LM in the medial pretectum, of three chickens. These injections did not label any neurons within the nBOR but resulted in the labeling of neurons in the OT in the same layers as the neurons labeled after injections into the LM. These results suggest that the nBOR provides an afferent projection to the LM but not the SS whereas the OT projects to both the LM and the SS.

### Discussion

#### Rationale for the Use of Retrograde and Anterograde Tract Tracing Techniques

HRP injections restricted to the LM enabled the identification of neurons within the telencephalon that project to the LM and revealed the spatial relationship between the location of these projection neurons and their termination within the LM. Unfortunately, the HRP retrograde tracing technique has drawbacks including the possibility of breaking fibers in passage during injection and the possibility of diffusion of injected HRP into neighboring nuclei resulting in some falsely labeled cells. Therefore, the telencephalic projection to the LM was confirmed with anterograde tract tracing techniques. In experiments comparing the terminal labeling of hatchlings and older chickens after injections into the HA, both axons and terminals were labeled similarly in hatchlings and six week old chickens. However, the results of these injections were not necessarily indicative of the ultrastructural maturity of the projection neurons or their synapses within the LM, or, of the functional efficacy of this projection. The projections from the nBOR and OT were not investigated with anterograde tract tracing techniques as they have already been described in detail in pigeons (nBOR: Brecha et al., 1980; OT: Brecha, 1978).

#### Topography of the Hyperstriatum in Birds

The avian telencephalon consists of five striatal masses. The hyperstriatum occupies the dorsalmost position of these masses, bulging out onto the dorsal surface of the cerebrum. There is a considerable interspecific variation among birds in the size of the hyperstriatum. On the one hand, in owls, the hyperstriatum extends over the entire dorsal surface of the rostral telencephalon while, on the other hand, in chickens, in agreement with the present study, it occupies only the rostromedial portion of the telencephalon (Adamo, 1967).

#### Organization of the HA to LM projection

This study identifies a population of neurons that is confined to a specific

portion of the HA of the visual telencephalon and that project to the LM in chicken. Furthermore, it reveals a spatial organization of the projection neurons. Neurons in the ventral portions of the projection area projected to the dorsal LM whereas labeled neurons in dorsal portions of the projection area projected to the ventral LM. Labeled neurons midway on the dorsoventral axis within the projection area projected midway within the LM.

These results are not only consistent with previous anterograde degeneration studies (Adamo 1967; Karten et al., 1973) and anterograde labeling studies (Miceli et al. 1978) that identified a Wulst projection to the pretectum in a variety of birds, but in addition, the results suggest that both the LMmc and the LMpc receive a direct input from projection neurons located exclusively in the lateral HA.

The finding that projection neurons are restricted to the HA is consistent with evidence identifying the HA layer as the source of extratelencephalic Wulst projections in pigeons (Reiner and Karten, 1983). Their report, in conjunction with reports identifying the IHA as the cell layer within the Wulst that receives visual input from the retinorecipient dorsolateral thalamic complex (Karten et al., 1973; Streit et al. 1980; Watanabe et al. 1983), suggest that the afferent thalamic terminals and efferent projection neurons of the visual Wulst are segregated from one another. The finding in the present study of projection neurons exclusively within the HA lends further support to this notion.

The segregation of inputs and outputs raises questions about the visuotopic organization of afferent projections and the visuotopic organization of efferent projections. A brief report of the response properties of units within the visual Wulst in pigeons (Revzin, 1969) and a study of the response properties of units in the visual Wulst of owls suggest that the visual field maps of IHA and HA are in register with one another (Pettigrew and Konishi, 1976). The implication is that

neurons in IHA project to HA although there is no direct evidence currently available for this projection.

Other neurophysiological studies of the visual Wulst in birds have suggested that there is a retinotopic organization of this area although it differs for different species. In owls, the temporal to nasal retina of the contralateral eye is mapped along the lateral to medial axis of the visual Wulst, while the inferior to superior retina is mapped along the caudal to rostral visual Wulst axis (Pettigrew and Konishi, 1976). In chicken, there appears to be a predominantly dorso-ventral topographic organization within the Wulst spanning the HA, IHA and HIS layers with the superior nasal retina represented in the most dorsal Wulst, the superior temporal and inferior temporal retina represented in dorso-middle and ventro-middle Wulst and the inferior nasal retina in the ventral most Wulst (Wilson, 1980). The topographic organization in the anterior-posterior axis of the Wulst is less clear though there is a greater representation of the superior retina in the anterior Wulst and a greater representation of the inferior retina in the caudal Wulst (Fig. 28). The predominance of a dorso-ventral topography is different from the topographical organization reported for the Wulst of owls. Given the restricted mediolateral extent of the chicken Wulst, the difference in the representation in these studies is not surprising.

Since the HA contains a retinotopic map and projects to visuotopically organized structures such as the tectum in owls and pigeons, it seems likely that the efferent projections of the Wulst would be retinotopically organized. This has been shown to be true for the telencephalic projection to the OT in owls and suggested in the pigeon (Bravo and Pettigrew, 1981; Karten et al, 1973; Brecha, 1978). The present study lends further support to the notion that a retinotopically organized visual area, the LM (see Chapter 5), also receives a spatially organized projection from the HA of the visual telencephalon. In

addition, the present study, in conjunction with the neurophysiological evidence for a retinotopic organization of the HA, suggests that specific portions of the LM receive an orderly projection from corresponding portions of the retina, either indirectly through the HA of the visual Wulst or directly from the retina (Fig. 27). The superior nasal retina projects indirectly via the dorsal and more rostral regions of the Wulst and directly to a small portion of the middle and caudal LM, the superior temporal retina projects indirectly via the middle Wulst and directly to the ventral LM from rostral to caudal, the inferior temporal retina projects indirectly via the middle Wulst and directly to the rostradorsal LM and the inferior nasal retina projects via the ventral and more posterior regions of the Wulst and directly to the caudodorsal LM. This finding suggests that in chickens, a specific visuotopic pattern is maintained in the spatial organization of the projecting axons and their terminals not only directly to the primary retinorecipient nuclei but also from these primary visual nuclei to the higher order telencephalic layers and then through the efferent projections of the HA to terminate in patterns that may be in register with the spatially organized direct retinal projection. Such a specific spatial organization is especially curious in light of the fact that the units in the LM respond to large field movement of the visual world, and the adaptive advantage of a spatially organized direct and indirect retinal projection to this area is not readily apparent. This spatial organization may be a consequence of developmental mechanisms as has been suggested for the retinal projection. Perhaps, it is the orderly arrangement of retinal axons in the optic tracts leading to primary visual areas together with some specific molecular markers common to these primary, secondary or tertiary terminal sites that dictate a very specific spatial organization of direct or indirect retinal pathways.

The present investigation provides evidence for the retinotopic organization of the efferent projections to the LM from the Wulst, a finding similar to that found

from the striate cortex of mammals to the NOT (Updyke, 1977). Both the Wulst and the striate cortex receive a topographically organized input from retinorecipient nuclei in the thalamus. This input appears restricted to deeper layers of the visual Wulst (IHA, HIS, IID) and layer 4 of the striate cortex segregated from the output; the neurons projecting to the LM are restricted to specific regions of the HA while the neurons of layers 5 and 6 are sources of extratelenchephalic efferents in mammals. The visual Wulst and striate cortex have other similar efferent projection targets including a reciprocal projection to the retinorecipient thalamic cell groups, the GLv, the tectum and several visual pretectal nuclei including the LM in birds and the NOT in mammals.

#### Development of the HA to LM projection

Previously, it has been suggested that the changes in the metabolic mapping pattern of the LM observed in older birds in comparison to hatchlings may be a result of the development of the telencephalic-pretectal pathway (McKenna and Wallman, 1985a). Specifically, the distribution of 2-DG label in response to temporal to nasal motion changes from a diffuse labeling of both LMmc and LMpc in hatchlings to the labeling of LMmc only in older birds whereas the labeling pattern after nasal to temporal motion changes from a diffuse labeling of the LMpc in hatchlings to a distinct diagonal band within the LMpc in older birds.

The results of the present study suggest that the telencephalic terminal innervation pattern within the LM is present at hatching and does not change postnatally. However, the techniques used in the present study to trace the presence of this projection could not assess the functional state of this projection. It is conceivable that, while the innervation pattern within the LM does not change postnatally, there is an improvement in the efficacy of transmission or selective amplification of this projection, perhaps due to the maturation of the projection neurons within the HA or a maturation of the synaptic terminals of

HA afferents with neurons in the LM. In support of this notion, it has been suggested previously that in kittens the afferents from the visual cortex to the NOT cannot be activated for some time after they first form synaptic contacts (Schoppmann, 1985).

The notion that the projection from the HA to the LM is inhibitory in nature has been suggested by McKenna and Wallman (1985a). The authors suggest that since the change in the 2-DG labeling pattern in the LMpc coincides with the reduction in OKN response in the nasal to temporal direction in older chicks (McKenna and Wallman, 1985a), the reduction may be due to the inhibition of nasal to temporal responsive units in the LM caused by the newly activated afferents from the Wulst (Wallman and Velez, 1985). Consistent with this notion is a preliminary finding (Letelier, personal communication) that after bilateral HA ablation in older chickens, the ability of the eye to follow large field slow velocity motion in the nasal to temporal direction improves. In addition, parallel evidence in pigeons indicates that the projection from the HA to the optic tectum, which arises from similar portions of the HA as the projection to the LM, is inhibitory (Bagnoli et al., 1979)

#### The nBOR and Optic Tectum Projections to the LM

In addition to the telencephalic projection to the LM, the present study identifies both the nBOR and the OT as sources of non-retinal afferent projections to the LM. For the nBOR, medium and large neurons located in all three of its subdivisions were found to project to the LM. These findings are in agreement with those reported in pigeons (Brecha et al., 1980). A similar projection has been identified in mammals from the medial terminal nucleus (MTN) of the accessory optic system to the NOT (Yamamoto, 1979).

The results of the present investigation have also identified neurons in tectal layers 2, 4, 6, 10, 13, and 14 that project to the LM. These findings are consistent

with the report of a tectal projection to the LMpc, LMmc and GT (Hunt and Kunzle, 1976) and the report of a tectal projection to the LM/PTO complex in pigeons (Brecha, 1978). A similar projection from the superior colliculus to the NOT has been reported in mammals (Graham, 1977; Berman, 1977).

In addition, the results of the present study demonstrate that injections into the SS result in the labeling of tectal neurons in similar positions and in the same layers as injections into the LM. This finding is in agreement with the report in pigeons of a tectal projection to the PTO in addition to the LM. Furthermore, the present study demonstrates that the LM receives a projection from the nBOR whereas the SS does not, a finding similar to that reported in pigeons (Brecha et al., 1980). The latter finding lends support to the notion that the LM and SS are indeed two distinct and separate nuclei within the avian pretectum and argues against the definition of the LM as suggested by Gamlin and Cohen (1988a,b).

## Chapter 7: THE ORGANIZATION OF THE EFFERENT PROJECTIONS OF THE LM

### Introduction

It has been suggested previously that the specific oculomotor function of the LM in birds may be to relay neural signals of horizontal visual field motion to oculomotor circuits through which optokinetic pursuit is generated (Winterson and Brauth, 1985). This notion is further supported by behavioral evidence implicating the LM in the generation of horizontal optokinetic pursuit such that after lesions of the LM, horizontal optokinetic pursuit is disrupted (Gioanni et al., 1983). The following experiments were undertaken to elucidate the organization of the efferent pathways of the LM through which horizontal optokinetic pursuit may be generated.

There are few neuroanatomical studies that describe the efferent connectivity of the LM in birds. A recent study by Gamlin and Cohen (1988b) identifies the efferent projection targets of the so-called LM in pigeons. These efferent target nuclei include the inferior olive (IO) cerebellum (Cb), n. papilliformis (nPap), nucleus of the basal optic root (nBOR), ventral nucleus of the deep mesencephalon (MPv), principal precommissural nucleus (PPC), stratum cellulare externum (SCE), lateral pontine nucleus (LP) and medial pontine nucleus (MP). Furthermore, HRP injections into several of these target nuclei revealed that different subpopulations of neurons within the LM project to different targets. However, as described previously, the interpretation of these results is confounded by a modified nomenclature for the pretectal nuclei and a definition of the LM that combines the SS and LM into a single area which, only conforms partially to the area defined here, both anatomically and functionally, as the LMmc and LMpc.

Several other studies in pigeons have identified projection neurons within the pretectal area, which corresponds to the LM, after retrograde tract tracing experiments of the Cb and LP (Clarke, 1977; Brauth and Karten, 1977), IO

(Brecha et al., 1980), OT (Brecha, 1978), and nBOR (Azevedo et al., 1983). However, little information is offered with regard to the position, size, or shape of these projection neurons.

Thus, the aim of this portion of the study was to identify the efferent projection pathways and target nuclei of the LM in chickens with the HRP and  $^3\text{H}$ -amino acid anterograde tract tracing techniques and to identify the projection neurons within the LM, with the retrograde tracing technique, after HRP injections into several of the efferent target areas.

## Results

### Identification of Efferent Targets

HRP injections into seven chickens and  $^3\text{H}$ -proline and leucine injections into two chickens were successfully restricted to only the LM. Similar results were obtained with both methods. Only the four largest injections resulted in labeled terminals in all of the efferent projection targets identified in this study. Although the smaller injections did not label all terminal target areas, they labeled fibers entering the projection target areas more clearly and thus enabled the use of two criteria, fibers entering into targets and the labeling of terminals within these areas, to identify the efferent projections targets of the LM.

After a typical injection (HRP-16) (Fig. 29a) into the LM, three groups of axons were seen leaving the injection site traveling caudally, each in a separate direction (Fig. 29b). They were designated the lateral, dorsal (which contains two branches), and ventral bundle.

The lateral bundle directly entered the adjacent optic tectum, coursing through the deeper tectal layers (see Fig. 30a, b) with most of the fibers terminating in layer 7, primarily within the more rostral and lateral portions of the tectum (Fig. 31). Additional light terminal labeling was evidenced in layers 4, 9, 11, 12, 13. Larger injections that included most of the LM resulted in a

heavier labeling of terminals in more caudal portions of the OT.

The dorsal bundle of axons that exited the LM first traveled caudally a short distance before dividing into two separate branches, the dorsomedial and ventromedial branches, that coursed around the dorsolateral and ventromedial borders of the lateral spiriform nucleus (Fig. 30a). Axons that made up the dorsomedial branch traveled dorsally and medially with some fibers from this group terminating in the medial portion of the ipsilateral pretectal nucleus (Pt) (Fig. 30a). Other axons from this branch continued medially with some terminating in the ipsilateral pretectal area (AP) (Fig. 30a, b). Those axons, which did not terminate in AP, continued medially towards the posterior commissure (Fig. 30a, b) eventually crossing to terminate in the contralateral dorsomesencephalic lateral reticular formation (FRL) (not illustrated). The ventromedial branch of the dorsal bundle traveled medially with some axons terminating in the ipsilateral principal precommissural nucleus (PPC) (Fig. 30a, b). Other axons continued medially moving in two separate directions, one group traveling dorsally toward the posterior commissure, the other group traveling ventrally to terminate in the ipsilateral nucleus Darkschewitsch (nD) (Fig. 30a, b; Fig. 32).

The ventral bundle of descending axons projected ventromedially with fibers dividing into two branches, the ventromedial and dorsomedial branches, that coursed around the ventrolateral and dorsomedial aspects of the subpretectal nucleus (SP) (Fig. 30a). The ventromedial branch contained fewer axons that coursed medially and entered the lateral aspect of the ipsilateral nucleus of the basal optic root to terminate in all three subdivisions, the nBORl, nBORp and nBORd (Fig. 30b; Fig. 33). The dorsomedial branch, which contained the bulk of axons of the ventral bundle, projected medially, but dorsal to the nBOR complex, although some axons were seen entering and terminating in the nBORd.

Caudal to the nBOR, the ventral bundle separated into two branches, one projecting medially and the other laterally. Axons in the medial branch continued caudally with some axons entering and terminating in the ipsilateral ventral portion of the nucleus of the deep mesencephalon (MPv), the papilliform nucleus (nPap) (Fig. 30c) and further caudally, the medial pontine nucleus (MP) (Fig. 3 d; Fig. 34). Some axons from this branch continued caudally to enter the ipsilateral inferior olive from the ventral aspect and terminated in the rostral portions of the inferior olive (Fig. 30e; Fig. 35). The axons in the lateral branch projected laterally and caudally coursing dorsal to the lateral pontine nucleus (LP) (Fig. 30d). Some axons turned ventrally to enter and terminate in the ipsilateral LP (Fig. 30d; Fig. 36); the rest turned dorsally and joined the brachium conjunctivum cerebellopetale (BCP) further caudally (Fig. 30d). Axons in the BCP projected both contralaterally and ipsilaterally to terminate in folia VI, VIIIa and b, and IXa and c of the Cb (Fig. 30f; Fig. 37).

In addition to the descending efferent projections described above, there was a group of ascending fibers that exited the dorsal LM and projected rostrally to ipsilateral thalamic areas. These fibers terminated in both dorsal and ventral thalamic areas including the ventrolateral geniculate nucleus (GLv), dorsolateral nucleus of the anterior thalamus, magnocellular portion, (DLAmc), dorsolateral nucleus of the anterior thalamus, lateral portion (DLL), and intercalated nucleus of the thalamus (ICT) (not illustrated). These efferent target nuclei of the LM were not verified with the HRP retrograde tract tracing technique.

#### Identification of Projection Neurons

The descending projections of the LM, defined by the anterograde tract tracing experiments, were examined using the HRP retrograde tract tracing technique. After injections into the nBOR, nD, pontine nuclei, IO, or Cb, 440 HRP-labeled LM neurons that were well-filled were drawn with a drawing tube and

measurements made from these drawings. Labeled neurons were classified on the basis of size and assigned to one of three categories, small (10-19  $\mu\text{m}$  along the longest axis), medium (20-29  $\mu\text{m}$  along the longest axis ) and large (30-39  $\mu\text{m}$  along the longest axis) neurons. These results suggest that different subpopulations of neurons based on size, some restricted to specific portions of the LM, project to different efferent target nuclei (Table 3).

After HRP injections that included all three subdivisions of the nBOR, small, medium and large neurons within both subdivisions of the LM were labeled in approximately equal numbers throughout the ipsilateral but some also in the contralateral LMmc and the LMpc. Of the 92 neurons identified, 33.7% were small, 40.2% were medium, and 26.1% were large neurons (Table 3). Most of the small and medium neurons tended to be round in shape whereas the large cells tended to be elongated in shape (Fig. 38).

HRP injections that included both the LP and MP resulted in the labeling of small, medium and large cells in both the LMmc and the LMpc. Of the 128 neurons identified, 21.1% were small, 44.5% were medium and 34.4% were large neurons (Table 3). Most of the small and medium neurons appeared stellate or round in shape whereas the large neurons tended to be round or elongated in shape (Fig. 39).

After HRP injections into the nD, most of the cells that were labeled were found in the LMmc. Of the 56 neurons identified, 80.4% were medium and only 19.6% were large neurons (Table 3). No small cells were labeled after injections into nD. Most of the labeled cells were round or elongated in shape (Fig. 40).

HRP injections into the IO labeled approximately equal numbers of medium and large neurons primarily within the LMmc. Of the 67 neurons identified, 52.2% were medium and 47.8% were large neurons. No small cells were labeled after these injections (Table 3). Most neurons that were labeled appeared round in

shape (Fig. 41).

After HRP injections into the Cb, more than twice as many large as medium neurons were labeled and these were found primarily within the LMmc. Of the 97 neurons identified, 69.1% were large whereas 30.9% were medium sized. Again, no small cells were labeled (Table 3). Labeled neurons were round or elongated in shape (Fig. 42).

## Discussion

### Rationale for Using the Anterograde and Retrograde Tracing Techniques

The HRP and tritiated amino acid anterograde tracing techniques enabled the labeling of the efferent projection pathways and the target nuclei of the LM. However, because of the possibility of false labeling as a consequence of the uptake of tracer by fibers in passage broken during injection, several of the efferent target nuclei of the LM including the nBOR, LP/MP, nD, IO, and Cb, thought to play a role in the generation of horizontal optokinetic pursuit were injected with HRP, thereby confirming these projections by retrogradely labeling the cells of origin within the LM.

### Efferent projections of the LM

The results of the present study suggest that the LM in chickens projects to several target nuclei including the ipsilateral OT, Pt, AP, PPC, nD, bilaterally to the nBOR, the contralateral FRL, the ipsilateral MPv, nPap, MP, LP, IO, and bilaterally to the Cb. Ascending projections of the LM terminate ipsilaterally in dorsal and ventral thalamic areas including the GLv, DLAmc, DLL and ICT.

A comparison of these results to another study in pigeons (Gamlin and Cohen, 1988b) is difficult because the pretectal area designated as the LM in pigeons in the available schematic drawings is not equivalent to the LM in the present study. For the pigeon, these authors have defined the LM as composed of two

subdivisions, the lentiform nucleus of the mesencephalon medialis and lateralis (LMm and LMI). These, however, are not equivalent to the LMmc and the LMpc. The portion of the pretectum designated as the LMm by Gamlin and Cohen appears to correspond to the SS in chickens as described by Ehrlich and Mark, (1985) and by the present study (see Table 1). The LMmc and LMpc defined both anatomically and functionally in this investigation are equivalent to the LMI and GI respectively as defined by Gamlin and Cohen. The differences in identification may be attributed to the indistinct boundaries of the pigeon pretectal nuclei when compared with the chicken pretectal nuclei (personal observation).

Despite these differences, the results of the present study are in general agreement with those reported for the pigeon LM (Gamlin and Cohen, 1988b). Both studies describe the IO, Cb, LP, nPap, MPv, PPC, and nBOR as receiving a projection from the LM. The present study also provides strong evidence for projections from the LM to the OT and MP; these have been only tentatively suggested in the pigeon.

There were, however, differences between the results of the present study and those reported in pigeons, some of which may be explained in part by the difference in the definition of the LM. On the one hand, the pigeon study suggests a projection from the LM to the stratum cellulare externum (SCE) whereas the present study does not. On the other hand the present study provides evidence for a projection from the LM to the AP, nD, and several thalamic nuclei whereas the pigeon study does not. The difference in the definition of the pretectal nuclei may account for the failure to find a projection from the LM to SCE in the present study when compared with the pigeon study. This projection may arise from the pretectal area designated as the LMm in the Gamlin and Cohen study and the SS in the present study. Although several HRP injections were made into the SS in the present study, the projection to the SCE could not be verified in these

experiments because of the technical problems associated with high background resulting from large injections. However, differences in the identification of the nuclei in the pretectal region does not explain the failure to find a projection from the LM to the AP and nD in pigeons as reported by Gamlin and Cohen. Neither the SS nor the GT as designated by Gamlin and Cohen (equivalent to the LMpc in the present study), project to either of these targets. However, the GT does give rise to ascending projections to thalamic areas including the DLAmc, DLL, ICT, GLv, (identified as targets of the LM in chickens in the present study) as well as the nucleus dorsolateralis medialis thalami (DLM), nucleus decussatio supraoptica, pars ventralis (nDSV), and nucleus posteroventralis thalami (PV) (not identified as targets in the present study). The pigeon GT also projects to the OT, a projection found to originate in the LM of chickens in the present study. Thus, most of the differences in the efferent connectivity of the LM in chickens and pigeons may be a consequence of different definitions of this area in these species; alternatively, these differences could be a result of species-specific variation.

#### Identification of cell populations projecting to target nuclei

The results of the present study suggest that within the LM, different subpopulations of neurons based on size project to different efferent target nuclei. Furthermore, several targets receive their projections from neurons primarily in one subdivision, the LMmc. These results are supported the scant evidence available in other avian species.

Although projections from the LM to nBOR, LP, and MP, have been reported previously in pigeons (nBOR: Azevedo et al., 1983; LP: Clarke, 1977; LP and MP: Gamlin and Cohen, 1988b), the cell types or sizes of the projection neurons within the LM were not identified. The results of the present study suggest that small, medium, and large cells within both the LMmc and LMpc, project to the nBOR whereas some small but mostly medium and large cells within both the LMmc

and LMpc project to the pontine nuclei.

A projection from the LM to the IO and from large cells in the LM to the Cb has also been identified previously in pigeons (Gamlin and Cohen, 1988b; Brecha et al., 1980; Clarke, 1977; Brauth and Karten, 1977). The present study in chickens identifies both medium and large cells found primarily in the LMmc that project to the IO whereas some medium but mostly large cells project to the Cb. Moreover, the present study suggests in birds for the first time that mostly medium size cells that lie primarily in the LMmc project to the n. Darkschewitsch.

Thus, subpopulations of different sized cells project to the different efferent target nuclei of the LM. This organization of the efferent pathways may reflect a differential distribution of different types of signals necessary for the generation of horizontal optokinetic pursuit to these target nuclei or alternatively, may carry different information regarding optokinetic functioning to these areas.

#### Efferent projections of the nBOR

Both the LM and nBOR have been implicated in the processing of retinal slip signals and in the generation of optokinetic pursuit. This similarity in function may also be reflected in the efferent connectivity of these areas. The efferent projections of the nBOR in pigeons include the vestibulocerebellum, inferior olive, oculomotor nuclei, interstitial nucleus of Cajal, contralateral nBOR, and LMmc (Brecha et al., 1980). Thus, coupled with the results of the present study, in birds, both the LM and nBOR project to vestibulocerebellum and the inferior olive. In contrast to the nBOR, no direct projection from the LM to the oculomotor nuclei or the interstitial nucleus of Cajal in birds has been found in this or other studies (Gamlin and Cohen, 1988b).

#### Efferent projections of the NOT in mammals

It has been previously suggested that the LM in birds may be homologous to the NOT in mammals. This suggestion is based on embryological evidence suggesting a common derivation from the tectal plate and their similar position within the pretectum (Kuhlenbeck and Miller, 1943). A comparison of the efferent connectivity would lend further support for this notion of homology. The evidence from mammalian studies of the efferent connections of the NOT detailed in Chapter 2 suggests that the NOT projects to the anterior pretectal nucleus, the contralateral NOT, MTN, DTN, superior colliculus, pontine nuclei, nRTP, and the dorsal cap of the inferior olive, mesencephalic reticular formation, interstitial nucleus of Cajal, n. Darkschewitsch and labels fibers in the posterior commissure (rat: Terasawa, 1979; cat: Graybiel, 1974; Berman, 1977; Itoh, 1977; rabbit: Holstege and Collewyn, 1982). The similarity of efferent targets of the NOT and the LM in both mammals and birds lends further evidence to support the notion that the LM in birds is homologous to the NOT in mammals.

## Chapter 8: GENERAL DISCUSSION

It has been previously suggested that the LM in birds is an integral part of the neural circuitry that generates horizontal optokinetic pursuit (chickens: Wallman et al., 1981; pigeons: Brauth and Karten, 1977; Brecha et al., 1980; Gianni et al., 1983). The results of the present study of the afferent and efferent projections of the LM (Fig. 43) reveal a connectivity scheme for the neural circuits that may generate this behavior. The LM receives a contralateral projection from the retina, the ipsilateral HA of the visual telencephalon, the ipsilateral optic tectum and ipsilateral nBOR. Ascending efferent projections of the LM terminate in ipsilateral thalamic areas including the GLv, DLAmc, DLL, and ICT. The descending efferent projections of the LM terminate ipsilaterally in the OT and bilaterally in nBOR (reciprocal connections), ipsilaterally in the nD, nPap, MPv, MP, LP, IO, contralaterally in FRL, and bilaterally in the Cb. Both the Cb (via the vestibular nuclei) and nD have been reported to project to the oculomotor nuclei presumably providing pathways for signals to modulate the activity of the extraocular muscles to generate the appropriate compensatory eye movement (Fig. 43). The anatomical evidence for the connectivity of the chicken LM as demonstrated in this study and the neurophysiological and behavioral evidence from other studies provide a basis on which to speculate about the functional role of the various afferent and efferent projections of the LM.

There is considerable evidence regarding the response properties of the LM in birds. A neurophysiological study of the LM in pigeons implicates the LM in receiving slip signals (the stimulus for OKN) from the retina. Units in the LM have large receptive fields, are direction selective responding to motion in mostly horizontal but also non-horizontal directions, and are velocity selective, preferring not only slow but also fast velocities (Winterson and Brauth, 1985). There is a segregation of units with particular response properties within the LM such that

the LMmc is responsive to temporal to nasal motion whereas both LMmc and LMpc are responsive to nasal to temporal motion (chickens: McKenna and Wallman, 1981, 1985a; pigeons: Morgan and Frost, 1983). Furthermore, there is a segregation within the LM such that units in the LMmc tend to prefer low velocity visual motion whereas units in the LMpc tend to prefer high velocity visual motion (Winterson and Brauth, 1985). The presence of units preferring fast velocities in addition to slow velocities is a characteristic shared by units in the mammalian NOT. These physiological properties suggest that the specific oculomotor function of the LM may be to relay retinal slip signals from movement of large portions of the visual field in mostly horizontal directions to oculomotor circuits through which optokinetic pursuit is generated (Winterson and Brauth, 1985).

#### Functional Role of Afferents

As demonstrated in the present study, the projection from the eye to the LM originates from retinal ganglion cells. Presumably, these retinal ganglion cells share similar functional properties with the neurons to which they project in the LM; that is, the retinal ganglion cells are direction selective in mostly horizontal directions and are velocity sensitive across a broad range of velocities. This similarity in functional characteristics has been demonstrated for the retinal ganglion cells and the neurons that receive their projection in the NOT (rabbits: Oyster, 1968; Oyster et al., 1972; cats: Hoffmann and Schoppmann, 1985). Thus, after detecting movement of portions of the visual field, retinal ganglion cells send signals coding for different velocities of mostly horizontal directional movement via these retinal afferents that converge onto neurons in the LM.

Some functional evidence, however, argues against the notion that the direct retinal projection is the sole pathway for optokinetic signals to reach the LM. Giovanni et al., (1983) report that after lesions of the LM, although temporal to

nasal optokinetic pursuit is eliminated, nasal to temporal optokinetic pursuit is only reduced, but not eliminated. This finding may be a result of the incomplete lesioning of the LM, a possibility because of the shape of the LM (see Chapter 4). Alternatively, this finding may suggest that the signals coding for nasal to temporal directional motion are processed in other areas. It has been previously reported that both the nBORI as well as the LM accumulate 2-DG in response to horizontal optokinetic stimulation (McKenna and Wallman, 1981; 1985a). Thus, despite the LM lesions, the nBORI may continue to process these nasal to temporal directional signals and, in turn, generate nasal to temporal optokinetic pursuit.

Similarly, the direct retinal pathway may be responsible for the responsivity of the LM to nonhorizontal directions or alternatively, these signals may reach the LM from other nuclei, perhaps the nBOR. This speculation is based on neurophysiological evidence that units in both the LM (Winterson and Brauth, 1985) and the nBOR (Burns and Wallman, 1981; Burns, 1985) are responsive to nonhorizontal directional movement of large portions of the visual field and the report of a direct projection from the nBOR to the LM in the present study. Thus, the projection from the nBOR (which also receives a reciprocal projection from the LM, discussed below) to the LM may provide a pathway for nonhorizontal retinal slip signals to reach the LM.

The function of the projection from the HA of the visual telencephalon to the LM that was identified in the present study has been speculated about previously. During postnatal development in mammals, the progressive loss of asymmetry in OKN and the improved response to fast velocity retinal slip signals has been attributed to the development of the cortico-pretectal pathway (humans and monkeys: Atkinson, 1979; cats: Malach et al., 1981; Naegele and Held, 1982). Similarly, it has been suggested that the projection from the HIA to the LM in birds develops postnatally and that its development may be responsible for

postnatal changes in the generation of horizontal optokinetic pursuit (McKenna and Wallman, 1985a; Wallman and Velez, 1985). This notion is based on metabolic mapping evidence suggesting postnatal changes in the labeling pattern of the LM and behavioral evidence suggesting a reduction in the ability to generate nasal to temporal optokinetic pursuit. The behavioral change in optokinetic responsiveness, manifested by the increase in directional asymmetry due to the reduction in the ability of the LM to generate nasal to temporal optokinetic pursuit, may be a result of the development of an inhibitory pathway from the HA to the LM (Wallman and Velez, 1985).

Some preliminary data from a study of the effects of ablations of the visual telencephalon on horizontal optokinetic pursuit (Letelier, personal communication) further supports the notion that the HA projection to the LM may indeed be inhibitory in nature. After bilateral ablation of the HA in chickens, the ability of the eye to execute horizontal optokinetic pursuit in the nasal to temporal direction improved over a wide range of velocities. Consistent with this notion of an inhibitory pathway is parallel evidence from a study of the interaction of visual Wulst and optic tract impulses on single units of the pigeon optic tectum. After excitation of tectal units through stimulation of the optic tract, subsequent visual Wulst stimulation exerts long lasting inhibitory effects on the tectal units (Bagnoli et al., 1979). The projection from the HA to retinorecipient neurons in the optic tectum arises from similar portions of the HA as the projection to the LM (personal observation).

The projection from the optic tectum (which also receives a reciprocal projection from the LM and is discussed below) to the LM originating from retinorecipient layers 2, 4, 8, and layers 10, 13, 14, may provide another indirect pathway for retinal slip signals that drive OKN to reach the LM or alternatively, it may serve some other function such as an activation pathway to the LM.

Evidence that contradicts the first notion comes from studies in mammals which demonstrate that optokinetic pursuit in horizontal directions can be executed even after ablation of the superior colliculus (Collewijn, 1975a). If, in a similar fashion in birds, the optic tectum is not relaying retinal slip signals necessary for the generation of horizontal OKN, then the OT may be providing information other than retinal slip signals to the LM. Presumably, this pathway could transmit signals to the LM which affect response threshold levels of units to the incoming retinal slip information similar to the manner in which the reticular formation exercises an effect on cortical threshold levels for detecting stimuli (Lindsley et al., 1950) resulting in an increased alertness of the subject (Fuster, 1958).

An ultrastructure study of the LMmc in chickens suggests the presence of both excitatory and inhibitory synapses onto neurons in this area (Gottlieb and McKenna, 1986) and fuels further speculation regarding the afferent connectivity of the LM. Neurons in the LMmc have primarily two types of presynaptic profiles. The first type of presynaptic profile encountered forms axodendritic synapses and shares characteristics associated with excitatory synapses. These may originate primarily in the retina. The second type of presynaptic profile forms axosomatic synapses and shares characteristics associated with inhibitory synapses. Although the authors suggest that the latter may originate primarily in the HA, one cannot eliminate the possibility that the inhibitory input may originate from the OT or the nBOR although there is no evidence to support this notion. Presumably, signals coding for direction and velocity, which are integral to the LM in generating optokinetic pursuit, are excitatory and may be transmitted through axodendritic synapses whereas inhibitory signals from the HA which may help reduce the ability of the LM to generate optokinetic pursuit may be transmitted at axosomatic synapses.

Thus, upon the initiation of movement of large portions of the visual field, the afferent projection from the optic tectum may provide a pathway for signals to reach the LM alerting it to incoming retinal slip signals. The major excitatory input coming primarily from the retina to the LM may carry most of the directional information in both temporal to nasal and nasal to temporal directions whereas the HA projection to the LM may have a modulatory function, inhibiting to some degree the generation of optokinetic pursuit in the nasal to temporal direction. The projection from the nBOR may provide a pathway for nonhorizontal retinal slip signals to reach the LM (Fig. 4.3).

#### Functional Role of Efferents

The effect of lesions of the LM on horizontal OKN lends support to the notion that some of the efferent pathways of the LM play a role in the generation of horizontal optokinetic pursuit (Gioanni et al., 1983) whereas other efferent pathways may have a different but related functional role.

Although there is no evidence for the function of most of the efferent projections of the LM identified in the present study (Fig. 4.3), the available connectivity studies provide a basis for speculation. The projection from the LM to the DLI and DLAmc may provide a pathway for signals, coding for the ongoing optokinetic functioning of the LM, to reach the visual Wulst. Both the DLI and DLAmc together with the anterolateral nucleus of the thalamus (LA) make up the primary retinorecipient area of the thalamus collectively referred to as the principal optic nucleus of the thalamus (OPT); the OPT is known to project to the visual Wulst in owls and pigeons (Karten et al., 1973). Thus, the pathway from the LM to the OPT may provide a means for signals to reach the visual Wulst presumably resulting in the modulation of LM units via the HA to the LM pathway described above. The projection from the LM to the DLL reported in the present study has been verified in pigeons with retrograde tract

tracing techniques (M. Wild, personal communication).

The LM projects to three additional visual areas in the midbrain, the OT, GLv, and AP, all of which receive a direct retinal projection and each of which subserves a different visual function. The finding of LM projections to these areas suggests that other visual areas in the chicken brain are not isolated from information regarding the optokinetic functioning of the LM.

The projection from LM to OT may transmit a signal regarding the retinal slip processing in the LM, or alternatively, it may transmit other forms of visual information. Although there is no functional evidence in support of the former notion, the projection from the LM to the neurons in retinorecipient layers 4 (which also sends an efferent projection to the LM) and 7 and the deeper tectal layers 9, 11, 12 and 13 (layer 13 sends an efferent projection to the LM), which give rise to descending pathways presumed to be involved in motor functions (Reiner and Karten, 1982), may modulate the activity of neurons in these layers. Connectivity studies in pigeons report that tectal layers 11, 12, and 13 project to the contralateral reticular formation of the hindbrain while layers 9, 11, and 13 project to the ipsilateral lateral pontine nucleus (Reiner and Karten, 1982). The terminals of the projection from the OT to the LP could overlap the terminals of fibers projecting directly from the LM to the LP (a finding in the present study). Thus, on the basis of connectivity evidence, it is conceivable that the projection from the LM to the OT may provide pathways along which signals, coding for the retinal slip processing in the LM, may travel. In support of the latter notion, that the LM projection to the OT may transmit other forms of visual information, is evidence in frogs that the pretectal region has been implicated in a variety of visuomotor functions including prey selection, habituation, predator avoidance, and detection of stationary objects and barriers (Fite, 1985). Since the OT is the main retinorecipient area of the avian brain, it may play a role in the generation

of these behaviors that require visual functioning. Thus, signals necessary for the generation of behaviors to occur could conceivably be processed in the LM and transmitted to the optic tectum.

The LM projection to the retinorecipient GLv may provide a pathway for signals regarding retinal slip processing to reach this visual area or alternatively, the pathway may modulate the activity of the GLv which has many color-opponent units and plays a role in the behavioral discrimination of chromatic categories (Maturana and Varela, 1982). Connectivity studies in birds suggest that the GLv also receives a large projection from the OT (Crossland and Uchwat, 1979); no functional evidence is available concerning the role of this projection in visual functions. The coincidental termination of projections from the OT and LM within the GLv allows for the possibility of the overlapping of these pathways and the consequent integration of optokinetic related information and color information with other visual information from the OT.

The projection from the LM to the retinorecipient AP suggests that the LM may provide information regarding its retinal slip processing to this visual pretectal area which has been implicated in the pupillary light reflex (Gamlin and Cohen, 1988b). The possible interrelationship between OKN and the pupillary light reflex has not been explored and the functional nature of this pathway remains unknown.

Several structures that do not receive a direct retinal projection, the pretectal PPC and Pt, the thalamic ICT, receive a projection from the LM. These areas, like the LM, also receive projections from the visual Wulst (Miceli et al., 1979). Conceivably, these pathways may allow for the integration of information regarding the retinal slip processing in the LM with other kinds of visual information from the visual Wulst. Similarly, the projection from the LM to the contralateral FRL reported in the present study, may provide a pathway for

information regarding retinal slip processing in the LM. The functional nature of the above-mentioned projections, however, remains unknown.

The remaining efferent projections from the LM to nBOR, nD, pontine nuclei, nPap, IO, and Cb can be considered in the functional context of the generation of asymmetric horizontal optokinetic pursuit in lateral-eyed birds. In light of the notion that the reduced ability of the eye to follow movement of the visual world in the nasal to temporal direction and especially at high velocities may have evolved for an animal with laterally placed eyes in order to reduce the continuous generation of temporally directed (nasal to temporal and nonhorizontal backward) optokinetic pursuit that would occur during forward locomotion or flight, it is not surprising to find these behavioral qualities reflected in the response properties of the LM units and the response properties of units in several target nuclei of the LM. First, half of the LM units prefer fast velocities and temporally directed motion whereas half prefer slow velocities and nasally directed motion. Second, there is a segregation of direction preferences within the LM such that only the LMmc responds to temporal to nasal visual motion whereas both LMmc and LMpc respond to nasal to temporal visual motion. Third, there is a differential projection from the LM to its different efferent targets (present study). Fourth, the response properties of units in the nBOR, LP, and Cb, suggest a role for these areas in the generation of horizontal optokinetic pursuit.

The projection from the LM to the nBOR, which terminates in all three subdivisions of the nBOR, together with the reciprocal projection from the nBOR may provide pathways for the integration of information between the horizontal and vertical optokinetic relay nuclei which eventually results in the appropriate compensatory eye movement. Presumably, this reciprocal connectivity has evolved because visual motion in the environment is usually a combination of horizontal and vertical directions and the LM responds preferentially to horizontal

directions whereas the nBOR responds preferentially to vertical and torsional directions (McKenna and Wallman, 1981, 1985; Burns, 1985).

The signals coding for temporally directed information and fast velocity information may travel along the pathways from the LM to the LP, Cb, and IO. This notion is supported by neurophysiological studies showing that units in the LP and the Cb which have similar response properties and also reflect some of the response properties of LM units. Units in the LP and Cb have large receptive fields and are responsive to moving targets at fast velocities from 20 to 60 deg/sec. In addition, some of these units tend to be direction sensitive preferring temporally directed motion (Clarke, 1974; 1977). In addition, the LP projects directly to folia VI-IXb of the Cb (Clarke, 1977), the same folia to which the LM projects directly (present study). Thus the pathways from the LM directly to the Cb or indirectly to the Cb via the pontine nuclei may transmit signals coding for fast velocity temporally directed motion.

The projection from the LM to folia IXc of the Cb, a portion of the vestibulocerebellum (folia IXc and X), presumably provides a pathway through which optokinetic signals may be integrated with vestibular information. This direct projection is not surprising in light of the complementary role of the optokinetic system and vestibular system in the stabilization of the visual image on the retina.

Although there is a lack of neurophysiological information regarding the visual response properties of neurons in the IO in birds, neuroanatomical studies suggest that the portion of the IO that receives its projection from the LM projects, in turn, to folia VII-X (Furber, 1983; Armstrong and Clarke, 1979). In light of the response properties of visual units in the Cb and the similarity in size of the neurons (medium and large) in the LM projecting to the IO, pontine nuclei and directly to the Cb, one might speculate that the projection from the LM to IO and

eventually to the Cb may also provide another pathway for signals coding for fast velocity temporally directed motion to reach the Cb. Alternatively, this pathway may also transmit signals coding for slow velocity backward motion or temporal to nasal motion, characteristics reflected by some units in the Cb. Evidence in rabbits suggests that the IO neurons are excited by large-field slow velocity movement of the visual world in the temporal to nasal direction (Barmack and Hess, 1980). In addition, the projection from the LM to IO may provide an indirect pathway for signals coding for retinal slip processing from the LM to be transmitted to folia IXc of the vestibulocerebellum.

The projection from the LM to the nPap, which is located in a topographically similar position to the nRTP in mammals, may provide another indirect pathway for LM signals to the Cb. Although the nPap does not project to the deep cerebellar nuclei in pigeons (Ziegler, personal communication), in mammals the nRTP, alternatively named the nucleus papilliformis (Olszewski and Baxter, 1954), is known to project to the Cb (Maekawa et al., 1981). A study of the visual response properties of the mammalian NOT cells projecting to the nRTP in rabbits reports that these units respond to a range of velocities from 5-50 deg/sec with most cells preferring temporal to nasal visual motion (Maekawa et al., 1984). Although there is no parallel functional information available for birds at the present time, the projection from the LM to the nPap and then to the Cb may provide a pathway for signals coding for both slow and fast velocity, temporal to nasal motion to be transmitted to the oculomotor nuclei which then generate the appropriate optokinetic pursuit movement.

Thus, based on the evidence provided above, it is conceivable that signals coding for mostly fast but possibly some slow velocity and mostly temporally directed but possibly some nasally directed motion, are generated by different neurons in the LM and transmitted either directly to the Cb or indirectly to the

Cb via the pontine nuclei, nPap, or the IO. Presumably, the reduction in the ability of the eye to generate backward pursuit may be the result of the integration by the Cb of fast velocity backward motion signals transmitted directly or indirectly from the LM, and the consequent generation of an inhibitory signal by the Cb, thereby modulating the output of the oculomotor nuclei in some manner.

Although there is no neurophysiological evidence regarding the units in the LM target nuclei that may receive signals coding for nasally directed slow velocity motion, perhaps these signals are processed and, in turn, transmitted by the neurons in the LM that project to nD, the other major source of afferents to the oculomotor nuclei in the connectivity scheme suggested by the present study (Fig. 4.3). It is conceivable that the LM units responsive to slow velocity motion that tended to be directionally selective in the temporal to nasal direction and tended to lie in the LMmc (Winterson and Brauth, 1985) may be the medium-sized neurons found primarily within the LMmc and identified in the present study as the neurons that project directly to nD. The nD in mammals, which is considered an accessory oculomotor nucleus, in turn, projects to the oculomotor nuclei (monkeys: Carpenter, 1970). Presumably, this projection provides an indirect pathway along which signals coding for slow velocity temporal to nasal motion may reach the oculomotor nuclei from the LM.

Thus, the projections from the LM to the Cb, either directly or indirectly via the pontine nuclei and the IO, along with the LM projection to the nD provide pathways along which signals leaving the LM may be transmitted to the oculomotor nuclei to result in the generation of the appropriate compensatory optokinetic pursuit eye movement (Fig. 4.3).

#### Homology of the LM and NOT

It has been suggested that a fundamental pattern of extratectal visual

pathways exists in nonmammalian vertebrates (Fite, 1985) such that, among highly visual species, there are three major retinorecipient zones located within the lateral superficial, central and dorsomedial portions of the pretectum. Although it has been suggested that there are at least six retinorecipient nuclei in the pretectum of chicken (Ehrlich and Mark, 1985a), it is conceivable to define only three retinorecipient zones in light of the diffuse cytology and the indistinct boundaries of nuclei within the pretectum and the topographical relationship of these individual nuclei. In all three cases, the LMmc and LMpc, SS and SM, and the AP and PD are adjoining areas with indistinct boundaries and could be considered as single retinorecipient zones. Thus, despite the broad range of variation found among species, a fundamental pattern may exist for the pretectal optic pathways of nonmammalian vertebrates.

Furthermore, as discussed in previous chapters, the notion that the LM in birds may be homologous to the NOT in mammals is based on evidence suggesting a similar embryological precursor and position within the pretectum (Kuhlenbeck and Miller, 1942). The present study provides further evidence for this notion. Consistent with the definition of homology as presented by Campbell and Hodos, (1970) the following types of data seem to be most useful in order to establish homologies in the CNS. They include similarity in embryology, topology, topography, cytoarchitectural features, behavioral changes resulting from lesions, neurophysiology, and fiber connections of areas. The greater the degree of concordance among these characteristics, the stronger becomes the justification for drawing the inference that structures in two different species may be homologous. The data gathered in the present study and the other available evidence in the literature strongly suggests that indeed the LM in birds is homologous to the NOT in mammals.

Both the LM and NOT are derived from the embryological tectal plate and

occupy similar positions in the pretectum, lateral to the adjoining optic tectum in birds and the superior colliculus in mammals. Both pretectal areas are characterized by large easily distinguishable neurons which sit in among the fibers of the optic tracts. In addition, after lesions of the LM or NOT the ability to generate horizontal optokinetic pursuit is greatly reduced or eliminated. Neurons within the LM and NOT have large receptive fields, are direction sensitive to mostly horizontal directions and are velocity sensitive preferring not only slow but also fast large field movement of the visual field. The notion of homology is further bolstered by the results of the present connectivity study. Both the LM and NOT receive afferent input from similar sources, the retina, the optic tectum (superior colliculus), the visual telencephalon (visual cortex), and the accessory optic system, the nBOR in birds and the MTN in mammals. Their similarity in connectivity is also extended to their efferent targets. Both the LM and NOT project to the optic tectum (superior colliculus), the nBOR (MTN), pontine nuclei, nPap (nRTP), IO, and the nD. Furthermore, similar to the results of the present study, there is neuroanatomical evidence in mammals which suggests that different populations of neurons in the NOT project to different target nuclei (Robertson, 1983). Thus, on the basis of the definition of homology as presented by Campbell and Hodos, (1970), including the connectivity results documented in the present study, the LM in birds should be considered homologous to the NOT in mammals.

Appendix A: TABLES

Table 1. Alternative nomenclatures used by various authors to describe the pretectal region designated as the LMinc, the LMpc and the SS in the present study.

Alternative Nomenclatures for the IM and SS

---

Lentiform Nucleus of the Mesencephalon, magnocellular portion (LMmc)

Nucleus Externus (NE)<sup>a,c</sup>  
 Nucleus Superficialis Synencephalon (SS)<sup>b</sup>  
 Nucleus Parageniculatus Tecti Optici (PTO)<sup>e</sup>  
 Lentiform Nucleus of the Mesencephalon, lateralis (IMl)<sup>f</sup>

---

Lentiform Nucleus of the Mesencephalon, parvicellular portion (LMpc)

Tectal Grey (GT)<sup>a,c,g</sup>  
 Nucleus Griseum Tectalis (GT)<sup>b</sup>  
 Nucleus Parageniculatus Tecti Optici (PTO)<sup>e</sup>

---

Superficial Synencephalic Nucleus (SS)










Nucleus Superficialis Synencephalon (SS) (includes LMmc)<sup>a,b</sup>  
 Nucleus Geniculatus Lateralis pars dorsalis principalis (GLdp)<sup>d</sup>  
 Lentiform Nucleus of the Mesencephalon, medialis (LMm)<sup>f</sup>

---

a= Huber & Crosby, '29  
 b= Reperant, '73  
 c= Cowan, '61  
 d= Karten & Hodrs, '67  
 e= Kuhlenbeck, '39  
 f= Gamlin and Cohen, '88

Table 2. Summary of the distribution of labeled ganglion cells in retinal quadrants after individual HRP injections into the LM. Injection sites are shown as cross-hatching on a parasagittal view of the LM, reconstructed from coronal sections through the nucleus.

## DISTRIBUTION OF LABELED GANGLION CELLS IN RETINAL QUADRANTS AFTER INDIVIDUAL HRP INJECTIONS INTO THE LM

Bird#	Injection Site <sup>1</sup>	Retinal			Quadrants	
		Inf. Temp.	Inf. Nasal	Sup. Temp.	Sup. Nasal	Total (100%)
HRP-27		17 (12.7%)	108 (80.6%)	9 (6.7%)	0 (0%)	134
HRP-48		87 (88.8%)	2 (2.1%)	9 (9.2%)	0 (0%)	98
HRP-57		68 (26.7%)	187 (73.3%)	0 (0%)	0 (0%)	255
HRP-115		0 (0%)	0 (0%)	245 (100%)	0 (0%)	245
HRP-70		5 (2.0%)	0 (0%)	246 (98%)	0 (0%)	251
HRP-153		1 (2.4%)	0 (0%)	30 (73.2%)	10 (24.4%)	41
HRP-15		265 (14.0%)	74 (3.9%)	1536 (81.4%)	12 (0.6%)	1887
HRP-14		104 (10.8%)	6 (0.6%)	836 (86.5%)	17 (1.8%)	963
HRP-36		79 (33.3%)	33 (13.9%)	50 (21.1%)	79 (33.3%)	241

<sup>1</sup>Injection sites are shown as crosshatching on a parasagittal view of the LM, reconstructed from coronal sections through the nucleus

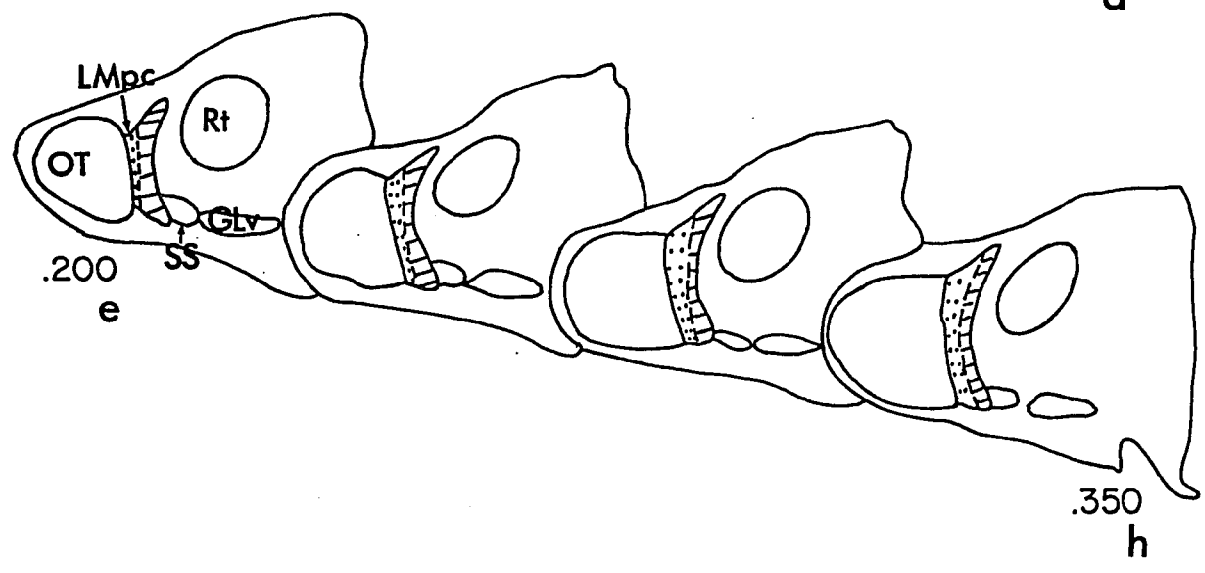
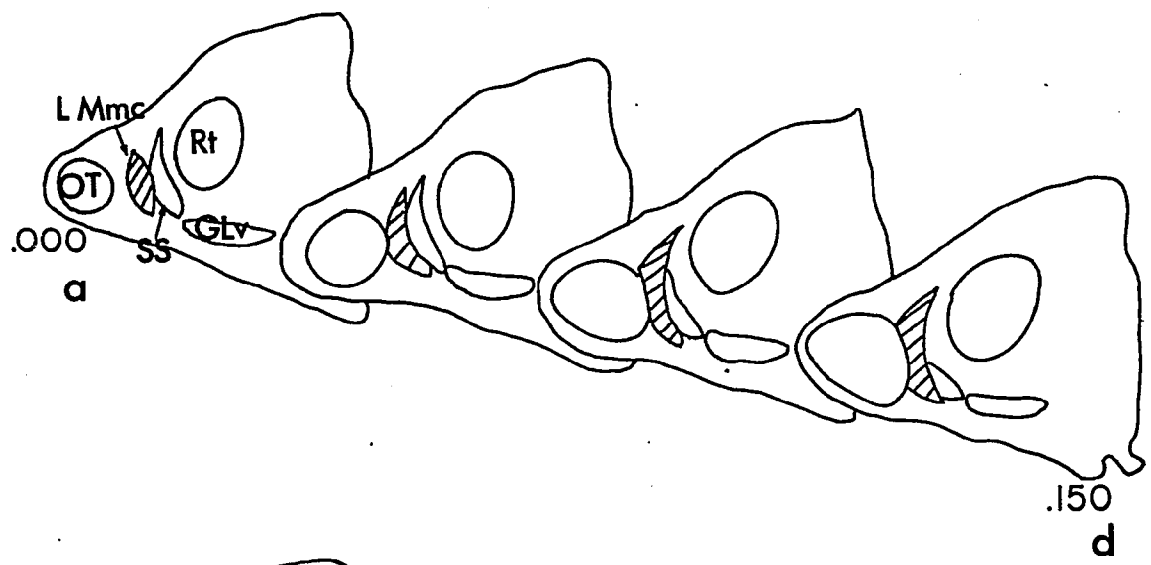
Table 3. Summary of the frequency of small, medium and large HRP-labeled neurons found in the LM after injections into target nuclei.

Target Nuclei	Retrogradely Labeled Neurons in LM		
	Small (10-19 $\mu$ m)	Medium (20-29 $\mu$ m)	Large (30-39 $\mu$ m)
Nucleus of the Basal Optic Root	31/92 (33.7%)	37/92 (40.2%)	24/92 (26.1%)
Pontine Nuclei (LP and MP)	27/128 (21.1%)	57/128 (44.5%)	44/128 (34.4%)
Nucleus Darkschewitsch	_____	* 45/56 (80.4%)	* 11/56 (19.6%)
Inferior Olive	_____	* 35/67 (52.2%)	* 32/67 (47.8%)
Cerebellum	_____	* 30/97 (30.9%)	* 67/97 (69.1%)

\*found only in LMmc

Appendix B: FIGURES

Fig. 1. Schematic line drawings of a series of coronal sections, stained with Klüver-Barerra stain, from the rostral (.000 mm) through the caudal pole (.750 mm) of the LM showing the position of both the magnocellular (lines) and parvocellular (dots) subdivisions. SS indicates the position of the superficial synencephalic nucleus, (O) indicates the position of the optic tectum, GLv indicates the position of the ventrolateral geniculate nucleus.



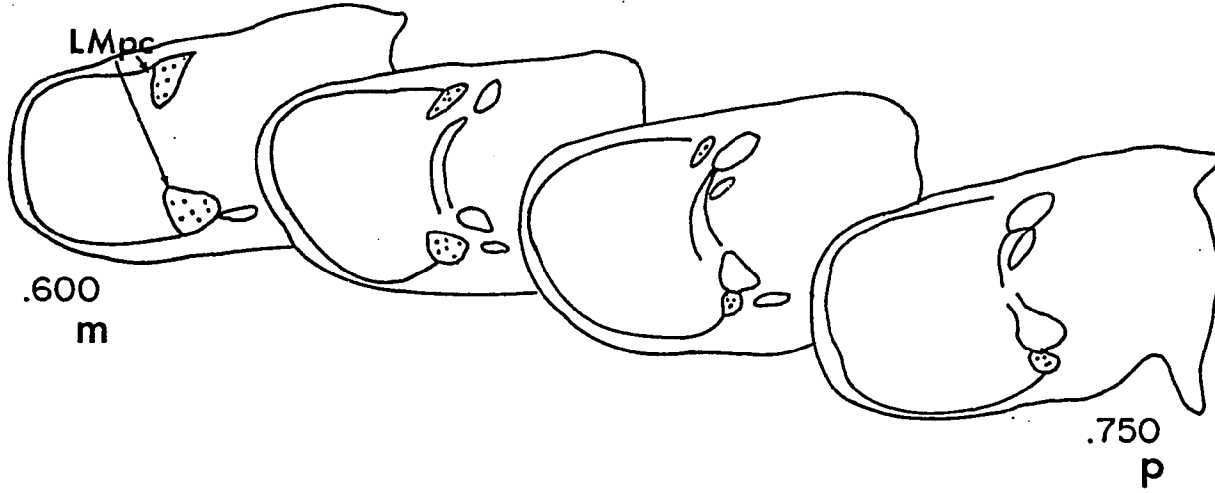
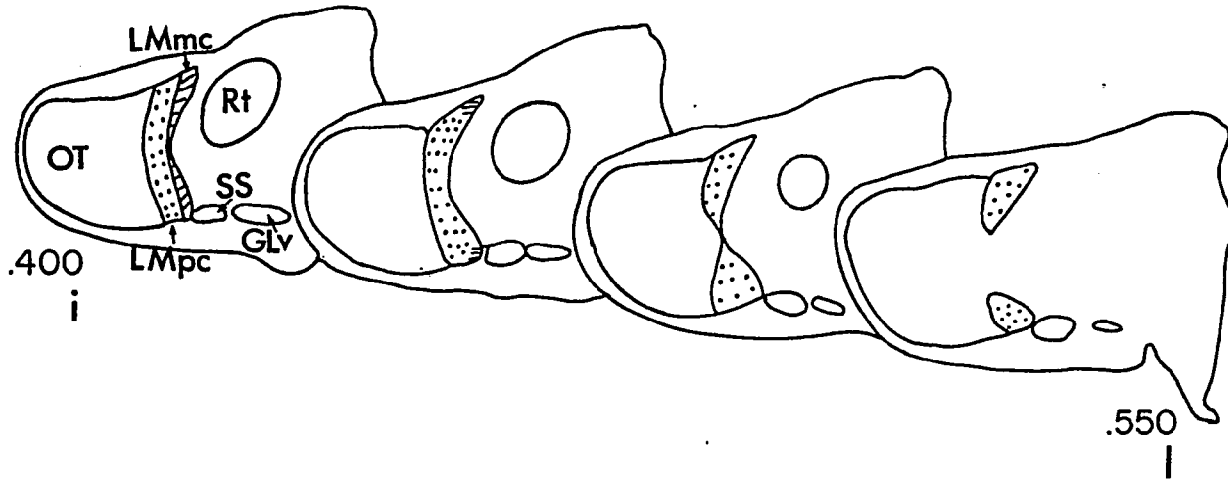
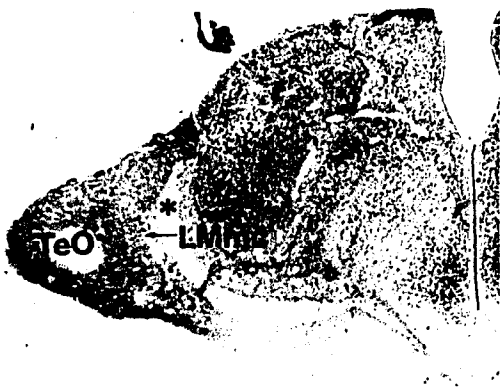


Fig. 2. Photomicrographs of coronal Klüver-Barrera-stained sections of the LM. A. At the rostral pole of the nucleus, the magnocellular portion (LMmc), is seen medial to the optic tectum and lateral to the SS (\*). B. The second subdivision, the parvicellular portion (LMpc), appears 200  $\mu\text{m}$  caudally. C. At 500  $\mu\text{m}$  from the rostral pole the LMmc is divided into a dorsal and a ventral limb (designated by asterisks); the LMpc narrows in its mediolateral aspect. D. At 650  $\mu\text{m}$  from the rostral pole, the LMpc also becomes divided into a dorsal and a ventral limb and the LMmc becomes limited to a few large cells in the ventral optic tract (x14).

2  
A



B

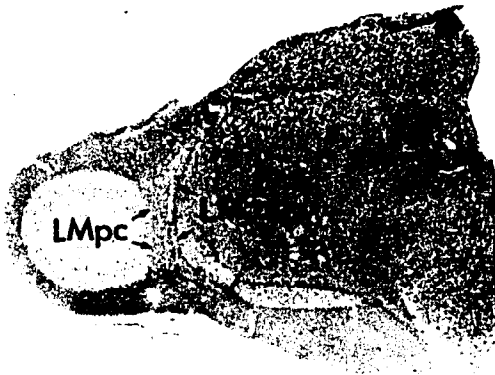


Fig. 3. High magnification photomicrograph of a coronal section through the rostral pretectum showing the cytoarchitectural features of the LMpc, LMmc, and the neighboring SS (x25).

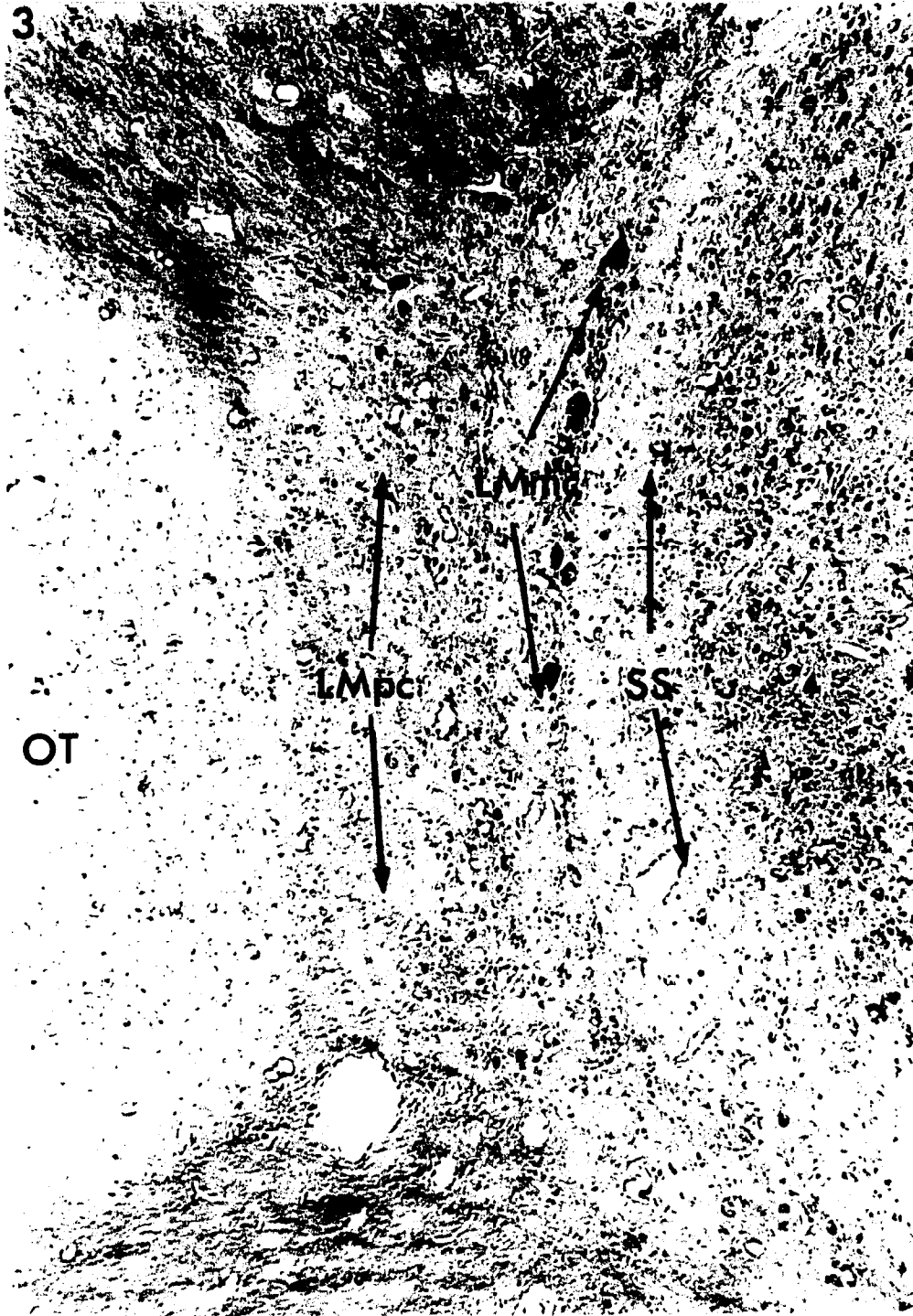
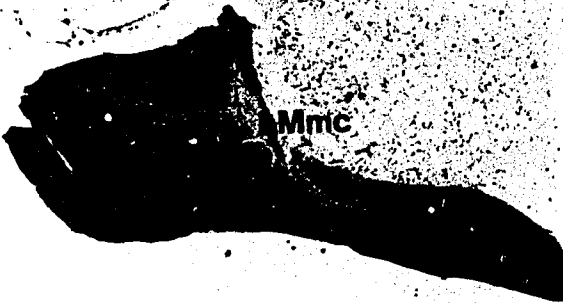


Fig. 4. Photomicrographs of coronal sections showing HRP-labeled terminals within the LM after intraocular injections of the contralateral eye with HRP-WGA. Labeled terminals are found in both subdivisions, the LMmc and the LMpc, throughout the rostrocaudal extent of the nucleus. These illustrated sections are at approximately the same level as the areas illustrated in Figure 2. A. Labeled retinal terminals in the LMmc at the rostral pole of the LM. B. Labeled retinal terminals in both LMmc and LMpc, 200  $\mu\text{m}$  from the rostral pole. C. Labeled retinal terminals in both the LMmc and the LMpc, 500  $\mu\text{m}$  from the rostral pole. D. At 650  $\mu\text{m}$ , labeled retinal terminals are found in both the dorsal and ventral limbs of the LMpc ( $\times 14$ ).

4  
A



C



B



D

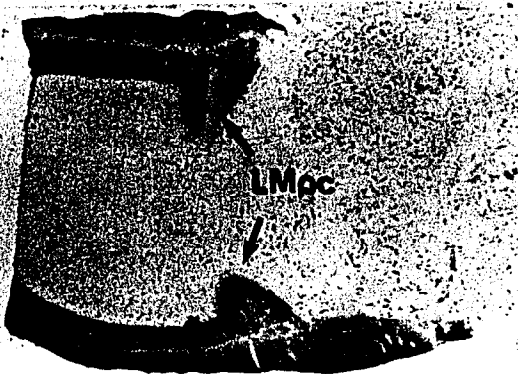


Fig. 5. Low magnification photomicrograph of a field of labeled cells (x225). b-d. High magnification photomicrographs of 3 labeled cells (x580). b. Example of a small cell. c-d. Examples of large cells with labeled dendrites stretching toward the inner nuclear layer.

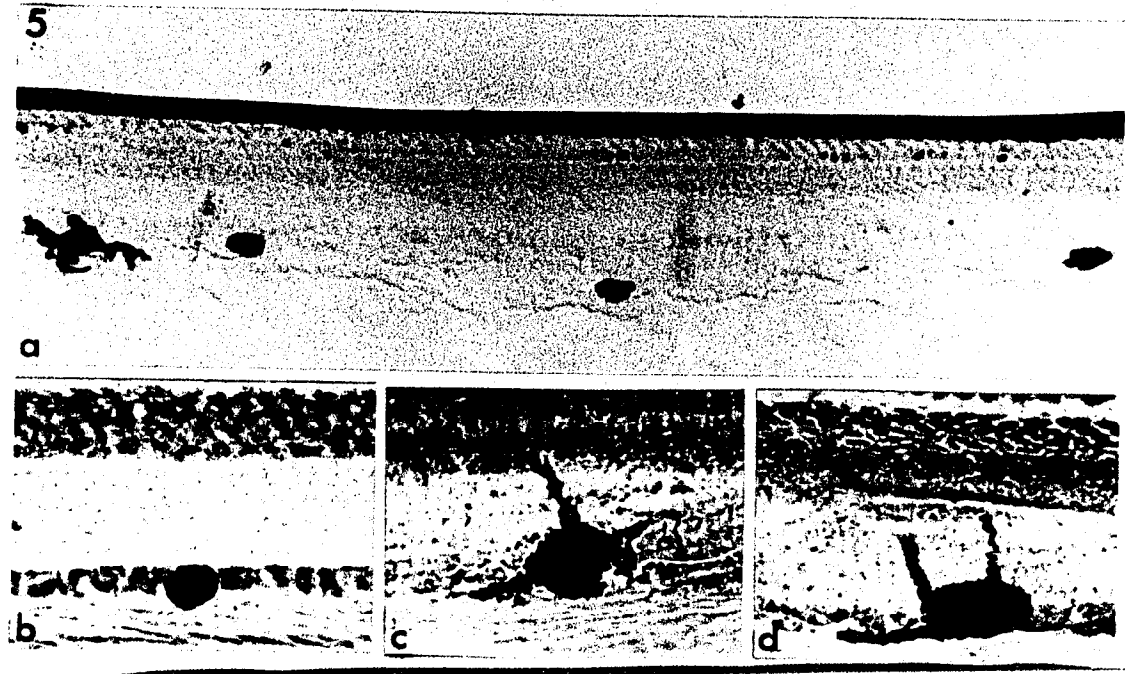


Fig. 6. Frequency histograms constructed from samples of HRP labeled retinal ganglion cells in the superior temporal (ST), inferior nasal (IN) and inferior temporal (IT) quadrants. Labeled cells in the superior nasal quadrant were insufficiently filled to be measured. Arrows indicate the means.

6

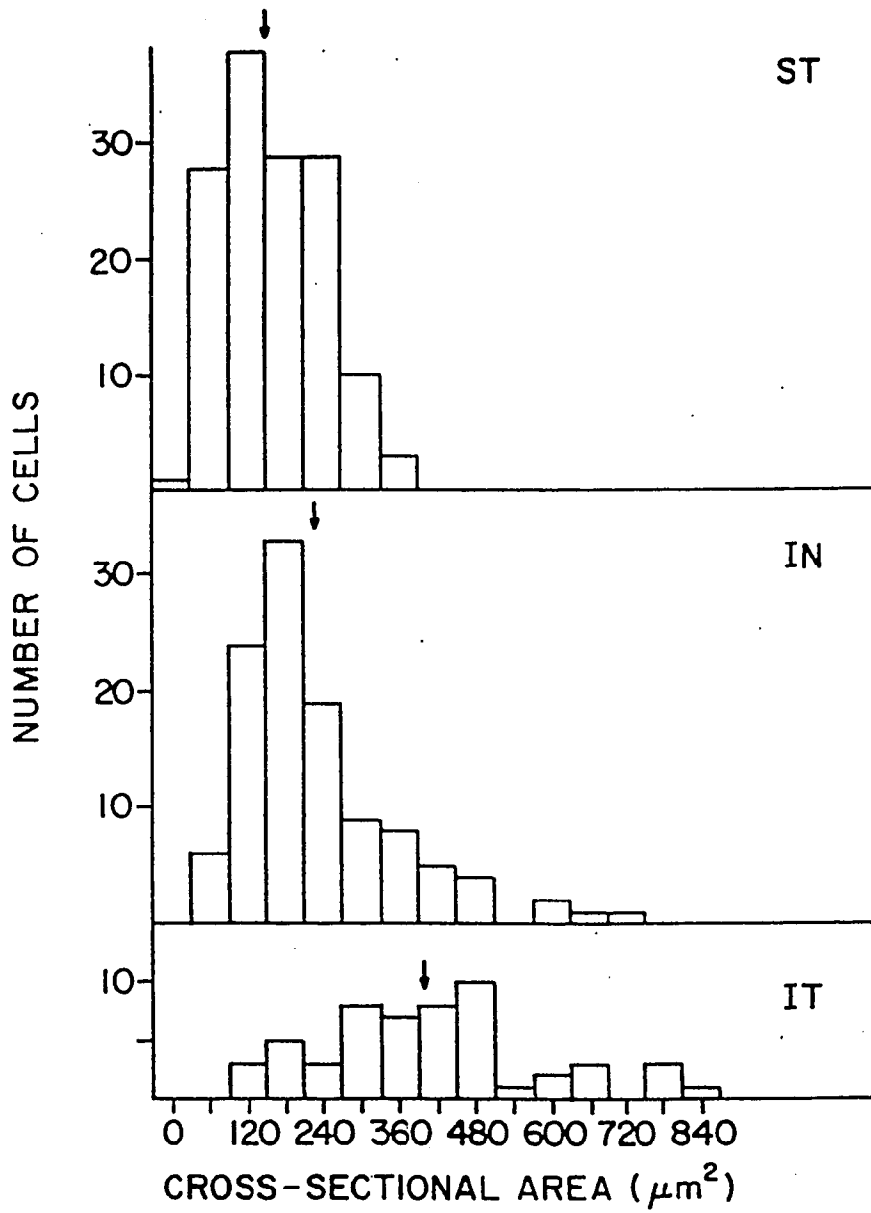


Fig. 7. Photomicrographs of HRP injection site (Fig. 7a-d) in the LM illustrated at the same intervals as in Figure 2 and a drawing of the reconstructed retina showing resulting distribution of labeled retinal ganglion cells (Fig. 7e) (x7). HRP injection located primarily in the dorsorostral LM resulted in labeling of ganglion cells mostly in the inferior nasal retina.

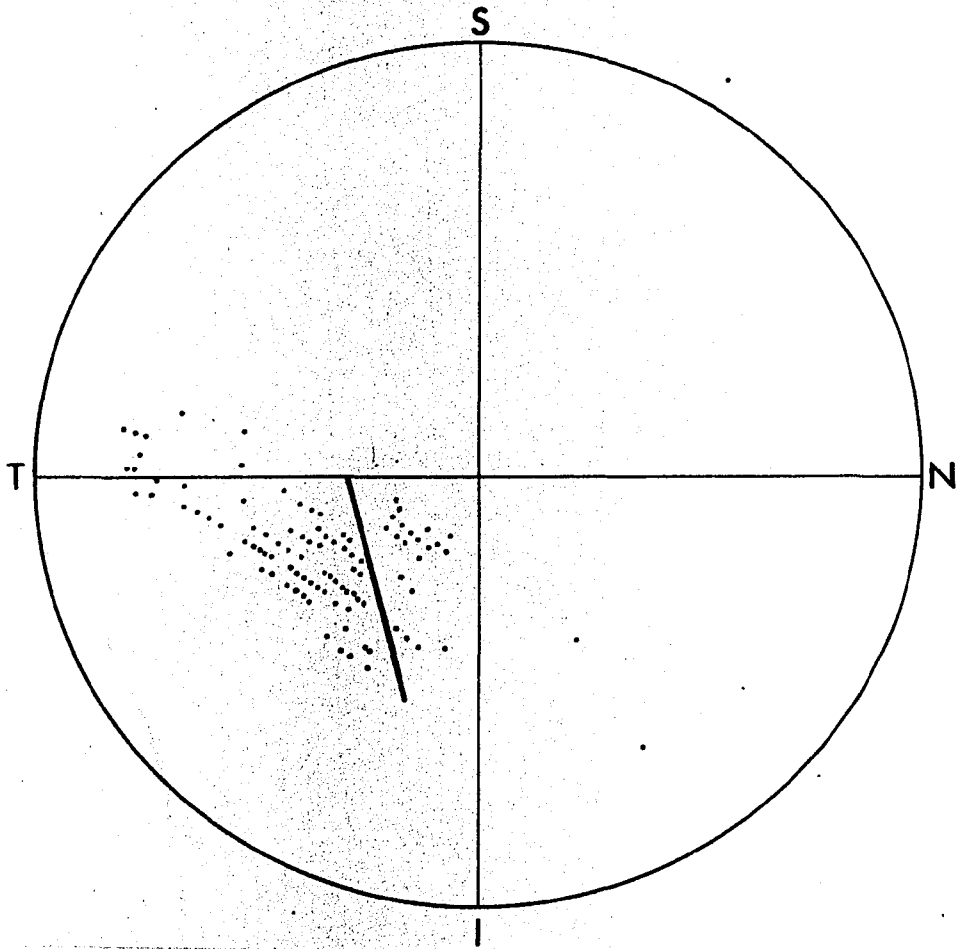
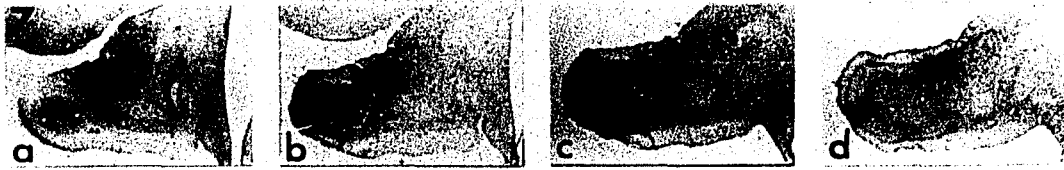
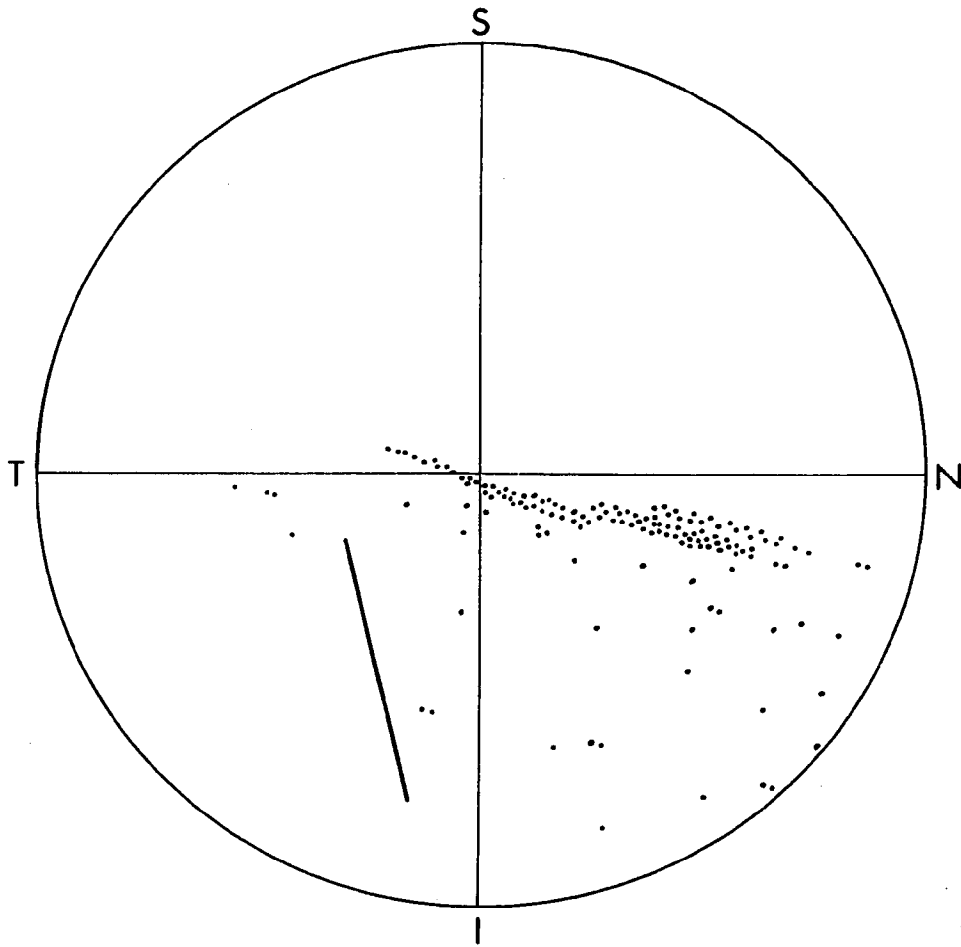
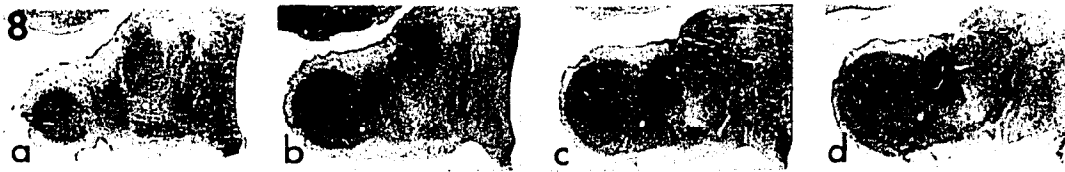


Fig. 8. Photomicrographs of HRP injection site (Fig. 8a-d) in the LM illustrated at same intervals as in Figure 2 and a drawing of the reconstructed retina showing resulting distribution of labeled retinal ganglion cells (Fig. 8e) (x7). HRP injection located primarily in the dorsocaudal LM resulted in labeling of ganglion cells mostly in the inferior temporal retina.



e

Fig. 9. Photomicrographs of HRP injection site (Fig. 9a-d) in the LM illustrated at same intervals as in Figure 2 and a drawing of the reconstructed retina showing the resulting distribution of labeled retinal ganglion cells (Fig. 9c) (x7). HRP injection located primarily in the ventral LM resulted in labeling of ganglion cells in the superior temporal retina.

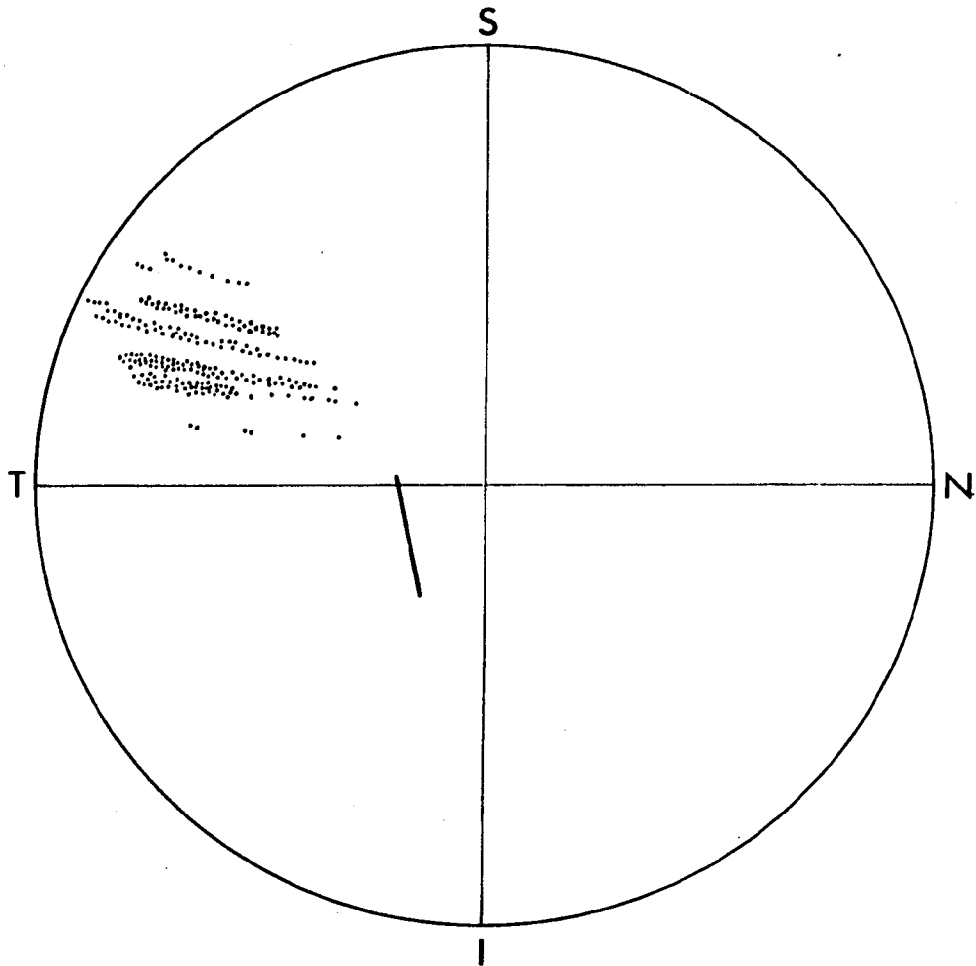
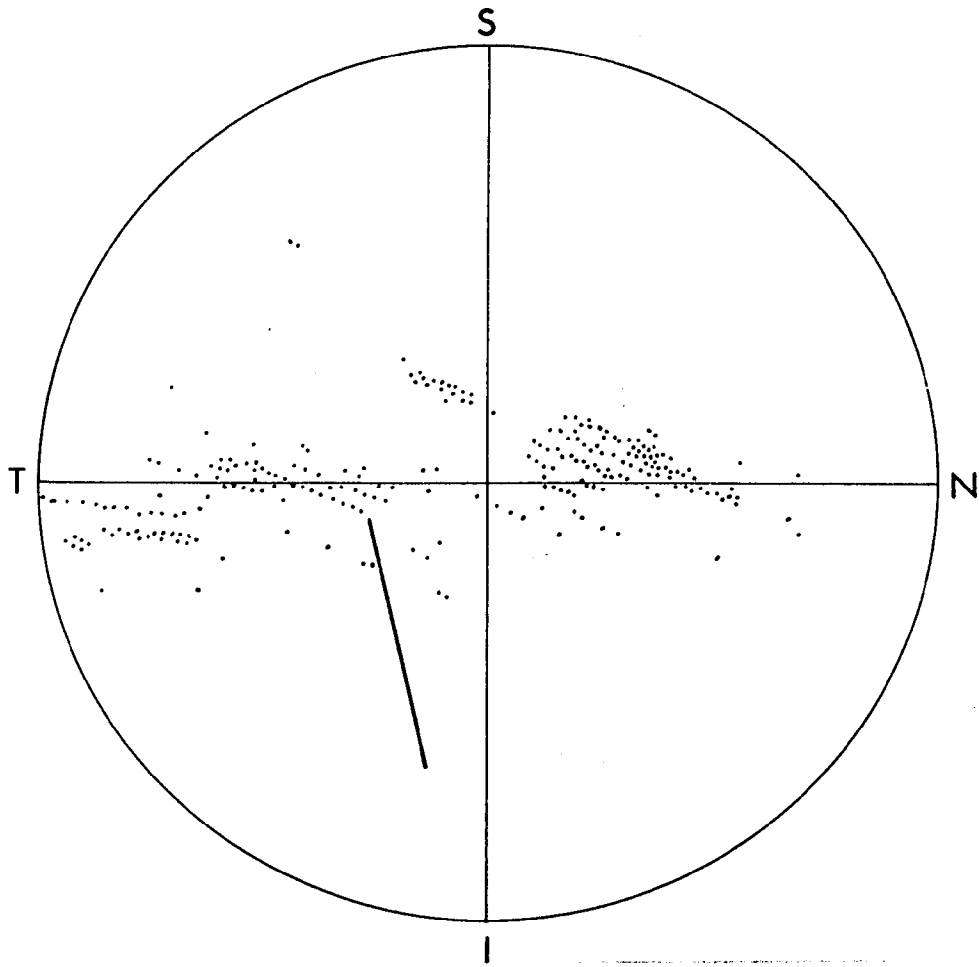
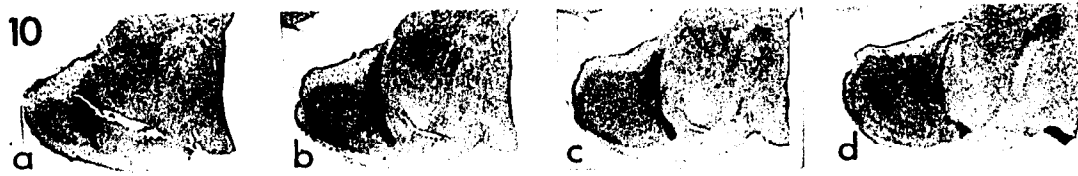


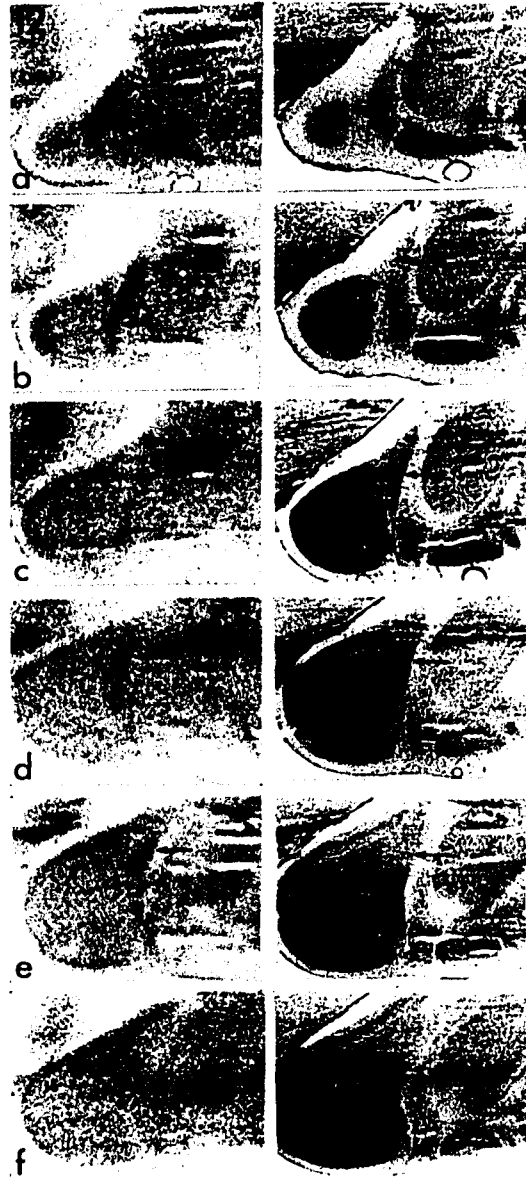
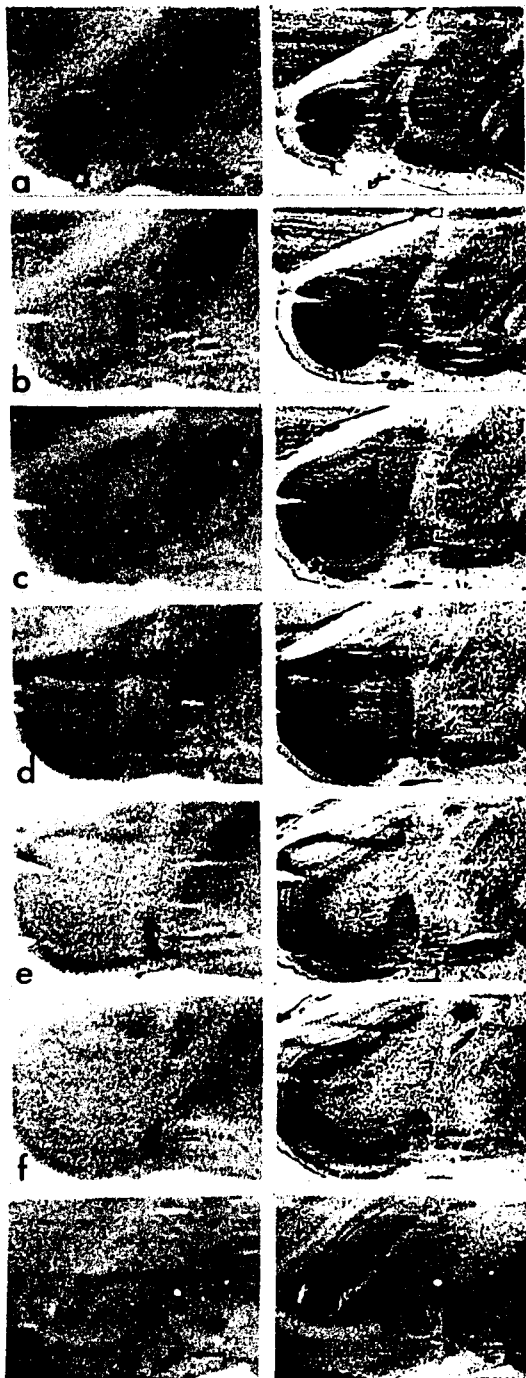
Fig. 10. Photomicrographs of HRP injection site (Fig. 10a-d) in the LM illustrated at same intervals as in Figure 2 and a drawing of the reconstructed retina showing resulting distribution of labeled retinal ganglion cells (Fig. 10e) (x7). HRP injection located throughout most of the LM resulted in a horizontal band of ganglion cells extending across the retina.



Figs. 11-12. Autoradiograms and matched stained sections from brains of chicks that viewed horizontal visual motion with half the retina after injection of 2-DG. Sections were cut rostrocaudally and are illustrated at approximately 120  $\mu\text{m}$  intervals. The 2-DG label in the autoradiograms and its corresponding position in the photomicrographs of the LM are indicated by arrows (x7).

Fig. 11. Superior retina stimulated with horizontal visual motion. a. The 2-DG label covered the dorsal half of the rostral LM but became progressively more ventral when traced caudally (Fig. 11b-f). The nBORI was also labeled (Fig. 11g).

Fig. 12. Inferior retina stimulated with horizontal visual motion. a. The dorsal half of the rostralmost LM was heavily labeled. b-c. As traced caudally the label extended ventrally and then became restricted to the dorsal LM (Fig. 12d-e). The caudalmost extreme was not labeled (Fig. 12f).



Figs. 13-14. Autoradiograms and matched stained sections from brains of chicks that viewed horizontal visual motion with half the retina after injection of 2-DG. Sections were cut rostrocaudally and are illustrated at approximately 120  $\mu\text{m}$  intervals. The 2-DG label in the autoradiograms and its corresponding position in the photomicrographs of the LM are indicated by arrows ( $\times 7$ ).

Fig. 13. Temporal retina stimulated with horizontal visual motion. a-c. Heavy label extended along the entire dorsoventral axis in the rostral half of the LM. d-f. In the caudal half the label was lighter and located in the ventral portion of the nucleus. The asterisk indicates a diagonal band that extends from the LM to the rostral nucleus principalis precommissuralis (PPC) that was also labeled.

Fig. 14. Nasal retina stimulated with horizontal visual motion. a-c. Label was absent from the rostral half of the LM. d-e. Label extended along the dorsoventral axis. f. At more caudal levels the label was located primarily in the dorsal portion of the LM.

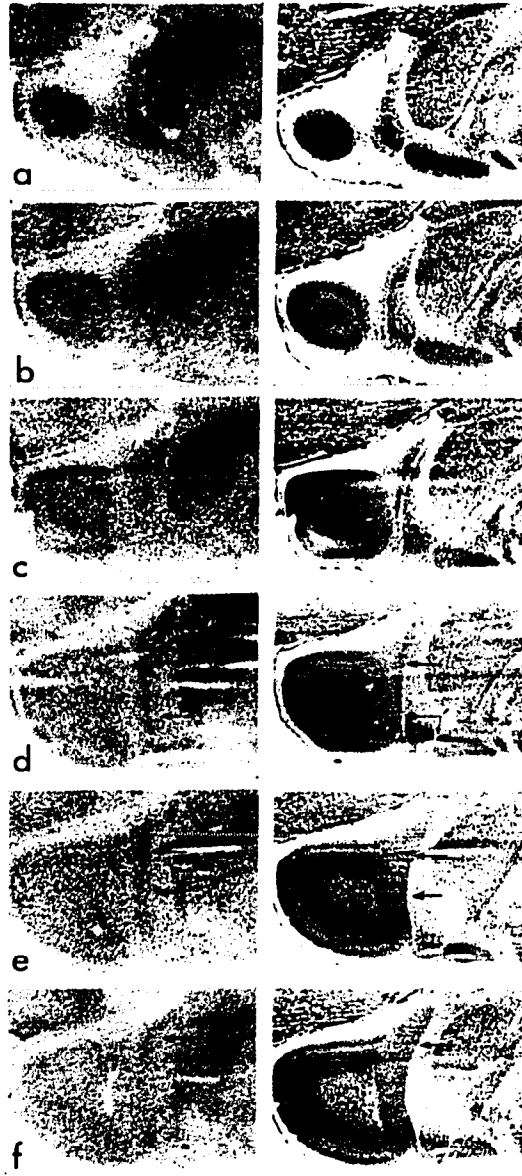
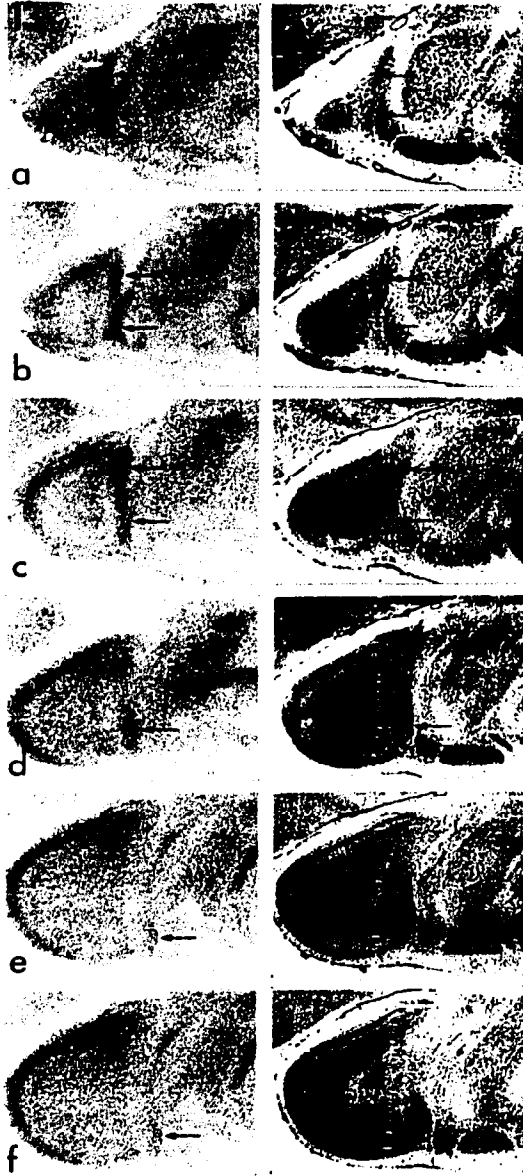


Fig. 15. Line drawing of a parasagittal view of the LM showing mapping of each retinal quadrant onto the nucleus. Inset in lower right corner shows similar retinotopic mapping onto the optic tectum (modified from Crossland and Uchwat, 1979).

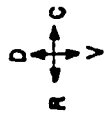
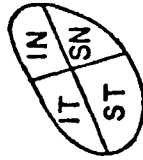
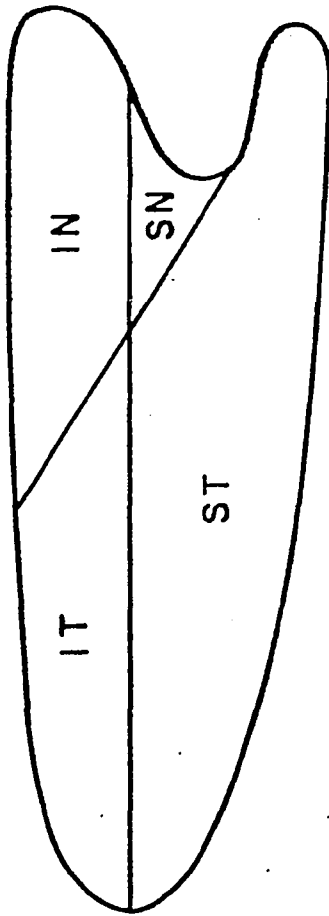
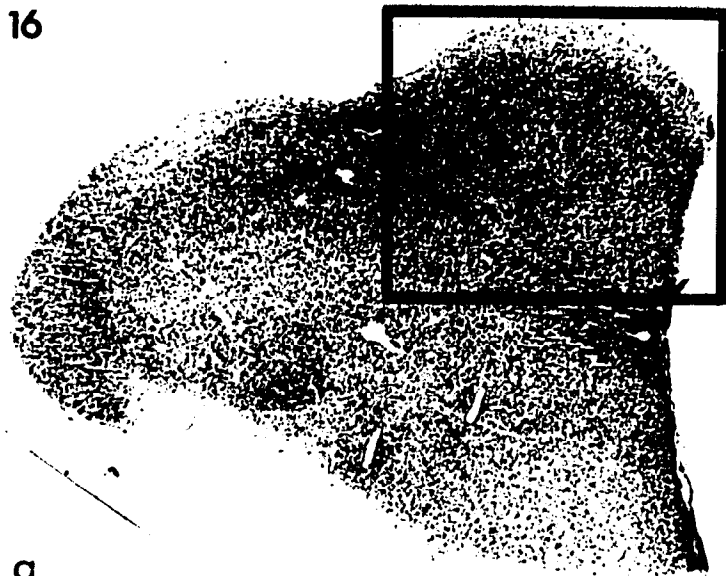
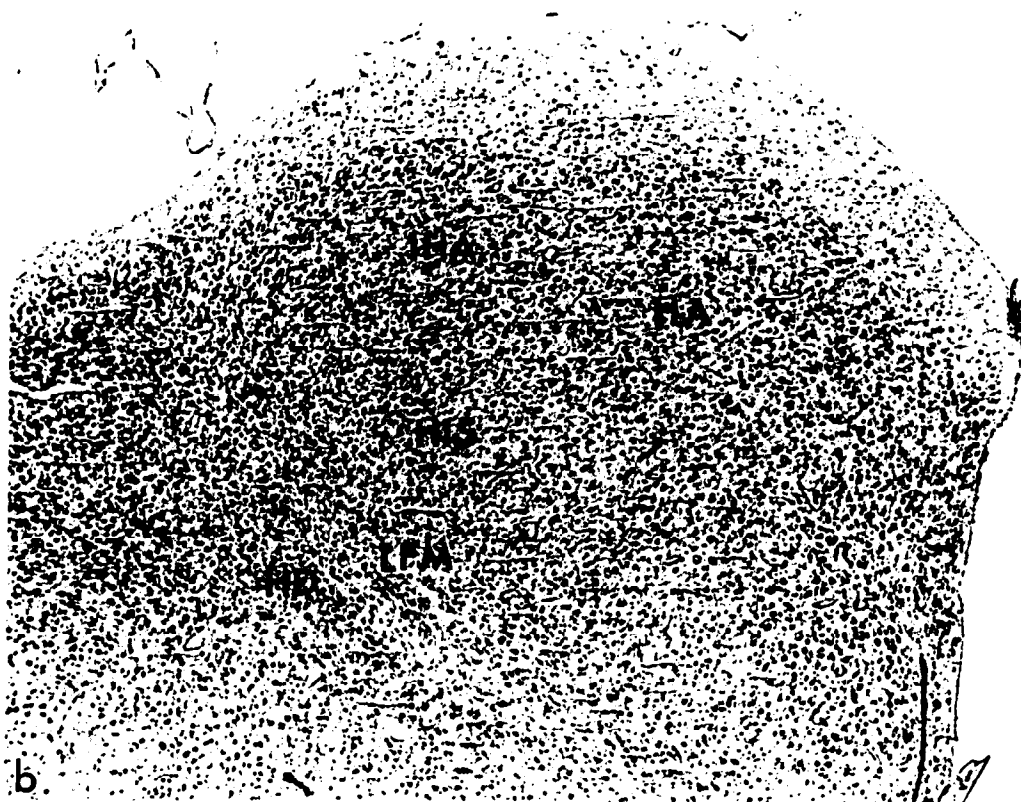


Fig. 16a. Photomicrograph of a Klüver-Barerra stained coronal section through the middle of the telencephalon (x4). The area within the box is depicted in the lower portion of this figure. b. A higher magnification photomicrograph of the hyperstriatum and the layers of the visual Wulst shows the accessory hyperstriatum (HA), intercalated accessory hyperstriatum (IHA), superior intercalated hyperstriatum (HIS), supreme frontal lamina (LFM) and dorsal hyperstriatum (HD) layers within the visual Wulst (x10).

16



a



b

Fig. 17. a-d. A series of photomicrographs of the HRP injection site in the LM (x7), illustrated at the same levels as in Fig. 2 along with an schematic illustration (e) of this injection site shown as crosshatching on a parasagittal view of the LM, reconstructed from coronal sections through the nucleus. f-k. A rostrocaudal series of line drawings through the caudal 4.0 mm of the telencephalon showing the distribution of labeled cells within the HA after a nearly complete injection into the LM. The line on the drawings represents the ventral border of the HA layer.



c



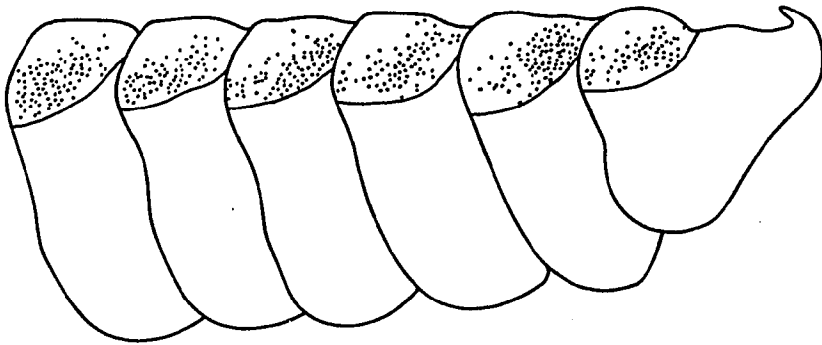
d



a



b



k

j

i

h

g

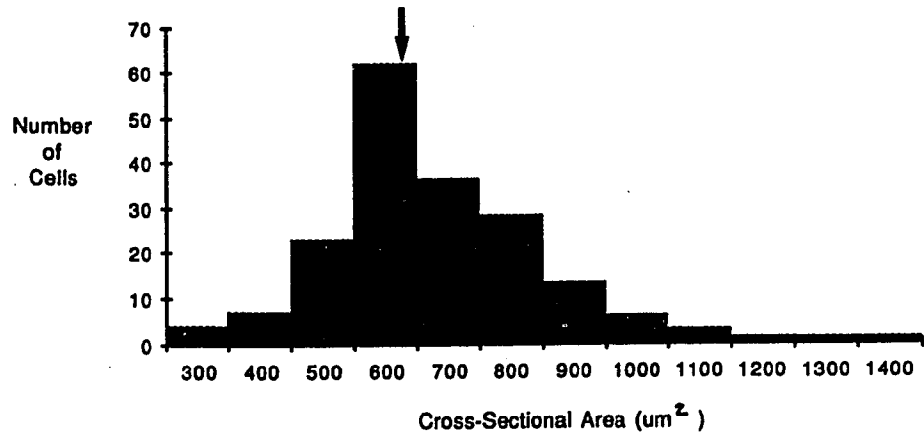
f



e

Fig. 18. a. Frequency histogram constructed from a sample of HRP labeled neurons in the HA layer of the visual Wulst after the injection shown in Fig. 17. Arrow indicates the mean. b. Photomicrographs of HRP-labeled neuron in the HA (x225). c. Photomicrograph of a field of HRP-labeled neurons in the HA (x90).

18



a



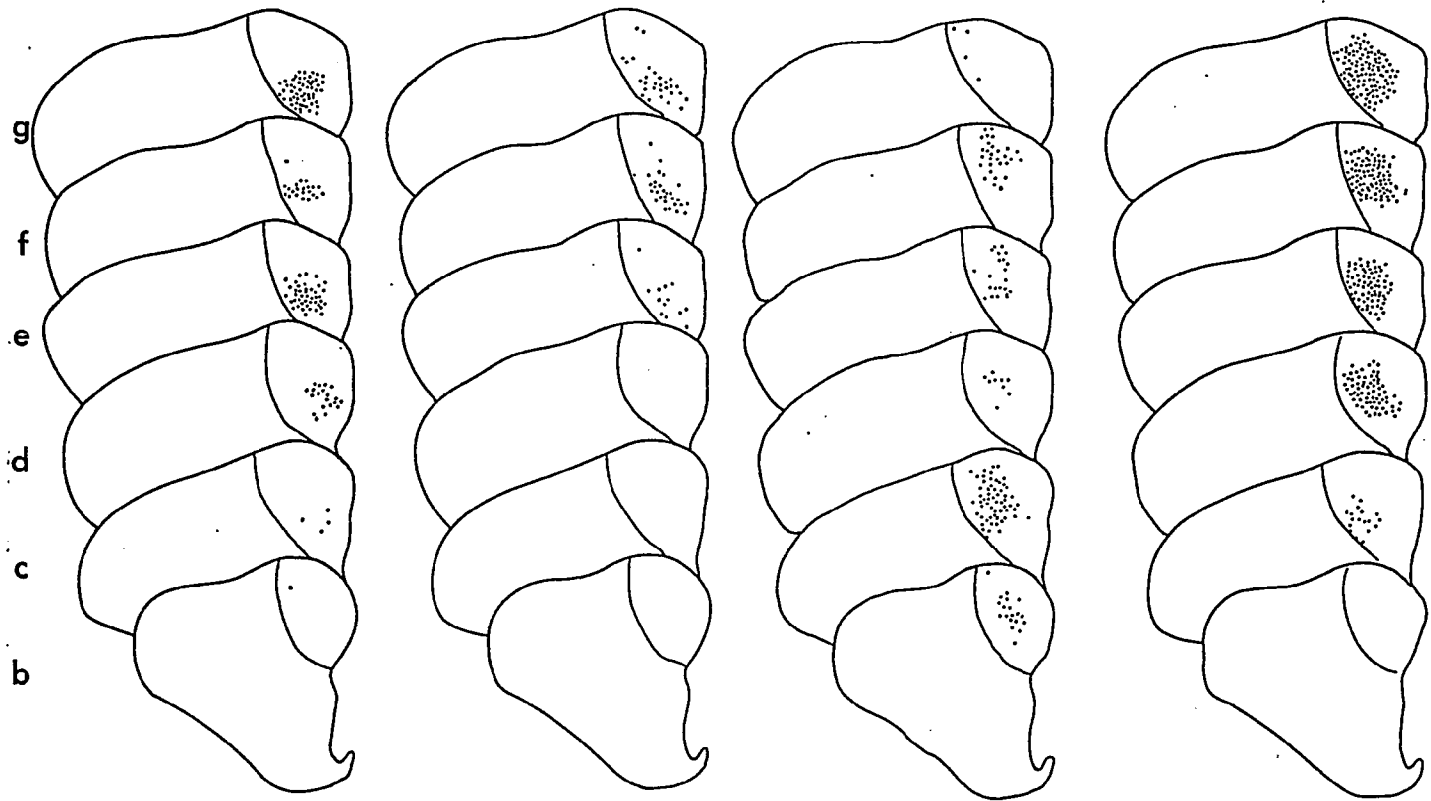
Figs. 19-22. Line drawings of a parasagittal view of the LM showing the position of four partial injection sites shown as crosshatching. (Figs. 19a, 20a, 21a, 22a). A rostrocaudal series of line drawings of sections through the caudal 4.0 mm of the telencephalon showing the distribution of labeled cells within the HA injections restricted to portions of the LM (Figs. 19b-g, 20b-g, 21b-g, 22b-g).

Fig. 19. HRP injection into dorsal LM labeled neurons primarily in ventral HA.

Fig. 20. HRP injection into a portion of the dorsal LM labeled neurons primarily in caudoventral HA.

Fig. 21 HRP injection into the ventral LM labeled neurons primarily in the dorsal portions of HA.

Fig. 22. HRP injection into the middle LM labeled neurons primarily in the central HA and not in dorsalmost or ventralmost portions of HA.



19 a HRP 4

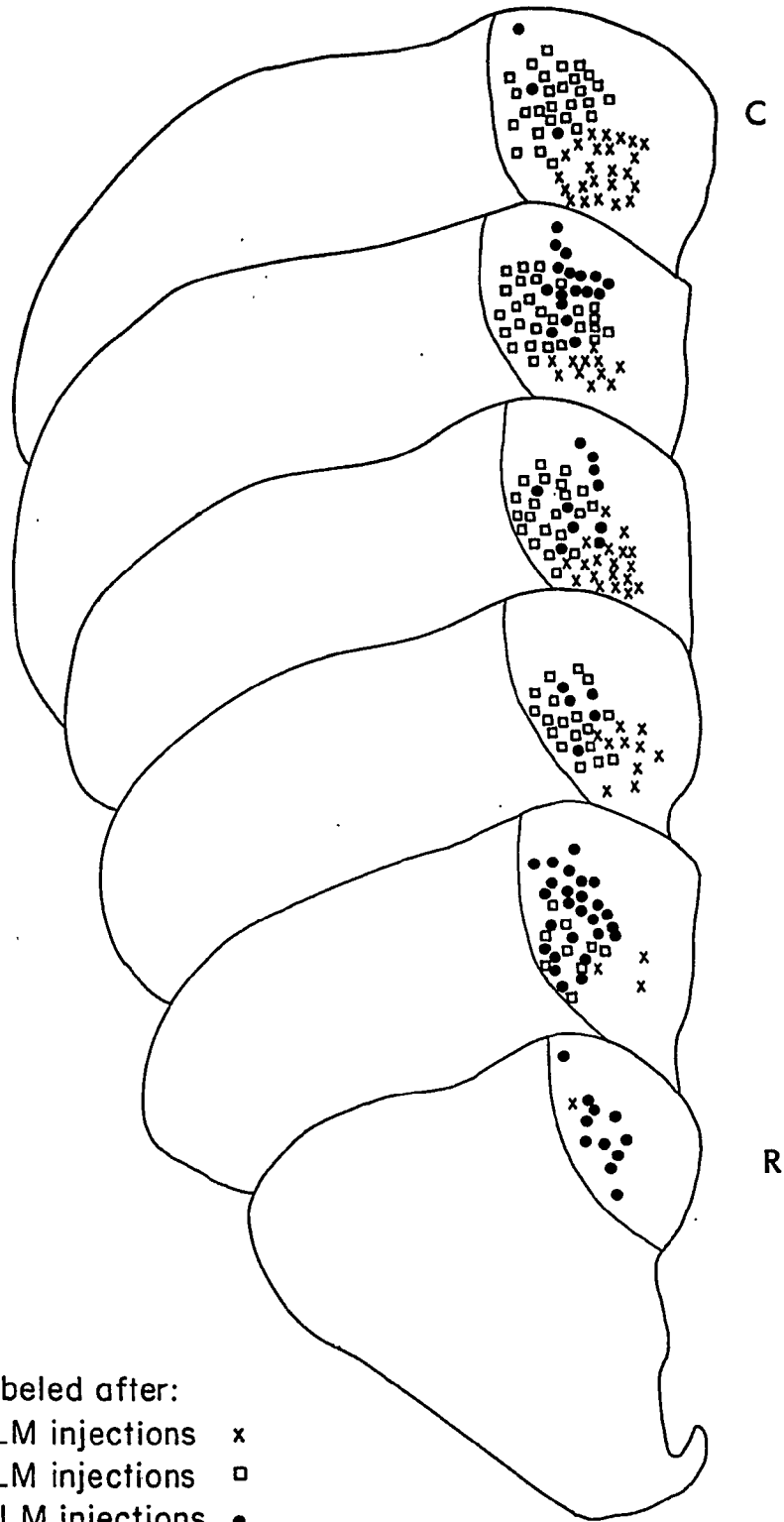
20 HRP 27

21 HRP 59

22 HRP 6

Fig. 23. Composite drawing of the distribution of labeled cells within the HA illustrated in Figs. 19-22 shown in a rostrocaudal series of line drawings through the telencephalon after injections of HRP restricted to portions of LM.

23



Figs. 24-25. A rostrocaudal series of line drawings through the LM showing the distribution of terminal labeling within this area after injections into the HA layer of the visual Wulst of older chickens (Fig. 24a-c) and hatchlings (Fig. 25a-c). Darkfield photomicrographs show the position of labeled terminals in the LM after injections into HA of older (Fig. 24d-f) and hatchling (Fig. 25d-f) chicken (x8).

Fig. 24. a-c. HRP injections into the HA of older chickens result in the labeling of terminals throughout the rostrocaudal extent of the LM. d-f. The distribution of terminal labeling appears uniform in rostral (d), middle (e) or caudal (f) LM and there is no apparent differential distribution of label within either subdivision of the LM (x8).

24

Six Weeks Old

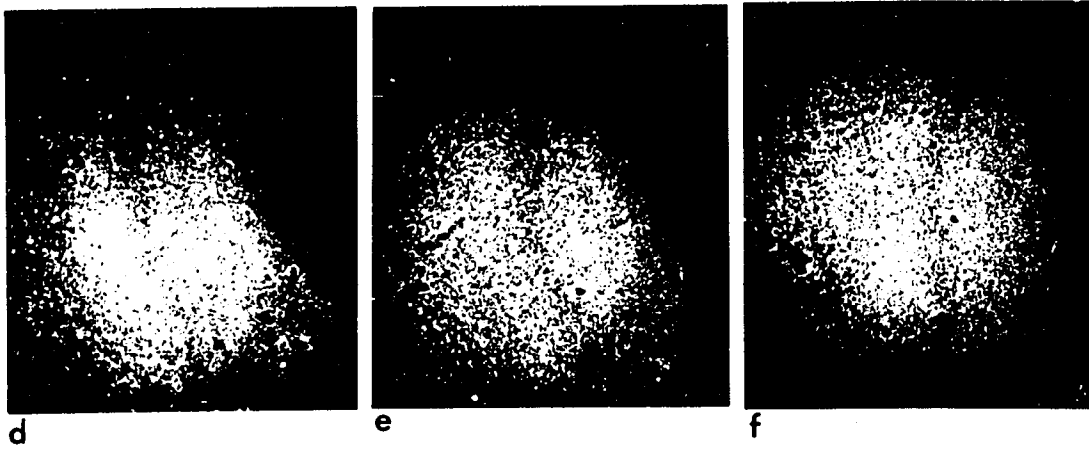
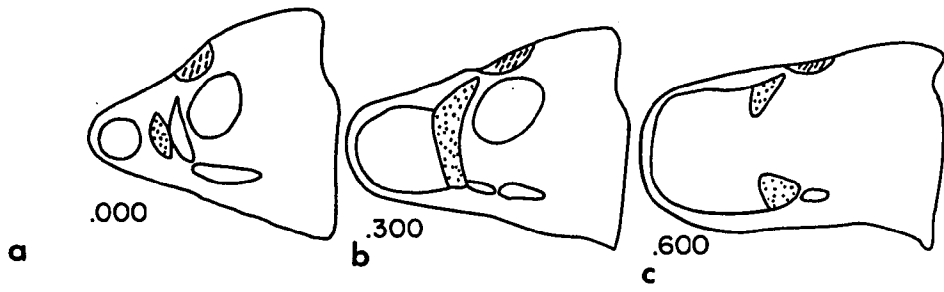


Fig. 25. a-c. HRP injections into the HA of hatchling chickens result in the labeling of terminals throughout the rostrocaudal extent of the LM. d-f. The distribution of labeled terminals is similar to that found in older chickens (Fig. 24d-f).

25

HATCHLING

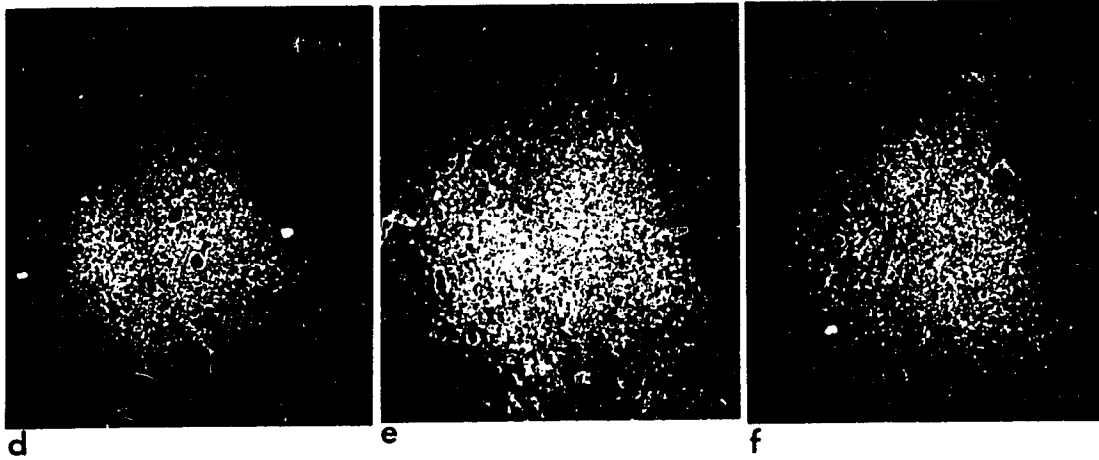
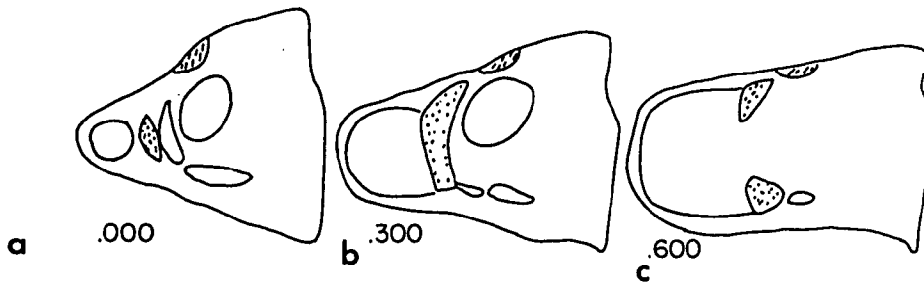
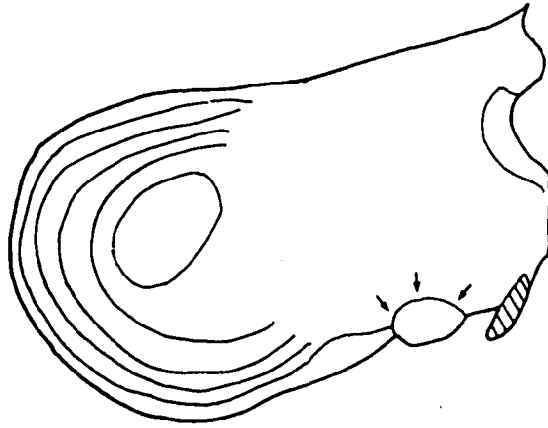


Fig. 26. a. A line drawing of a coronal section at the level of the nBOR as designated by the arrows. b. Photomicrograph of a field of HRP-labeled cells in the nBOR (x70). Retrogradely labeled neurons are found in all three subdivisions of the nBOR. c-e. Photomicrographs of labeled neurons in nBOR (x210). HRP-labeled neurons in the nBOR are generally medium (M) or large-sized (L) neurons round or stellate in shape.

26



a

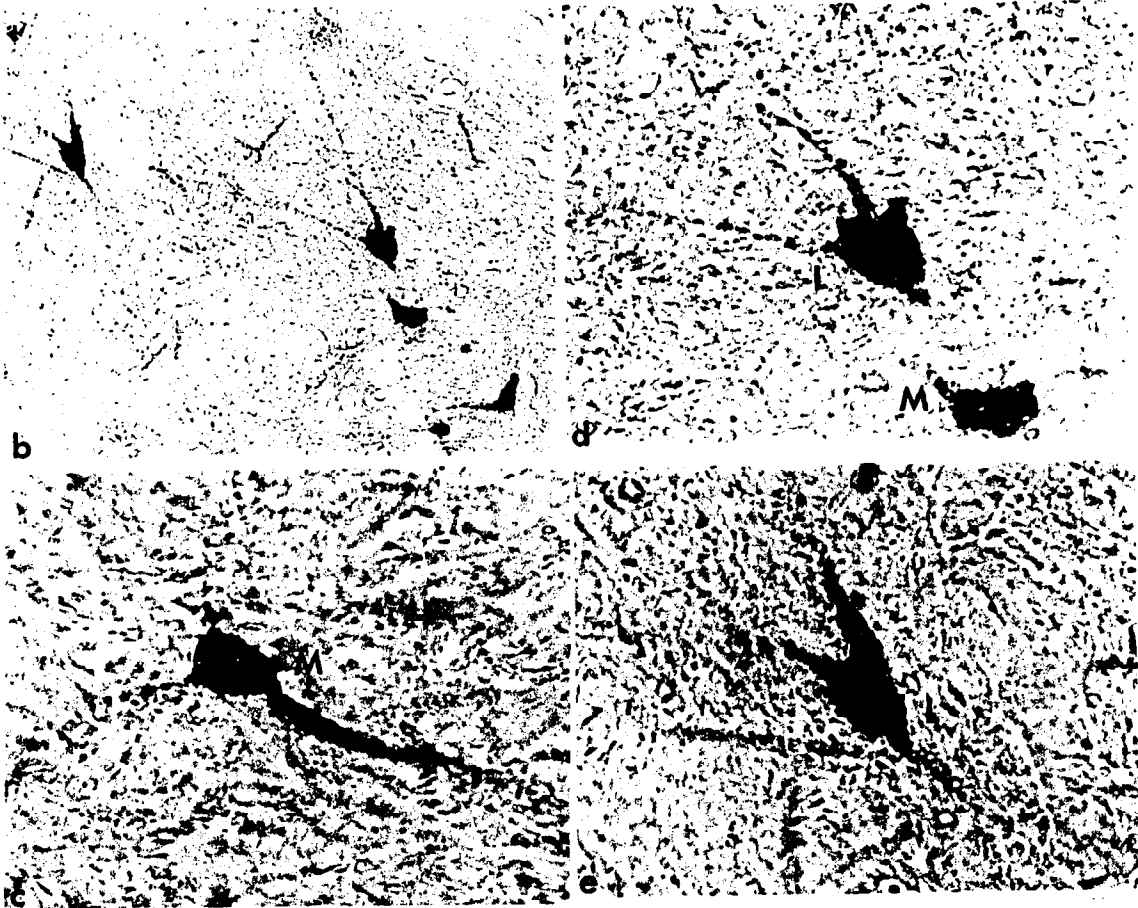
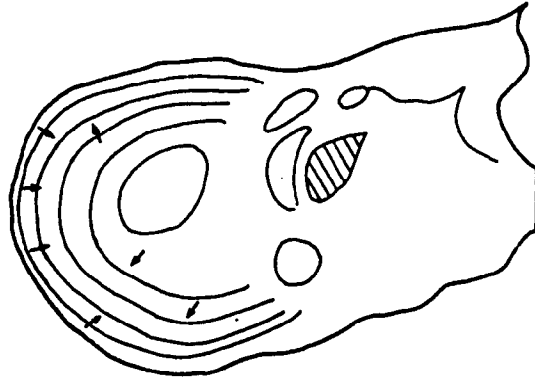
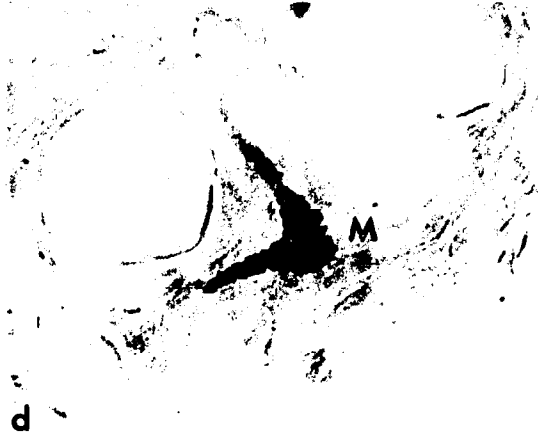
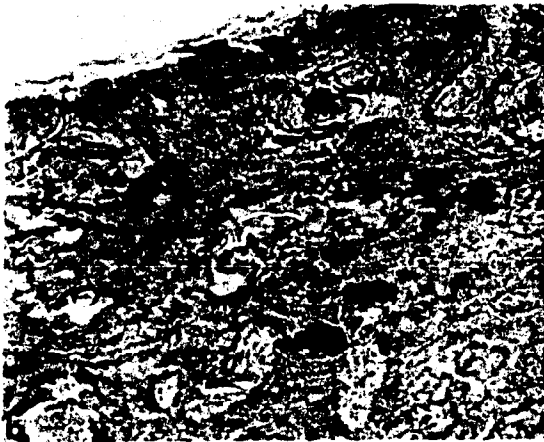


Fig. 27. a. A line drawing of a coronal section through the rostral optic tectum. Arrows indicate regions in which HRP-labeled neurons are found. b. Photomicrograph of a field of labeled neurons in layers 8 and 10 of the OT (x125). c-e. Higher magnification photomicrograph of labeled neurons in OT (x195). Retrogradely labeled neurons in the optic tectum are small (S) and medium sized (M) and round or elongated in shape.

27



a



d

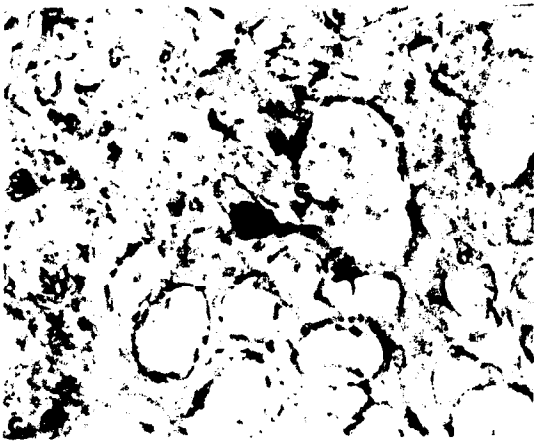


Fig. 28. Schematic representations of the mapping of the retinal quadrants in the hyperstriatum and the LM. The hyperstriatum and LM are shown in parasagittal views reconstructed from coronal sections through these areas. Evidence suggests that specific portions of the LM receive an orderly projection from corresponding portions of the retina, either indirectly through the HA of the visual Wulst or directly from the retina.

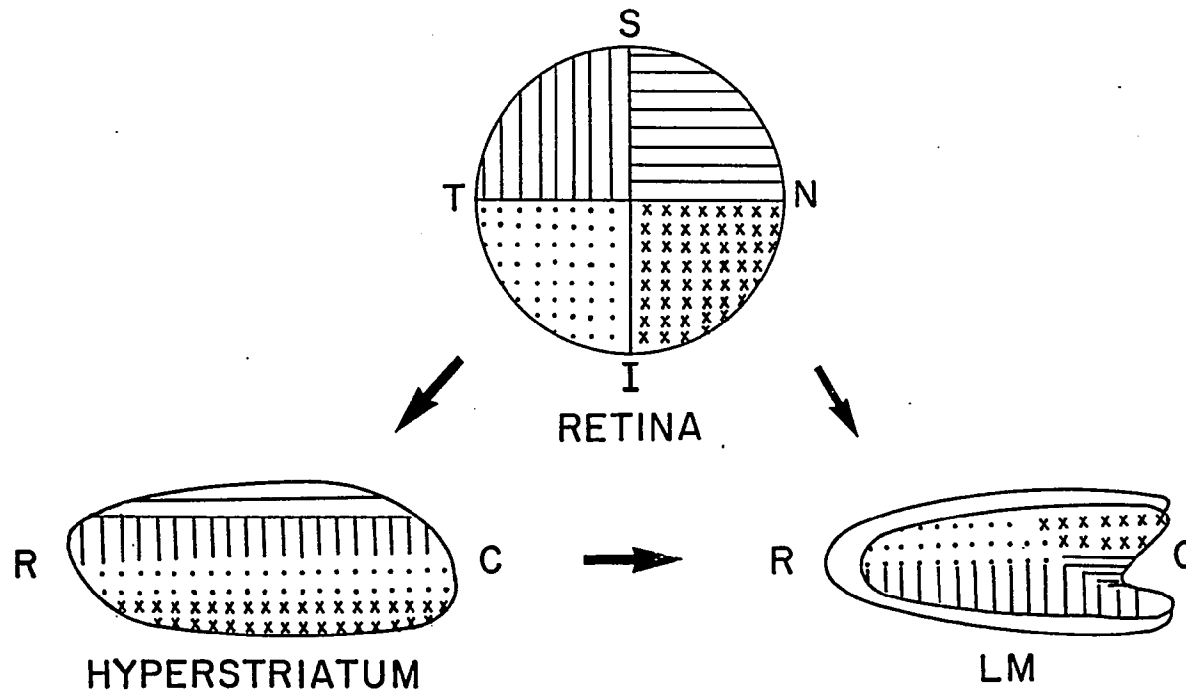
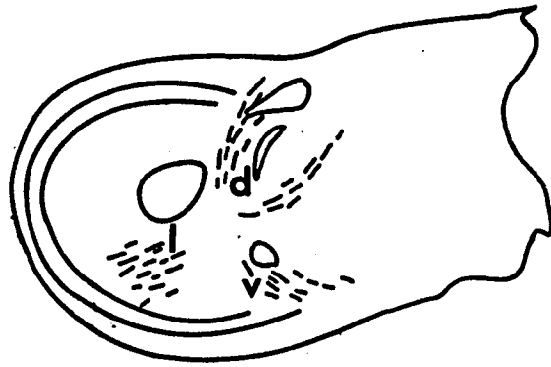
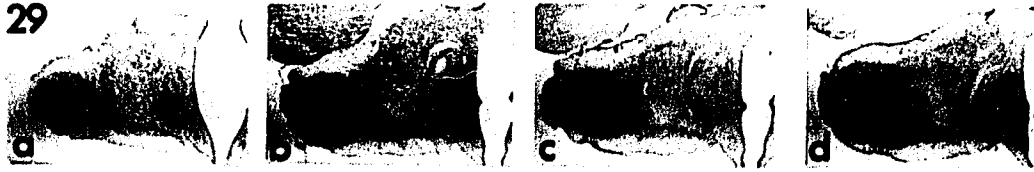


Fig. 29. Photomicrographs of HRP injection site (Fig. 29a-d) in the LM illustrated at the same intervals as in Fig. 2 (x7). e. The lower illustration is a line drawing of a coronal section just caudal to the caudal pole of the LM showing the antero-  
grade labeling of three bundles of axons, the dorsal (d), ventral (v), and lateral (l), exiting the LM.

29



e

Fig. 30. Line drawings of a rostrocaudal series of coronal sections through the brain (Fig.30A-E) showing the distribution of labeled axons and terminals in OT (30A,B), Pt (30A), AP (30A,B), PPC (30A,B), nI (30A,B), PC (30A,B), nBOR (30B), MPv (30C), nPap (30C), MP (30D), LP (30D), BCP (30D) and IO (30E). F. A parasagittal section through the Cb, illustrating the resultant anterograde labeling of axons and terminals in folia VI, VIII and IXa and c, after HRP injections into the LM.

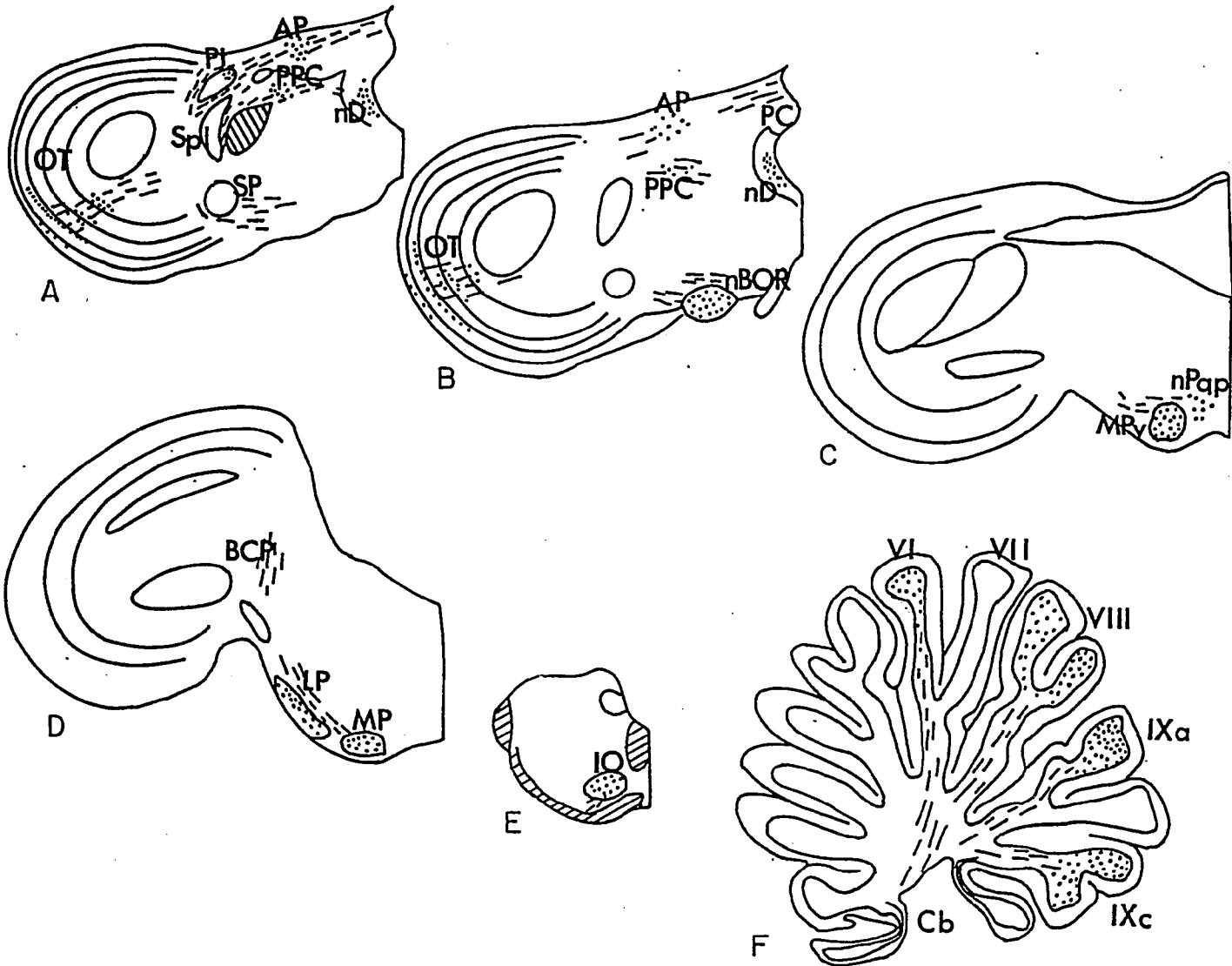


Fig. 31. a. A bright-field photomicrograph of a Nissl-stained coronal section through the rostral OT. The area designated by the box is represented in the dark-field photomicrograph below. b. Darkfield photomicrograph showing the resultant anterograde terminal labeling in layer 4, 7, 9, 11, 12, 13 of the OT (x34).

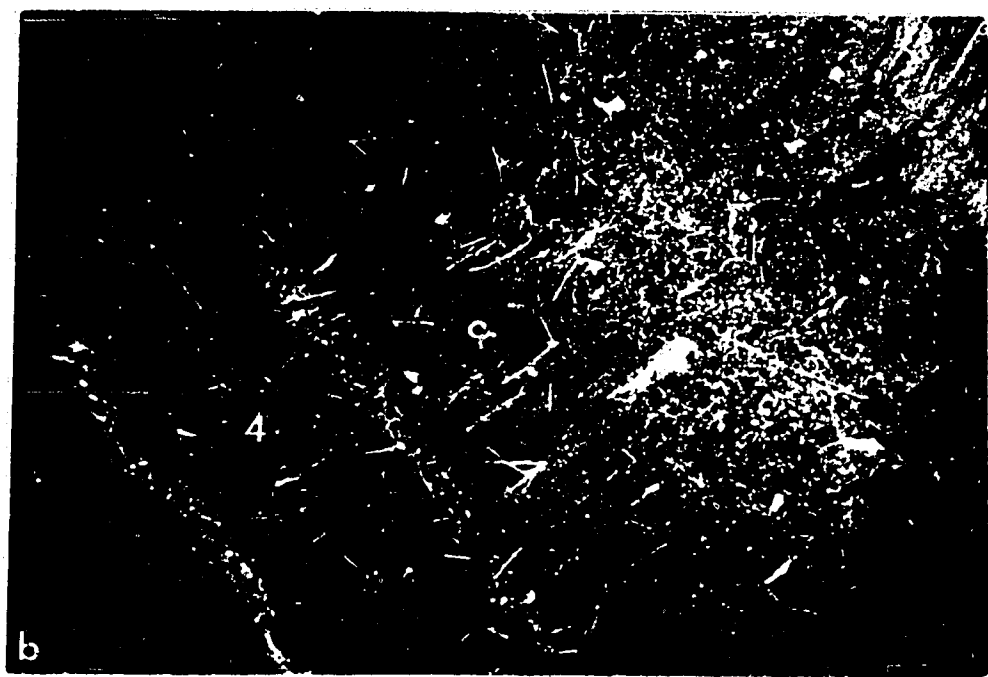
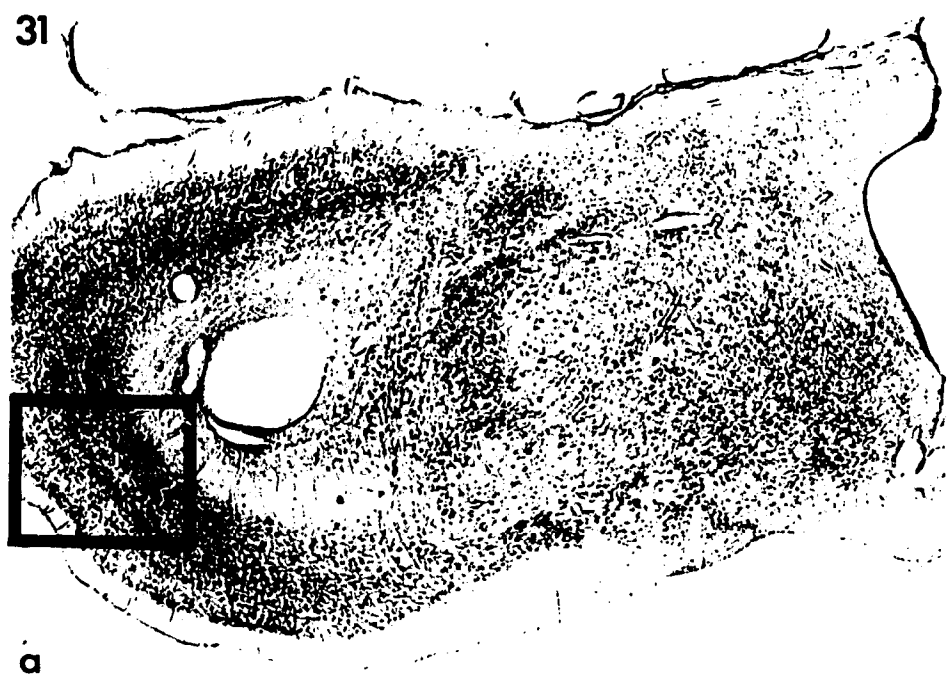


Fig. 32. a. A bright-field photomicrograph of a Nissl-stained coronal section through the nD. The area designated by the box is represented in the dark-field photomicrograph below. b. Darkfield photomicrograph showing resultant anterograde labeling within the nD (x34).

32

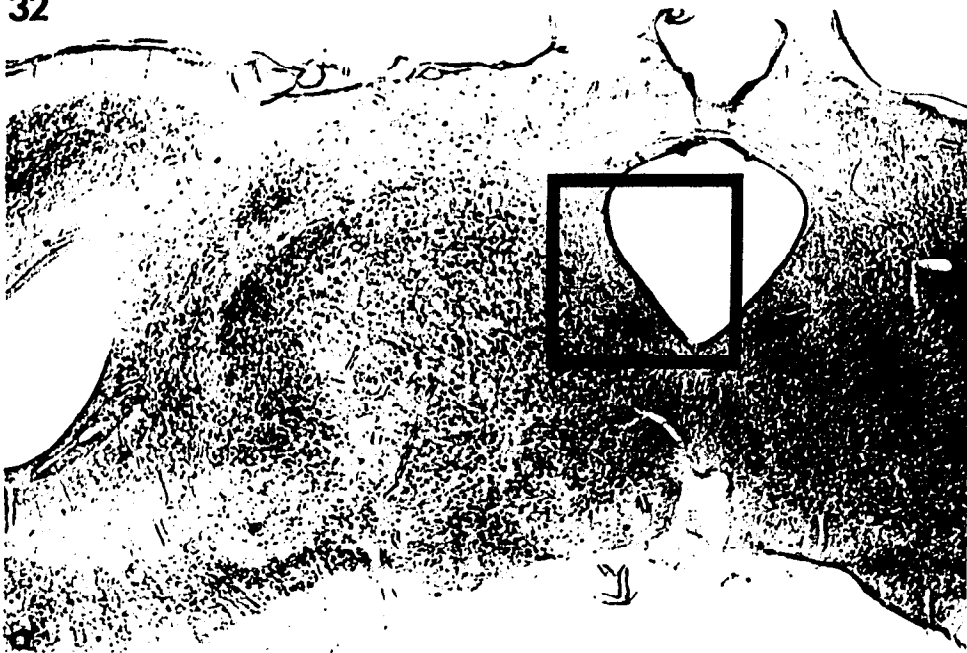


Fig. 33. a. A bright-field photomicrograph of a Nissl-stained coronal section through the nBOR. The area designated by the the box is represented in the dark-field photomicrograph below. b. Darkfield photomicrograph showing resultant anterograde labeling of terminals in all three subdivisions of the nBOR (nBORd, nBORp and nBORl)(x34).

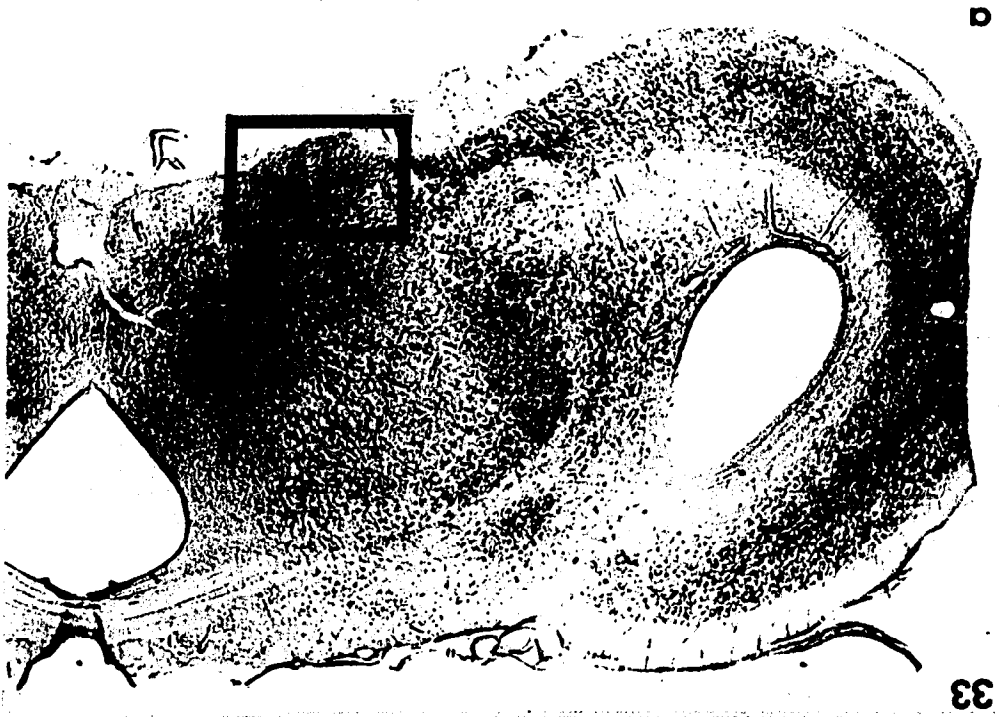
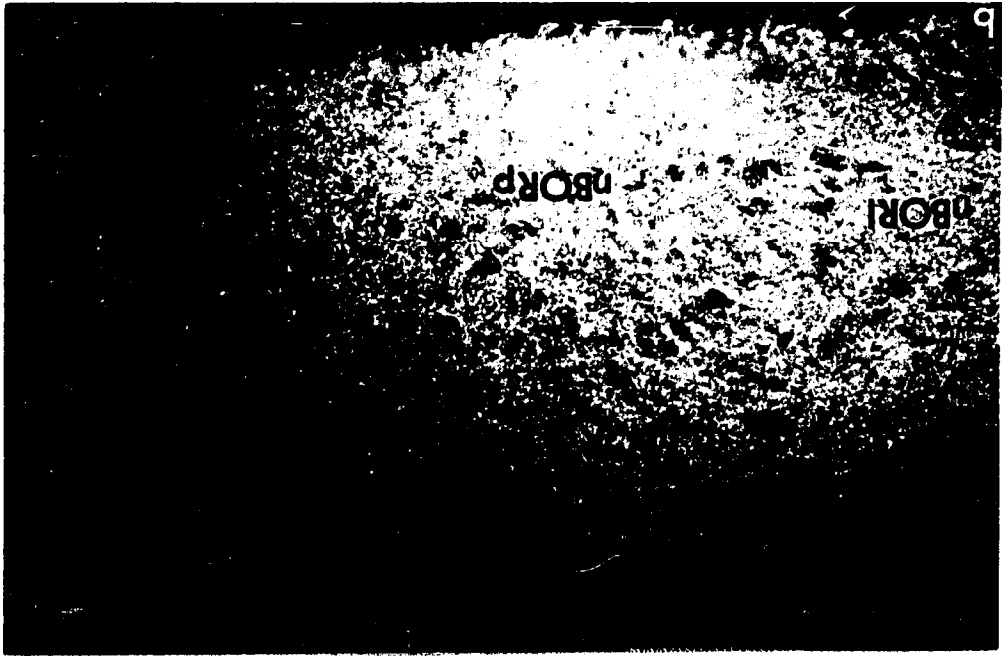


Fig. 34. a. A bright-field photomicrograph of a Nissl stained coronal section through the MP. The area designated by the box is represented in the dark-field photomicrograph below. b. Darkfield photomicrograph showing the resultant anterograde labeling of terminals in the MP (x34).

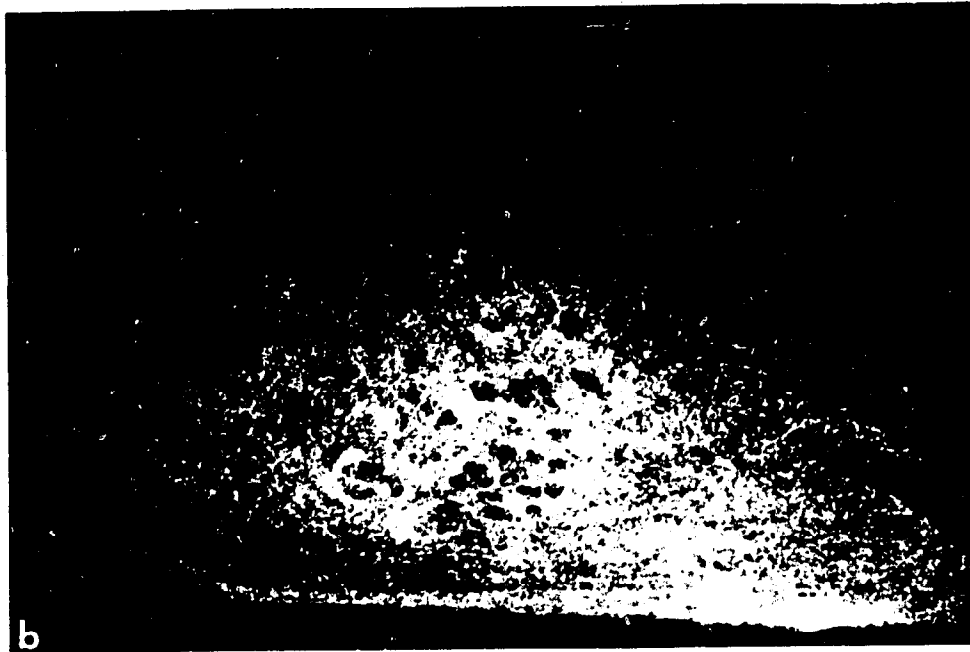
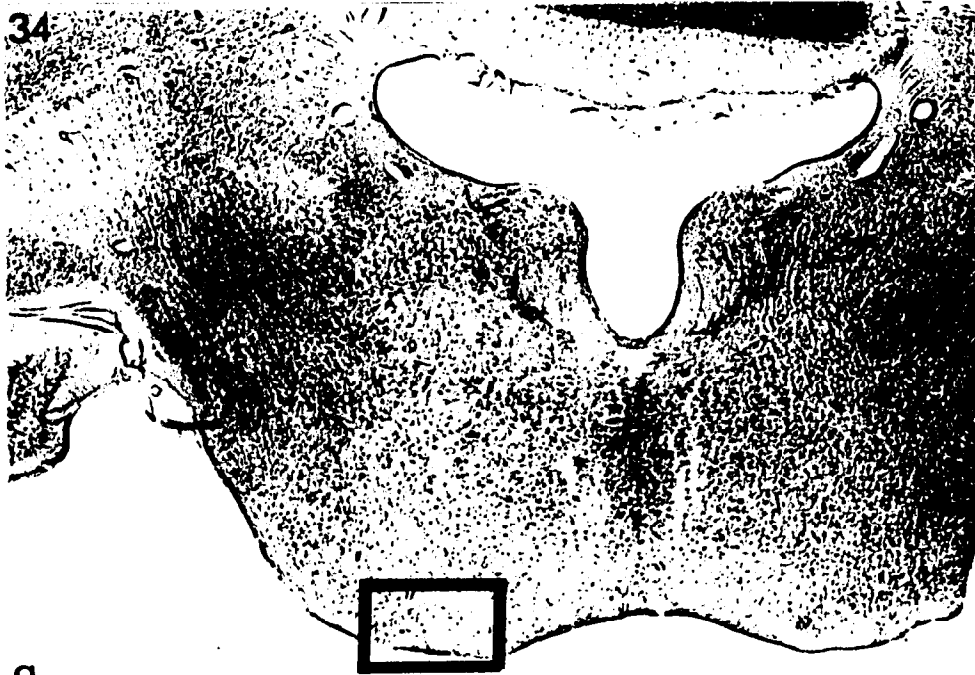
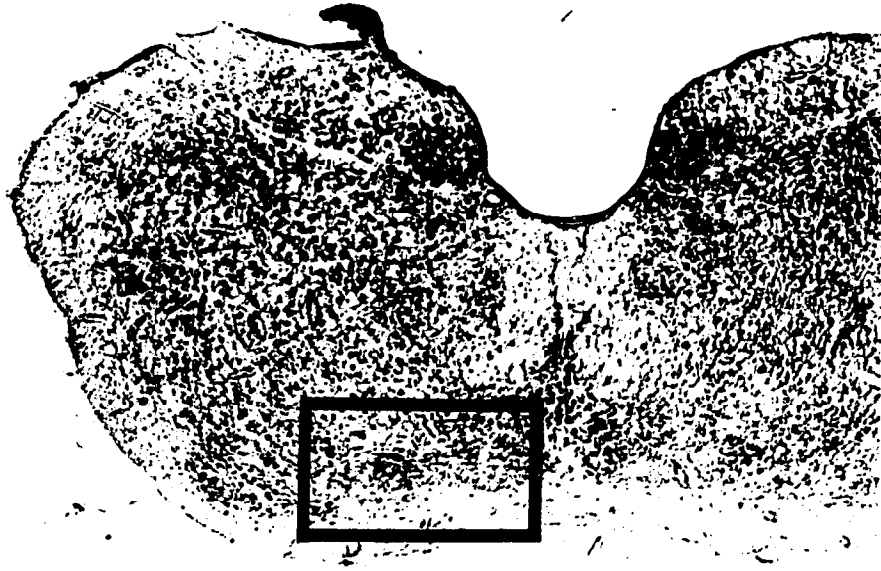
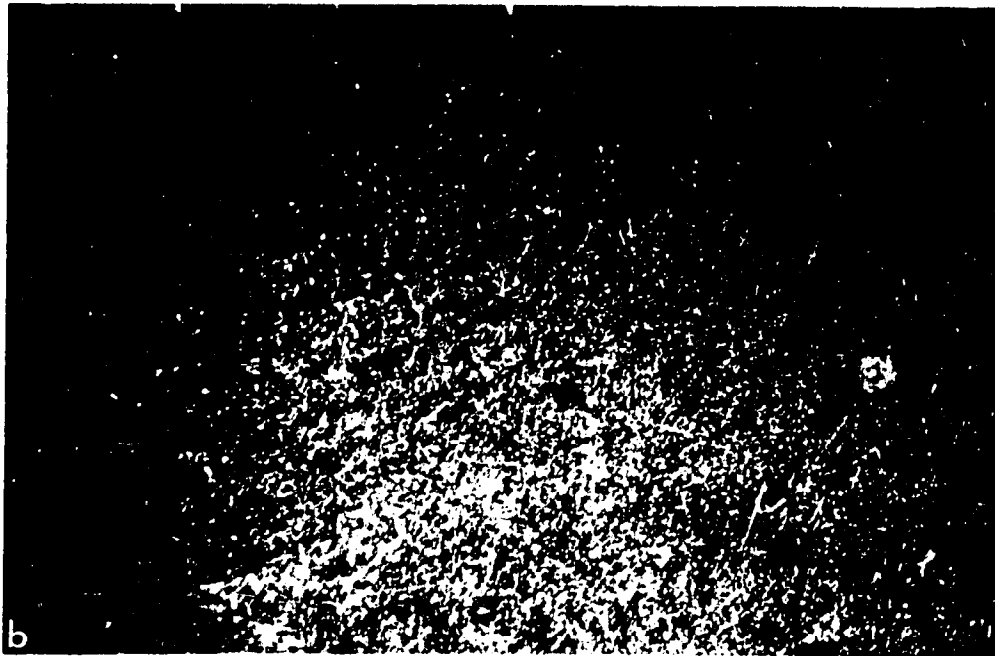


Fig. 35. a. A bright-field photomicrograph of a Nissl-stained coronal section through the rostral IO. The area designated by the box is represented in the dark-field photomicrograph below. b. Darkfield photomicrograph showing the resultant anterograde labeling of terminals in rostral IO ( $\times 34$ ).

35

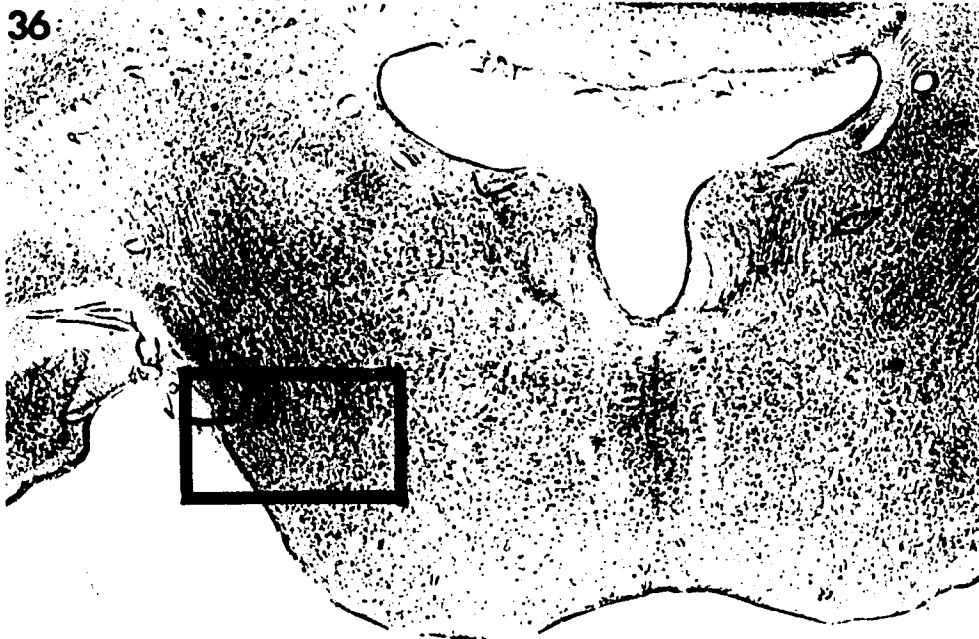


a



b

Fig. 36. a. A bright-field photomicrograph of a Nissl-stained coronal section through the LP. The area designated by the box is represented in the dark-field photomicrograph below. b. Darkfield photomicrograph showing the resultant anterograde labeling in the LP (x34).



a

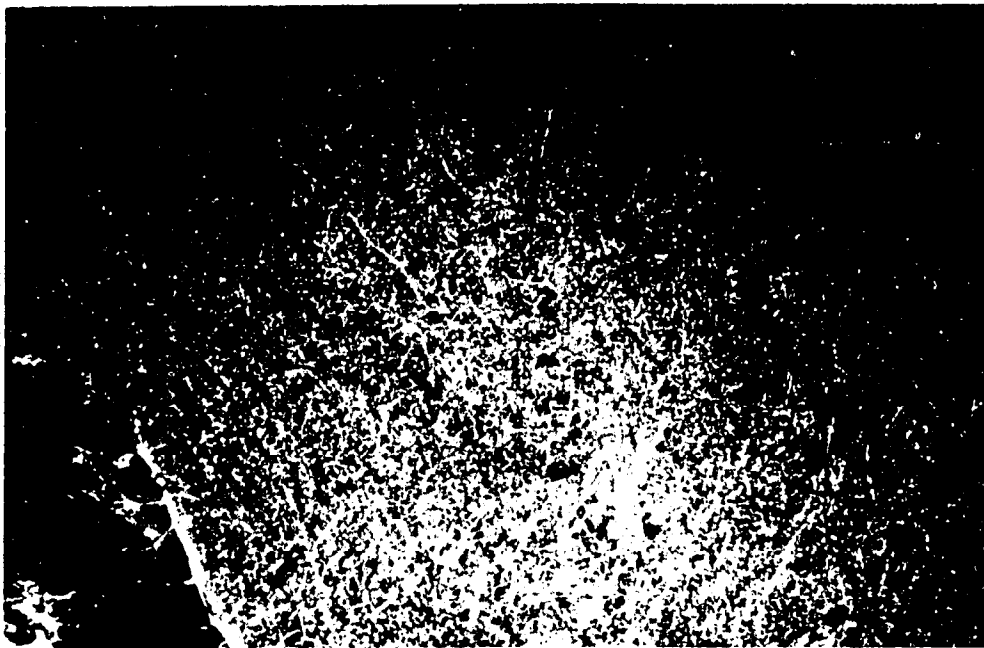


Fig. 37. a. A bright-field photomicrograph of a Nissl-stained parasagittal section through folia V-IX of the Cb. The area designated by the box is represented in the dark-field photomicrograph below. b. Darkfield photomicrograph showing the resultant terminal labeling in folia IXc of the Cb (x23).

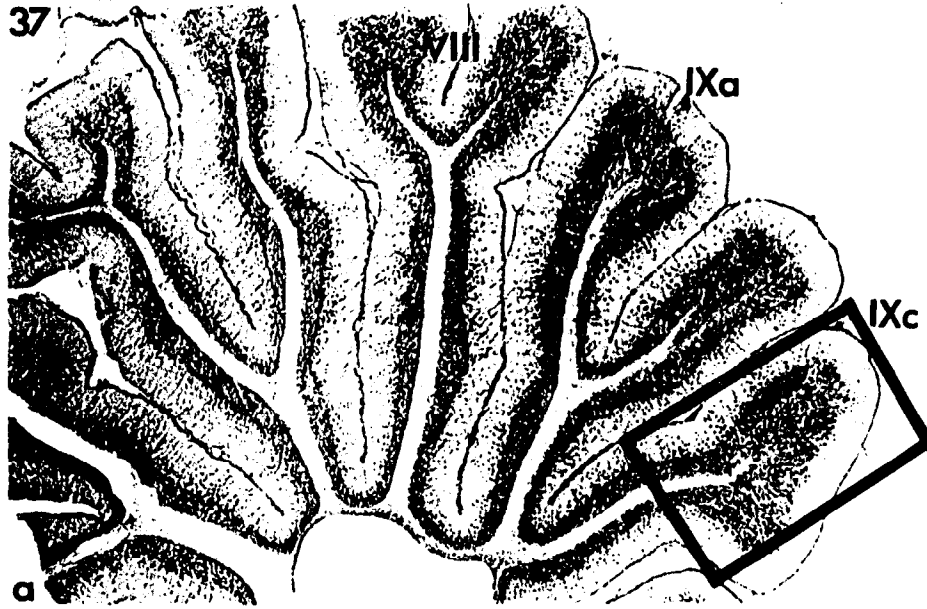


Fig. 38. Photomicrographs of HRP-labeled neurons found in the LM after injection into the nBOR (x163). a. Example of a medium (M) sized neuron. b. Examples of small (S) and large (L) sized neurons.

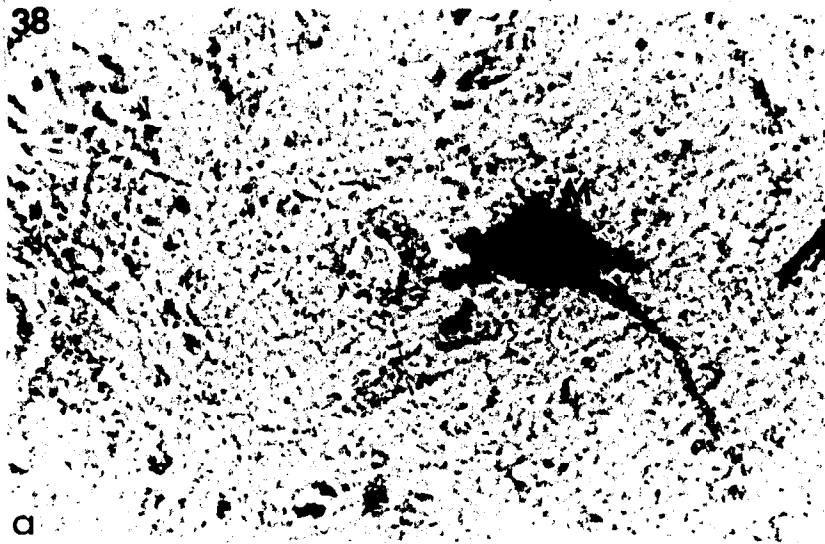


Fig. 39. Photomicrographs of HRP-labeled neurons found in LM after injection into LP/MP (x163). a. Example of a small (S) sized neuron. b and c. Examples of medium (M) sized neurons. d and e. Examples of large (L.) sized neurons.

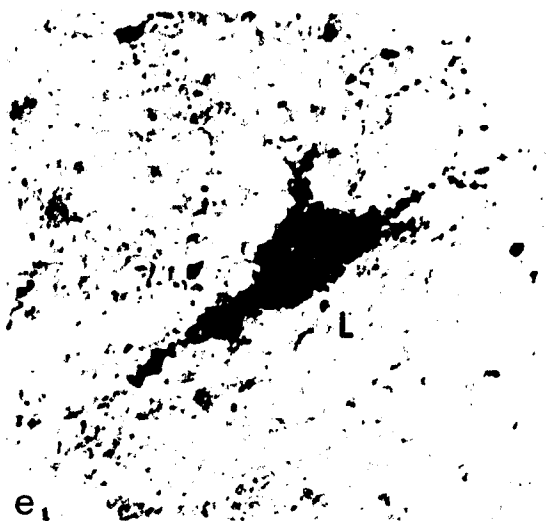
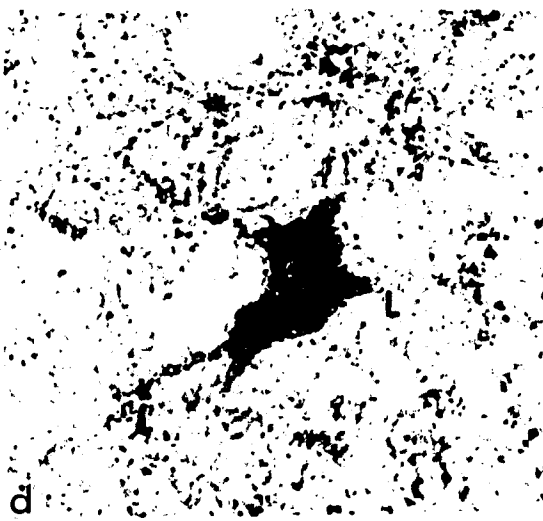
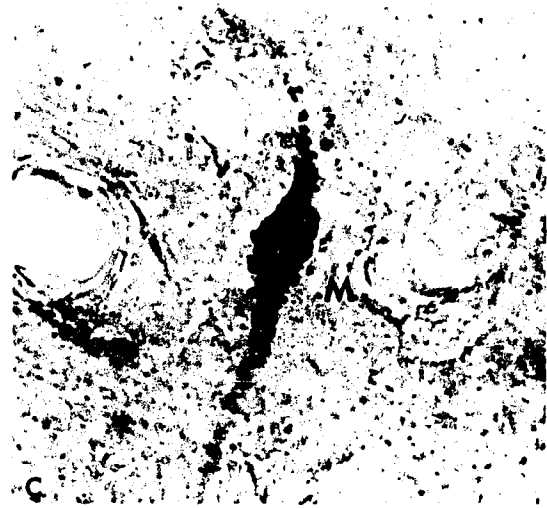
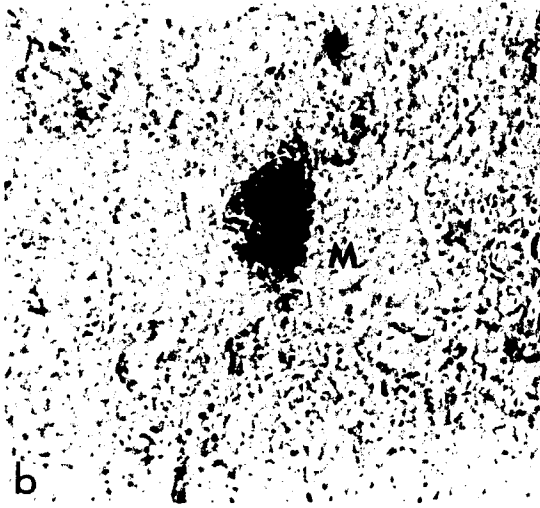
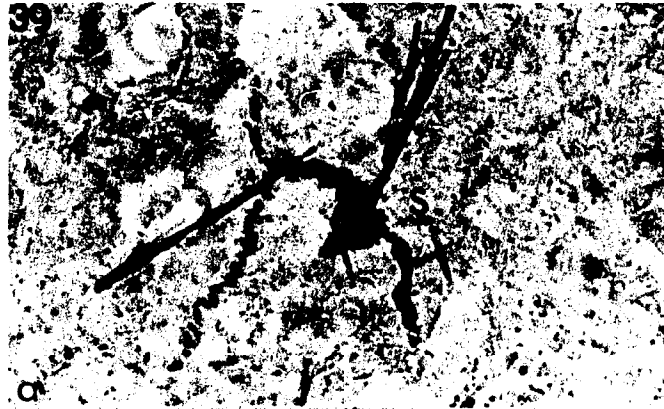


Fig. 40. Photomicrographs of HRP-labeled neurons found in LM after injection into nD ( $\times 163$ ). a and b. Examples of medium sized neurons.

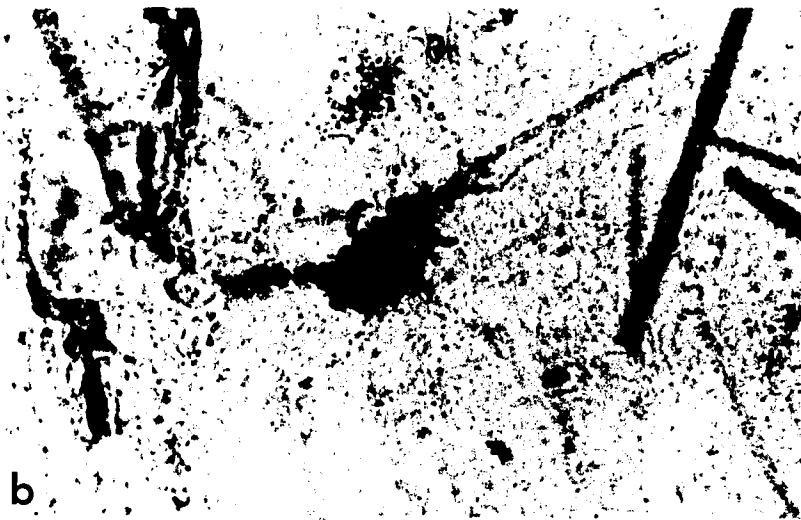
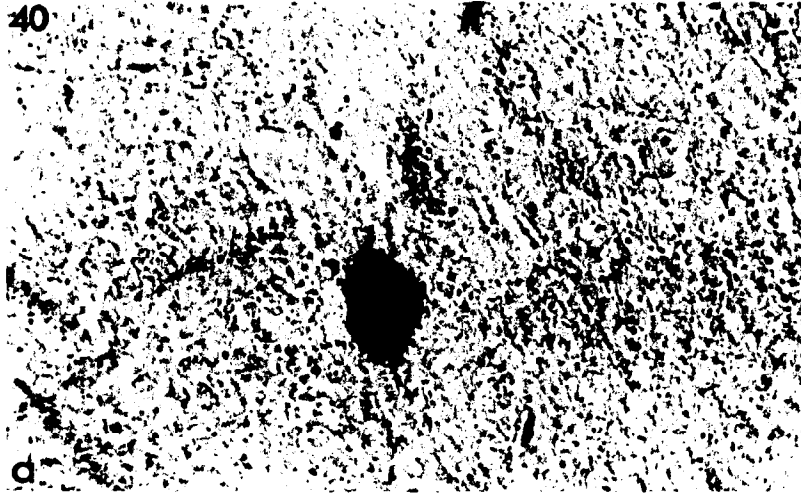


Fig. 41. Photomicrographs of HRP-labeled neurons found in LM after injection into IO ( $\times 16.3$ ). a. Example of a large (L) sized neuron. b and c. Examples of medium (M) sized neurons.

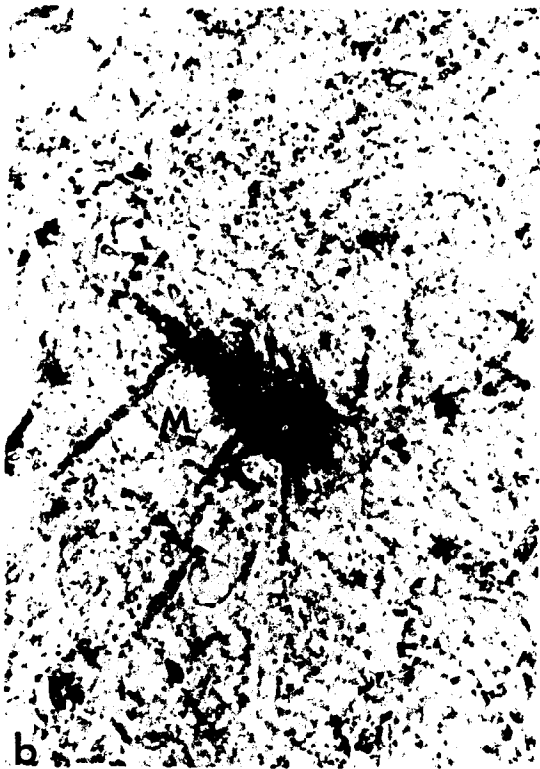
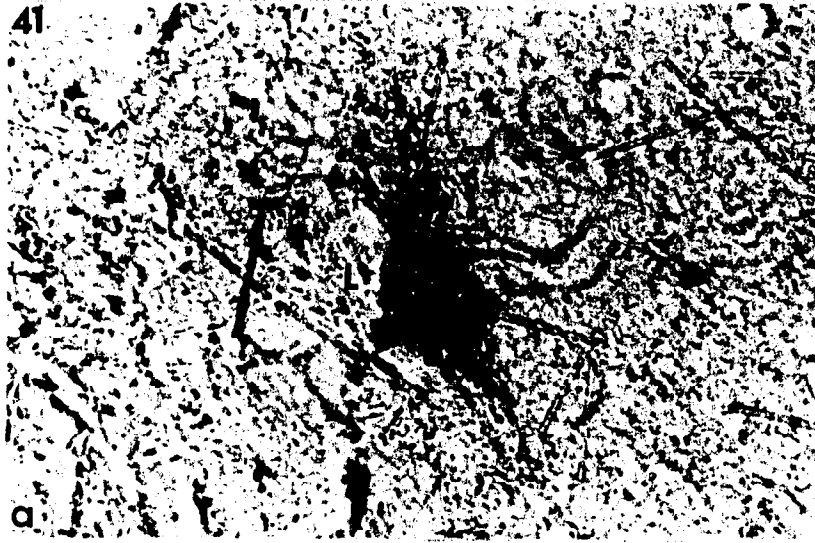


Fig 42. Photomicrographs of HRP-labeled neurons found in LM after injection into Cb (x163). a and b. Examples of large (L.) and medium (M) sized neurons.

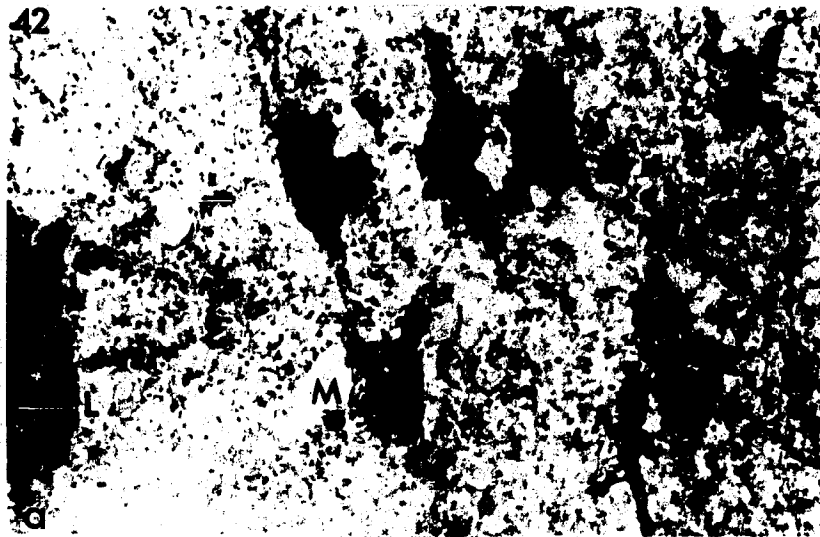
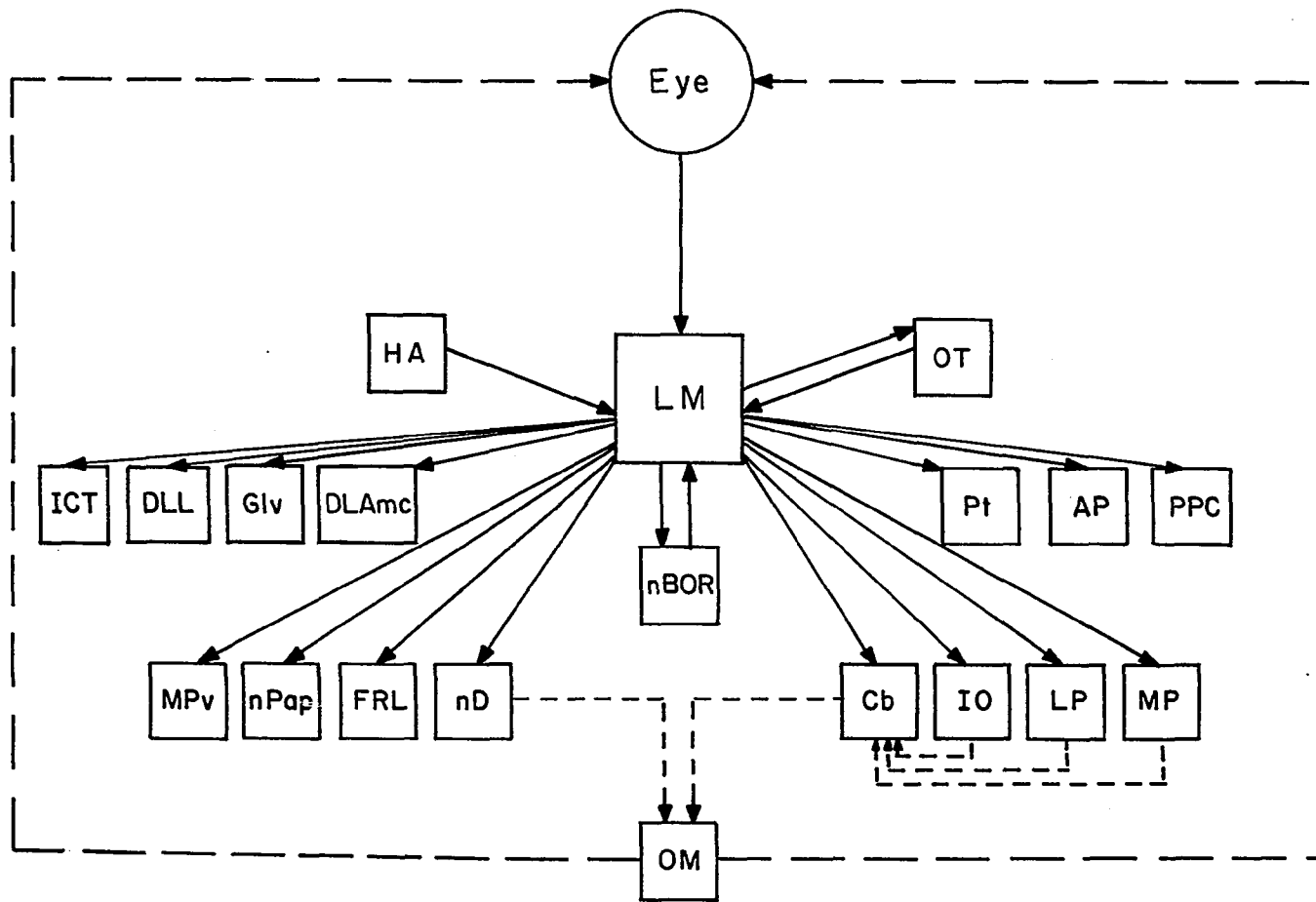


Fig. 43. Summary diagram of the proposed neural circuitry of the LM and its relationship to the eye. The afferent and efferent connections of the LM in chickens identified in the present study are drawn with solid lines whereas connections determined by other studies are drawn with dotted lines.



## REFERENCES

- Adamo, N.J. (1967) Connections of efferent fibers from hyperstriatal areas in chicken, raven and African lovebirds. *J. Comp. Neurol.* 131: 337-356.
- Atkinson, J. (1979) Development of optokinetic nystagmus in the human infant and monkey infant: An analogue to development in kittens. In *Developmental Neurobiology of Vision*, R.D. Freeman, ed., 277-287, Plenum Press, N.Y.
- Azevedo, T.A., Cukiert, A. and L.R.G. Britto (1983) A pretectal projection upon the accessory optic nucleus in the pigeon: an anatomical and electrophysiological study. *Neurosci. Lett.* 43: 13-18.
- Bagnoli, P., Francesconi, W. and F. Magni (1979) Interaction of optic tract and visual wulst impulses on single units of the pigeon optic tectum. *Brain Behav. Evol.* 16: 19-37.
- Ballas, I., Hoffmann, K.P., and H.J. Wagner (1981) Retinal projection to the nucleus of the optic tract in the cat as revealed by retrograde transport of horseradish peroxidase. *Neurosci. Lett.* 26: 197-202.
- Ballas, I., and K.P. Hoffmann (1985) A correlation between receptive field properties and morphological structures in the pretectum of the cat. *J. Comp. Neurol.* 238: 417-428.
- Barlow, H.B., Hill, R.M., and W.R. Levick (1964) Retinal ganglion cells responding selectively to direction and speed of image motion in the rabbit. *J. Physiol. (London)* 173: 377-407.
- Barmack, N.H. and D.T. Hess (1980) Multiple unit activity evoked in the dorsal cap of the inferior olive of the rabbit by visual stimulation. *J. Neurophysiol.* 43: 151-164.
- Berman, N. (1977) Connections of the pretectum in the cat. *J. Comp. Neurol.* 174: 227-254.
- Braun, J.J. and F.P. Gault (1969) Monocular and binocular control of horizontal optokinetic nystagmus in cats and rabbits. *J. Comp. Physiol. Psychol.* 69: 12-16.
- Brauth, S.E. and H.J. Karten (1977) Direct accessory optic projections to the vestibulo-cerebellum: A possible channel for oculomotor control systems. *Exp. Br. Res.* 28: 73-84.
- Bravo, H. and J.D. Pettigrew (1981) The distribution of neurons projecting from the retina and visual cortex to the thalamus and tectum opticum of the barn owl, *Tyto alba*, and the burrowing owl, *Speotyto cunicularia*. *J. Comp. Neurol.* 190: 419-441.
- Brecha, N. (1978) Some observations on the organization of the avian optic tectum: afferent nuclei and their tectal projections. Ph.D. dissertation SUNY Stony

- Brook, N.Y..
- Brecha, N., H.J. Karten and S.P. Hunt (1980) Projections of the nucleus of the basal optic root in the pigeon: an autoradiographic and horseradish peroxidase study. *J. Comp. Neurol.* 189: 615-670.
- Burns, S. (1985) The avian accessory optic system: neurophysiology, development and oculomotor function. Ph.D. dissertation, CUNY, N.Y., NY.
- Campbell, C.B.G. and W. Hodos (1970) The concept of homology and the evolution of the nervous system. *Brain Behav. Evol.* 3: 353-367.
- Cardozo, J.J.N. and J.J.L. Van Der Vant (1987) Synaptic organization of the nucleus of the optic tract in the rabbit: a combined Golgi-electron microscopic study. *J. of Neurocytol.* 16: 389-401.
- Carpenter, M.B., Harbison, J.W. and P. Peter (1970) Accessory oculomotor nuclei in the monkey: projections and efferents of discrete lesion. *J. Comp. Neurol.* 140: 131-154.
- Cazin, L., W. Precht and J. Lannou (1980) Pathways mediating optokinetic responses of vestibular nucleus neurons in the rat. *Pflugers Arch. ges. Physiol.* 384: 19-29.
- Cazin, L., J. Lannou, and W. Precht (1984) An electrophysiological study of pathways mediating optokinetic responses to the vestibular nucleus in the rat. *Exp. Br. Res.* 54: 337-348.
- Chown, P.J., P. Ramm, B. Morgan, and B. Frost (1984) Functional analysis of L.Mmc of pigeon accessory optic system. *Soc. Neurosci. Abstr.* 10: 574.
- Clarke, P.G.H. (1974) The organization of visual processing in the pigeon Cb. *J. Physiol.* 243: 267-285.
- Clarke, P.G.H. (1977) Some visual and other connections to the Cb of the pigeon. *J. Comp. Neurol.* 174: 535-552.
- Collewijn, H. (1969) Optokinetic eye movements in the rabbit: input-output relations. *Vis. Res.* 9: 117-132.
- Collewijn, H. (1975a) Oculomotor areas in the rabbit's midbrain and pretectum. *J. Neurobiol.* 6: 3-22.
- Collewijn, H. (1975b) Direction selective units in the rabbits nucleus of the optic tract. *Br. Res.* 100: 489-508.
- Cowan, W.M., L. Adamson and T.P.S. Powell (1961) An experimental study of the avian visual system. *J. Anat. (London)* 95: 545-563.

- Cynader, M. and L. Harris (1980) Eye movements in strabismic cats. *Nature (London)* 286: 64-65.
- Crossland, W.J. and C.J. Uchwat (1979) Topographic projections of the retina and the optic tectum upon the ventral lateral geniculate nucleus in the chick. *J. Comp. Neurol.* 185: 87-106.
- Dubois, M.F.W. and H. Collewijn (1979) The optokinetic reactions of the rabbit: relation to the visual streak. *Vis. Res.* 19: 9-17.
- Ehrlich, D. (1981) Regional specialization of the chick retina as revealed by the size and density of neurons in the ganglion cell layer. *J. Comp. Neurol.* 195: 643-657.
- Ehrlich, D. and R. Mark (1984a) An atlas of the primary visual projections in the brain of the chick, *Gallus, gallus*. *J. Comp. Neurol.* 223: 592-610.
- Ehrlich, D. and R. Mark (1984b) Topography of the primary visual centers in the brain of the chick, *Gallus, gallus*. *J. Comp. Neurol.* 223: 611-626.
- Feldon, S., P. Feldon and L. Kruger (1970) Topography of the retinal projection upon the superior colliculus of the cat. *Vis. Res.* 10: 135-143.
- Fite, K.V., N. Brecha, H.J. Karten and S.P. Hunt (1981) Displaced ganglion cells and the accessory optic system of pigeons. *J. Comp. Neurol.* 195: 279-288.
- Furber, S.E. (1983) The organization of the olivocerebellar projection in the chicken. *Brain Behav. Evol.* 22: 198-211.
- Fuster, J.M. (1958) The effects of stimulation of brain stem on tachistoscopic perception. *Science* 127: 150.
- Galifret, Y. (1968) Les diverses aires fonctionnelles de la retine du pigeon. *Z. Zellforsch.* 86: 535-545.
- Gamlin, P.D.R. and D.H. Cohen (1988a) The retinal projections to the pretectum in the pigeon (*Columba livia*). *J. Comp. Neurol.* 269: 1-17.
- Gamlin, P.D.R. and D.H. Cohen (1988b) Projections of the retinorecipient pretectal nuclei in the pigeon (*Columba livia*). *J. Comp. Neurol.* 269: 18-46.
- Garey, L.J. and T.P.S. Powell (1968) The projections of the retina in the cat. *J. Anat.* 102: 189-222.
- Gioanni, H., Rey, J., Villalobos, J., Richard, D. and A. Dalbera (1983) Optokinetic nystagmus in the pigeon (*Columba livia*) II. Role of the pretectal nucleus of the accessory optic system (AOS). *Exp. Br. Res.* 50: 237-247.
- Gioanni, H., Rey, J., Villalobos, J., Bouyer, J.J. and Y. Gioanni (1981) Optokinetic nystagmus in the pigeon (*Columba livia*). *Exp. Br. Res.* 44: 362-370.

- Gottlieb, M.D. and O.C. McKenna (1986) Light and electron microscopic study of an avian pretectal nucleus, the lentiform nucleus of the mesencephalon, magnocellular division. *J. Comp. Neurol.* 248: 133-145.
- Graham, J. (1977) An autoradiographic study of the efferent connections of the superior colliculus in the cat. *J. Comp. Neurol.* 173: 629-654.
- Grasse, K.J. and M.S. Cynader (1986) Response properties of single units in the accessory optic system of the dark-reared cat. *Dev. Br. Res.* 27: 199-210.
- Giolli, R.A., Towns, L.C., Takahashi, T.T., Karamanlidis, A.N. and D.D. Williams (1978) An autoradiographic study of the projections of the visual cortex area 1 to the thalamus, pretectum, and superior colliculus in the rabbit. *J. Comp. Neurol.* 180: 743-752.
- Giolli, R.A. and M.D. Guthrie (1971) Organization of subcortical projections of visual areas I and II in the rabbit. An experimental degeneration study. *J. Comp. Neurol.* 142: 351-376.
- Graybiel, A. (1974) Some efferents of the pretectal region of the cat. *Anat. Rec.* 178: 365.
- Gregory, K.M. (1985) The dendritic architecture of the visual pretectal nuclei of the rat: a study with the golgi-cox method. *J. Comp. Neurol.* 234: 122-135.
- Hobbelein, J. F. and H. Collewijn (1971) Effect of cerebro/cortical and collicular ablations upon the optokinetic reactions in the rabbit. *Doc. Ophthalmol.* 30: 227-236.
- Hoffmann, K.P., and A. Schoppmann (1975) Retinal input to direction selective cells in the nucleus tractus opticus of the cat. *Br. Res.* 99: 359-366.
- Hoffmann, K.P., and A. Schoppmann (1981) A quantitative analysis of the direction specific responses of neurons in the cat's nucleus of the optic tract. *Exp. Br. Res.* 42: 146-157.
- Hoffmann, K.P., and J. Stone (1985) Retinal input to the nucleus of the optic tract of the cat assessed by antidromic activation of ganglion cells. *Exp. Br. Res.* 59: 395-403.
- Hollander, H. (1974) On the origin of the corticopretectal projection in the cat. *Exp. Br. Res.* 21: 433-439.
- Holstege, G. and H. Collewijn (1982) The efferent connections of the nucleus of the optic tract and the superior colliculus in the rabbit. *J. Comp. Neurol.* 209: 139-175.
- Howard, L.P. and M. Ohmi (1984) The efficiency of the central and peripheral retina in driving human optokinetic nystagmus. *Vis. Res.* 24: 969-976.

- Huber, G.C. and E.C. Crosby (1929) The nuclei and fiber paths of the avian dien-cephalon with consideration of telencephalic and certain mesencephalic centers and connections. *J. Comp. Neurol.* 48: 1-225.
- Hunt, S.P. and H. Kunzle (1976) Observations on the projections and intrinsic organization of the pigeon optic tectum: an autoradiographic study based on anterograde and retrograde axon and dendritic flow. *J. Comp. Neurol.* 170: 153-172.
- Hutchins, B. and J.T. Weber (1985) The pretectal complex of the monkey: a rein-vestigation of the morphology and retinal terminations. *J. Comp. Neurol.* 232: 425-442.
- Hutchins, B. and J.T. Weber (1986) Ultrastructural analysis of retinal and visual cortical projections within the cat's pretectal nucleus of the optic tract. *Soc. for Neurosci. Abstr.* 12: 1032.
- Itoh, K. (1977) Efferent projections of the pretectum of the cat. *Exp. Br. Res.* 50: 89-105.
- Kaneski, T. and J. M. Sprague (1974) Anatomical organization of pretectal nuclei and tectal laminae in the cat. *J. Comp. Neurol.* 158: 319-338.
- Karten, H.J. and W. Hodos (1967) A stereotaxic atlas of the brain of pigeon (*Columba livia*). Johns Hopkins Press, Baltimore, MD.
- Karten, H.J., Hodos, W., Nauta, W.J.H. and A.M. Revzin (1973) Neural connec-tions of the visual Wulst of the avian telencephalon: experimental studies in the pigeon (*Columba livia*) and owl (*Speotyto cunicularia*). *J. Comp. Neurol.* 150: 253-278.
- Karten, H.J., Fite, K.V., and N. Brecha (1977) Specific projection of displaced reti-nal ganglion cells upon the accessory optic system in the pigeon (*Columba livia*). *Proc. Natl. Acad. Sci. USA* 74: 1753-1756.
- Kawamura, S.J., Sprague, M., and K. Niimi (1974) Corticofugal projections from the visual cortices to the thalamus, pretectum, and superior colliculus in the cat. *J. Comp. Neurol.* 158: 339-362.
- Koontz, M.A., Rodieck, R.W., and S.G. Farmer (1985) The retinal projection to the cat pretectum. *J. Comp. Neurol.* 236: 42-59.
- Kuhlenbeck, H. (1939) The development and structure of the pretectal cell masses in the chick. *J. Comp. Neurol.* 71: 361-387.
- Kuhlenbeck, H. and R. Miller (1942) The pretectal region of the rabbit's brain. *J. Comp. Neurol.* 76: 323-365.
- Laties, A.M. and J.M. Sprague (1966) The projection of optic fibers to the visual centers of the cat. *J. Comp. Neurol.* 127: 35-70.

- Lindsley, D.B., Schreiner, L.H., Knowles, W.B. and H.W. Magoun (1950) Behavioral and EEG changes following chronic brainstem lesions in the cat. *Electroencephal. Clin. Neurophysiol.* 2: 483-498.
- Maekawa, K., Takeda, T. and M. Kimura (1981) Neural activity of nucleus reticularis tegmentis pontis- the origin of visual mossy fiber afferents to cerebellar flocculus of rabbits. *Br. Res.* 210: 17-30.
- Maekawa, K., Takeda, T. and M. Kimura (1984) Responses of the nucleus of the optic tract neurons projecting to the nRTP upon optokinetic stimulation in the rabbit. *Neurosci. Res.* 2: 1-25.
- Malach, R. Strong, N.P. and R.C. Van Sluyters (1981) Optokinetic nystagmus in long-term monocularly deprived cat. *Soc. Neurosci. Abstr.* 7: 733.
- Maturana, H.R. and F.J. Varela (1982) Color opponent responses in the avian lateral geniculate: a study in the quail (*Coturnix coturnix japonica*). *Brain Res.* 247: 227-235.
- McGill, J. I., Powell, T.P.S., and W. M. Cowan (1966) The retinal representation upon the optic tectum and isthmo-optic nucleus in the pigeon. *J. Anat.* 100: 5-33.
- McKenna, O.C., and J. Wallman (1981) Identification of avian brain regions responsive to retinal slip using 2-deoxyglucose. *Brain Res.* 210: 455-460.
- McKenna, O.C., and J. Wallman (1985a) Functional postnatal changes in avian brain regions responsive to retinal slip: a 2-deoxy-D-glucose study. *J. Neurosci.* 5: 330-342.
- McKenna, O.C., and J. Wallman (1985b) Accessory optic system and pretectum of birds: comparisons with those of other vertebrates. *Brain Behav. Evol.* 26:91-116.
- Mesulam, M.M. (1976) The blue reaction product in horseradish peroxidase neurohistochemistry: incubation parameters and visibility. *J. Histochem. Cytochem.* 24: 1273-1280.
- Mesulam, M.M. (1978) Tetramethyl benzidine for horseradish peroxidase neurohistochemistry. A non-carcinogenic blue reaction-product with superior sensitivity for visualizing neural afferents and efferents. *J. Histochem. Cytochem.* 26: 106-117.
- Miceli, D., Gioanni, H., Reperant, J. and J. Peyrichoux (1979) The avian visual Wulst. I. An anatomical study of the afferent and efferent pathways; in Granda Maxwell, *Neural Mechanisms of Behavior in the Pigeon*, Plenum Press, NY. 223-254.
- Miceli, D., Reperant, J. and L. Dionne (1985) A quantitative autoradiographic study of visual Wulst projections to the diencephalic and brainstem of the pigeon. *Suppl. to Inv. Ophthalm. Vis. Sci.* Vol. 26, No.3, 326.

- Montgomery, N., Fite, K.V. and A.M. Grigonis (1985) The pretectal nucleus lenticularis mesencephali of *Rana pipiens*. *J. Comp. Neurol.* 234: 264-275.
- Mowrer, O.H. (1936) Maturation vs. learning in the development of vestibular and optokinetic nystagmus. *J. Genet. Psychol.* 48: 383-404.
- Naegle, J.R., and R. Held (1982) The postnatal development of monocular optokinetic nystagmus in infants. *Vis. Res.* 22: 341-346.
- Nakamura, Y., Mizuno, N. and A. Konishi (1981) Electron microscopic identification of axon terminals of retinopretectal fibers in the cat by a combined horseradish peroxidase and tritiated amino acids tracing method. *Br. Res.* 212: 127-130.
- Olszewski, J. and D. Baxter (1954) *Cytoarchitecture of the human brain stem.* S. Karger, New York.
- Oyster, C.W. and H.B. Barlow (1967) Direction-selective units in rabbit retina: distribution of preferred directions. *Science* 155: 841-842.
- Oyster, C.W., Takahashi, E. and H. Collewijn (1972) Direction-selective retinal ganglion cells and control of optokinetic nystagmus in the rabbit. *Vis. Res.* 12: 183-193.
- Pasik, T. and P. Pasik (1964) Optokinetic nystagmus: an unlearned response altered by section of chiasma and corpus callosum in monkeys. *Nature (London)* 203: 609-611.
- Pasik, P., Pasik, T. and H.P. Krieger (1959) Effects of cerebral lesions upon optokinetic nystagmus in monkeys. *J. Neurophysiol.* 22: 298-304.
- Pearlman, A.L. and C.P. Hughes (1976) Functional role of efferents to the avian retina. I. An analysis of retinal ganglion cell receptive fields. *J. Comp. Neurol.* 166: 111-122.
- Petrossi, V.E. and D. Troiani (1983) Cortical modulation of the nucleus of the optic tract in the rabbit. *Exp. Neurol.* 81,(3): 627-639.
- Pettigrew, J.D. and M. Konishi (1976) Neurons selective for orientation and binocular disparity in the visual wulst of the barn owl (*Tyto alba*). *Science* 193: 675-678.
- Precht, W. and P. Strata (1980) On the pathways mediating optokinetic responses in vestibular nuclear neurons. *Neuroscience* 5: 777-787.
- Precht, W. (1981) Functional organization of optokinetic pathways in mammals. In A.F. Fuchs and W. Becker (eds.) *Progress in Oculomotor Res.*, Elsevier, North Holland, 425-442.

- Rager, G., Rager, U. and A. Kabiersch (1986) Organization of fibers in the retinotectal pathway of the chick. *Soc. Neurosci. Abstr.* 12: 436.
- Reiner, A., Brecha, N. and H.J. Karten (1979) A specific projection of retinal displaced ganglion cells to the nucleus of the basal optic root in the chicken. *Neuroscience* 4: 1679-1688.
- Reiner, A. and H.J. Karten (1983) The laminar organization of efferent projections from the avian wulst. *Br. Res.* 275: 349-354.
- Reperant, J. (1973) Nouvelles donnees sur les projections visuelles chez le pigeon (*Columba livia*). *J. Hirnforsch.* 14: 151-188.
- Revzin, A.M. (1969) A specific visual projection area in the hyperstriatum of the pigeon. *Br. Res.* 15: 246-249.
- Robertson, R.T. (1983) Efferents of the pretectal complex: separate populations of neurons project to lateral thalamus and to inferior olive. *Br. Res.* 258: 91-95.
- Scalia, F. (1972) The termination of retinal axons in the pretectal region of mammals. *J. Comp. Neurol.* 145: 223-258.
- Scalia, F. and V. Arango (1979) Topographic organization of the projection of the retina to the pretectal region in the rat. *J. Comp. Neurol.* 186: 270-292.
- Schoppmann, A. (1981) Projections from A 17 and 18 of visual cortex to the nucleus of the optic tract. *Br. Res.* 223: 1-17.
- Schoppmann, A. (1985) A developmental study of retinal afferents and visual responses in the cat pretectum. *Exp. Br. Res.* 60: 350-362.
- Siminoff, R., Schwassmann, H.O. and L. Kruger (1966) An electrophysiological study of the visual projection to the superior colliculus of the rat. *J. Comp. Neurol.* 127: 435-444.
- Stein, B.E. and S.B. Edwards (1979) Corticotectal and other corticofugal projections in neonatal cat. *Br. Res.* 161: 399-409.
- Strong, N.P., Malach, R., Lee, P. and R. C. Van Sluyters (1984) Horizontal optokinetic nystagmus in the cat: recovery from cortical lesions. *Dev. Br. Res.* 13: 179-192.
- Streit, P., Stella, M. and M. Cuenod (1980) Transneuronal labeling in the pigeon visual system. *Neurosci.* 5: 763-775.
- Tauber, E.S. and A. Atkins (1968) Optomotor responses to visual stimulation: relation to visual system organization. *Science* 160: 1365-1367.

- Terasawa, K., Otani, K. and J. Yamada (1979) Descending pathways of the nucleus of the optic tract in the rat. *Br. Res.* 173: 405-417.
- Ter Braak, J.W.G. (1936) Research on optokinetic nystagmus. *Dutch Arch. Human Anim. Physiol.* 21: 309-375.
- van Tienhoven, A. and L.P. Juhasz (1962) The chicken telencephalon, diencephalon and mesencephalon in stereotaxic coordinates. *J. Comp. Neurol.* 118: 185-198.
- Tsumoto, T., Suda, K., and H. Sato (1983) Postnatal development of corticotectal neurons in the kitten striate cortex: a quantitative study with horseradish peroxidase technique. *J. Comp. Neurol.* 219: 88-99.
- Updyke, B.V. (1977) Topographic organization of the projections from cortical areas 17, 18, and 19 onto the thalamus, pretectum and superior colliculus in the cat. *J. Comp. Neurol.* 173: 81-122.
- Visser, J.A. and G.G.J. Rademaker (1934) Die optischen reaktionen groszhirnloser tauben. *Arch. neer physiol.* 19: 482-501.
- Wallman, J. and J. Velez (1985) Directional asymmetries of optokinetic nystagmus: developmental changes and relation to the accessory optic system and to the vestibular system. *J. Neurosci.* 5: 317-329.
- Watanabe, M., Itoh, H. and H. Masai (1983) Cytoarchitecture and visual receptive neurons in the wulst of the japanese quail (*Coturnix coturnix japonica*). *J. Comp. Neurol.* 213: 188-198.
- Weber, J.T. and J. K. Harting (1980) The efferent projections of the pretectal complex: and autoradiographic and horseradish peroxidase analysis. *Br. Res.* 194: 1-28.
- Weber, J.T. (1985) Pretectal complex and the accessory optic system of primates. *Brain Beh. Evol.* 26: 117-140.
- Wilson, P. (1980) The organization of the visual hyperstriatum in the domestic chick. I. Topology and topography of the visual projection. *Br. Res.* 188: 319-332.
- Winterson, B.J. and S.E. Brauth (1985) Direction selective single units in the n. lentiformis mesencephali of the pigeon (*Columba livia*). *Exp. Br. Res.* 60: 215-226.
- Wood, C.C., Spear, P.D. and J.J. Braun (1973) Direction specific deficit in horizontal optokinetic nystagmus following removal of visual cortex in the cat. *Br. Res.* 60: 231-237.
- Yamamoto, M. (1979) Topographical representation in rabbit cerebellar flocculus for various afferent inputs from the brainstem investigated by means of retrograde axonal transport of horseradish peroxidase. *Neurosci. Lett.* 12:

29-34.